Diss. ETH No. 11137

A statistical analysis and climatological interpretation of hailstorms in Switzerland

A dissertation submitted to the
Swiss Federal Institute of Technology (ETH)
Zürich

for the degree of
Doctor of Natural Sciences

presented by
Saskia Willemse
Dipl. Nat. ETH
born on January 2, 1966
citizen of Tesserete (TI)

Accepted on the recommendation of
Prof. A. Waldvogel, examiner
Prof. C.-D. Schönwiese, co-examiner
Dr. D. Heimann, co-examiner

Zürich, 1995

Il cielo è di tutti

Qualcuno che la sa lunga
mi spieghi questo mistero:
il cielo è di tutti gli occhi,
di ogni occhio è il cielo intero.

E' mio, quando lo guardo.
E' del vecchio, del bambino,
del re, dell'ortolano,
del poeta, dello spazzino.

Non c'è povero tanto povero
che non ne sia il padrone.
Il coniglio spaurito
ne ha quanto il leone.

Il cielo è di tutti gli occhi,
ed ogni occhio, se vuole,
si prende la luna intera,
le stelle comete, il sole.

Ogni occhio si prende ogni cosa
e non manca mai niente:
chi guarda il cielo per ultimo
non lo trova meno splendente.

Spiegatemi voi dunque,
in prosa od in versetti,
perché il cielo è uno solo
e la terra è tutta a pezzetti.

Gianni Rodari
Il libro degli errori

Contents

Abstract

In these days of concern about the anticipated increase in greenhouse warming the question arises as to the influence of climatic change on the frequency of natural hazards. However, the term natural hazards includes a range of different phenomena, which cannot be described with one common data-set. For reasons of availability of time and data, the present study concentrates on (severe) hailstorms. As we decided to search for an answer to the above question on an experimental way, we need a reasonable hailstorm climatology which goes back beyond the era of RADAR measurements.

The best set available data on the distribution of severe hailstorms are hail damage claims collected by the Swiss crop-hail insurance (SHV), and these enable a spatial analysis to be derived of hailstorm events since 1949. These data have a simple structure: for each Swiss community, on a given day, it is known whether a damage claim has been registered or not. No indication on the amount of damage and its extension in the community itself is available. The reliability of the crop insurance data has been checked with the help of agrarian land-use statistics for the time interval considered. For the period between 1983 to the present hail-damage distributions have been compared with radar data of the "Schweizerische Meteorologische Anstalt". The best agreement between the hail patterns and the RADAR patterns is found for the larger storms, which mainly cross Switzerland from the West or South-West to the East or North-East. Since the calibration and the reliability test show that the quality of the data is best in the Mittelland and in the Prealps, this hailstorm-climatology project has been limited to the Swiss area north of the alpine ridge.

All days recording more than 30 damage claims have been plotted in daily hail-maps and the main features (length, area, orientation, beginning- and endpoint) of all clusters with a length of more than 25 km were stored in a data-base. For the period between 1949 and 1993, 651 clusters were collected with this method. The length of the clusters varies between 25 km (minimum condition) and 179 km, with a mean of 43 km; the smallest area measures 88 km^2, the largest 2'156 km^2 and the mean 395 km^2. The largest clusters are always oriented in a south - west direction.

An analysis of the time series of the number of damage claims and damage clusters shows a strong variability of the thunderstorm occurrence during the observed time span. Periods of stronger

hailstorm activity are observed around 1970 and after the mid 80's. Although one might be tempted to extrapolate the time series of the damage claim-frequency and of the hail cluster-frequency to try to predict the future thunderstorm activity, the data on which these series are based do not allow such kind of predictions because they hide too many uncertainties; furthermore, the considered time period is still too short for climatological interpretations.

Therefore, an attempt is made to find a set of meteorological measures and parameters which characterise strong hailstorm days and whose possible future development is, at least partially, known from other climatological studies. The main features favouring large hailstorms are:

- airflow from the Southwest (mostly maritime tropical air)
- frontal disturbances (particularly cold fronts)
- moisture advection around the 700 hPa level
- 0 °C - level between 3'000 and 4'500 m ASL

As thunderstorms are complex phenomena depending on many meteorological factors each of which follows a different evolution, it is not possible to define one single future scenario. Some possible scenarios are discussed at the end of the study . We come to the conclusion that, as long as the uncertainties on the future evolution of the meteorological factors favouring thunderstorm development are not reduced, it is not possible to make a meaningful forecast of thunderstorm activity.

Riassunto

Una domanda che emerge sempre piú spesso nell'ambito delle recenti discussioni sull'aumentato effetto serra riguarda l'influsso che questo cambiamento climatico puó avere sull'occorrenza di catastrofi naturali. D'altronde, il termine *catastrofi naturali* comprende un gran numero di fenomeni che non possono venir descritti da un unico insieme di dati. Per ragioni di disponibilitá di tempo e di dati il lavoro qui presentato si concentra sullo studio di (forti) tempeste di grandine. La decisione di affrontare questo tema dal punto di vista sperimentale ci ha posti davanti al problema della disponibiltá di dati climatologici del tempo precedente l'era delle misurazioni RADAR.

Gli annunci di danni dovuti alla grandine raccolti dall'assicurazione svizzera contro la grandine (SHV) si sono rivelati i migliori dati a nostra disposizione. Questi dati rendono possibile un'analisi della distribuzione della grandine a partire dal 1949 ed hanno una struttura molto semplice: per ogni giorno dell'anno é conosciuto il numero di comuni che hanno registrato danni della grandine e la loro posizione geografica. Non si hanno informazioni sulla percentuale e sull'estensione del danno all'interno del comune. L'attendibiltá di questi dati é stata controllata con l'aiuto di statistiche agricole del periodo considerato. I dati riguardanti gli anni dal 1983 ad oggi sono stati confrontati con misurazioni radar dell'Istituto Svizzero di Meteorologia. La congruenza tra la distribuzione dei danni e le immagini registrate dal RADAR é migliore per le tempeste piú grandi, che generalmente attraversano l'altipiano svizzero do ovest o sud-ovest a est o nord-est. Dato che sia l'esame dell'attendibiltá che il confronto con le immagini RADAR mostrano che la qualitá dei dati é migliore nell'altipiano e nelle prealpi, la nostra analisi climatologica é limitata al territorio svizzero a nord delle alpi.

Il metodo di raccolta dei dati consiste nella rappresentazione geografica dei comuni danneggiati dalla grandine in giorni con piú di trenta comuni coinvolti. Si ottiene cosí una rappresentazione di cosiddetti *clusters* di grandine di cui puó venir misurata la lunghezza, l'area, il punto d'inizio e il punto terminale e la direzione di spostamento. Per esser sicuri di registrare soltanto le tempeste piú grandi, abbiamo stabilito un limite inferiore di lunghezza al di sotto del quale i clusters non vengono piú registrati. Durante il periodo tra 1949 e il 1993 sono strati osservati 651 clusters, la cui lunghezza varia tra 25 km (limite inferiore) e 179 km, con una media di 43 km. Il cluster piú piccolo misura 88 km^2, quello piú grande 2'156 km^2 e la

media é di 395 km^2. Tutti i clusters piú grandi presentano una direzione di spostamento da sud-ovest a nord-est.

Un analisi dell'evoluzione temporale del numero di annunci di grandine e del numero di clusters mostra una grande variabilitá dell'attivitá temporalesca durante tutto periodo osservato. Periodi di maggiore attivitá si osservano attorno al 1970 a dopo la metá degli anni 80.

Un'estrapolazione della futura attivitá temporalesca a partire dagli annunci di grandine o dal numero di clusters non é possibile a causa delle numerose incertezze nascoste nei dati usati per questa climatologia e a causa del fatto che il periodo analizzato, dal punto di vista climatologico, é piuttosto corto.

In alternativa all'estrapolazione diretta, abbiamo cercato misure e parametri meteorologici che caratterizzano i giorni di forti tempeste di grandine e di cui la possibile evoluzione futura é conosciuta in seguito ad altri studi climatologici. Le principali caratteristiche meteorologiche che favoriscono la formazione di grandi tempeste di grandine sono:

- flusso d'aria (generalmente marittima tropicale) da sud-ovest
- passaggio di una pertubazione (soprattutto fronti freddi)
- apporto di aria umida ad un livello di circa 700 hPa
- limite di 0 °C tra 3'000 e 4'500 m s.l.m.

Temporali sono fenomeni molto complessi che dipendono da numerosi fattori meteorologici, ognuno dei quali segue un' evoluzione differente. Ció rende impossibile la definizione di un unico scenario caratterizzante la futura evoluzione dell'attivitá temporalesca. Una delle conclusioni piú importanti di questo lavoro é che, fintanto che il futuro climatologico dei fattori meteorologici caratterizzanti lo sviluppo di temporali é incerto come lo é attualmente, non sará possibile fare previsioni sensate sulla futura attivitá temporalesca.

Foreword

Climate and climate change are increasingly becoming a matter of discussion in the scientific and public domain.

The awareness that human activities might influence the climate system has motivated mankind to seek a better knowledge of the mechanisms governing this system to determine how much he can be made responsible for the detected and predicted changes.

The beginning of the computer era enabled theoretical studies of the climate system with mathematical models. With these models single phenomena can be isolated and studied separately or in combination with a small selected number of other processes.

The performance and calibration of measuring instruments are being improved continuously and the density of measuring networks is growing almost everywhere, allowing a better detection of the short-term climate signals. The development of increasingly refined methods for the indirect detection of long-term climate signals (paleoclimatology) enables a more precise insight on the climate evolution of the past millennia.

But why are we so concerned about climatic change?

Climate variation has a large impact on man's activities and on the economy. Occurrences of extreme variations of precipitation leading to droughts and floods have always been a cause of concern, increasingly so in recent years as the greater world-demand for food resources, especially in developing countries, has created a greater vulnerability.

Even quite small, average hemispheric temperature changes can be reflected in large regional variations. In the Little Ice age, for instance, winters in Europe were, on average, much more severe than now, glaciers and the cover of sea ice advanced considerably although the hemispheric average temperature only changed by a little over 1°K (Houghton 1984).

The growth of earth's population favours settlements in areas which are very sensitive to climate changes. For instance, in case of an increase of mean temperature, settlements located below sea level (e.g. Bangladesh and Holland) would be flooded. An important change of the precipitation pattern would cause

mountain slopes which are in a precarious equilibrium to slip down and to bury cities and villages that are placed at their feet. An increase of the number and intensity of hailstorms and windstorms would endanger crops and properties like buildings and vehicles.

1 Introduction

1.1 Climate and climate system

The word *climate* is derived from a Greek word meaning *to incline* and the original zones of climate were zones in which the inclination of the sun's rays at noon was the same, that is, zones of latitude. The accumulation of meteorological data has shown that winds and rainfall, as well as temperature, have a zonal arrangement, but that the true climatic zones do not run strictly parallel to lines of latitude. Eight principal zones are distinguished: near the equator a zone of tropical rain climate, then two subtropical zones of *steppe* and *desert* climate, then two zones of temperate rain climate, then, in the northern hemisphere only, an incomplete zone of *boreal* climate with a great annual range of temperature and finally, two polar caps of snow climate (Meteorological Glossary, 1991).

It is impossible to define climate in a unique, clear and generally valid way. Many definitions have been suggested in the past, leading to a real history of climate definitions (see Schönwiese 1994). Some definitions are mentioned below.

WMO (1979): climate is the synthesis of weather over a time interval which is long enough to enable the definition of statistical ensemble characteristics (averages, variances, probabilities of extreme events, etc.) and which is independent from any momentary state.

Houghton (1984): it is generally recognised that climate is in some sense the average of weather, its fluctuations, and its influence on the surface of the earth. The main problem in the definition of climate is to make this intuitive idea sufficiently precise to serve as a basis for a theory of climate.

Hantel, Kraus and Schönwiese (1987): climate is the statistical behaviour of the atmosphere, which is characteristic for a relatively large time scale.

Meteorological Glossary (1991): the climate of a locality is the synthesis of the day-to-day values of the meteorological elements that affect the locality. Synthesis here implies more than simple averaging. Various methods are used to represent climate, e.g. both average and extreme values, frequencies of values within stated ranges, frequencies of weather types with associated values of

elements. The main climatic elements are precipitation, humidity, sunshine, wind velocity, and such phenomena as fog, frost, thunder, gale; cloudiness, grass minimum temperature, and soil temperature at various depths may also be included. Climatic data are usually expressed in terms of an individual calendar month or season and are determined over a period (usually about 30 years) long enough to ensure that representative values for the month or season are obtained. The climate of a locality is mainly governed by the factors of:

i) latitude,
ii) position relative to continents and oceans,
iii) position relative to large-scale atmospheric circulation patterns,
iv) altitude,
v) local geographical features

A broad classification is made into *continental climate* and *maritime climate.*

These definitions consider climate only in the sense of a mean state

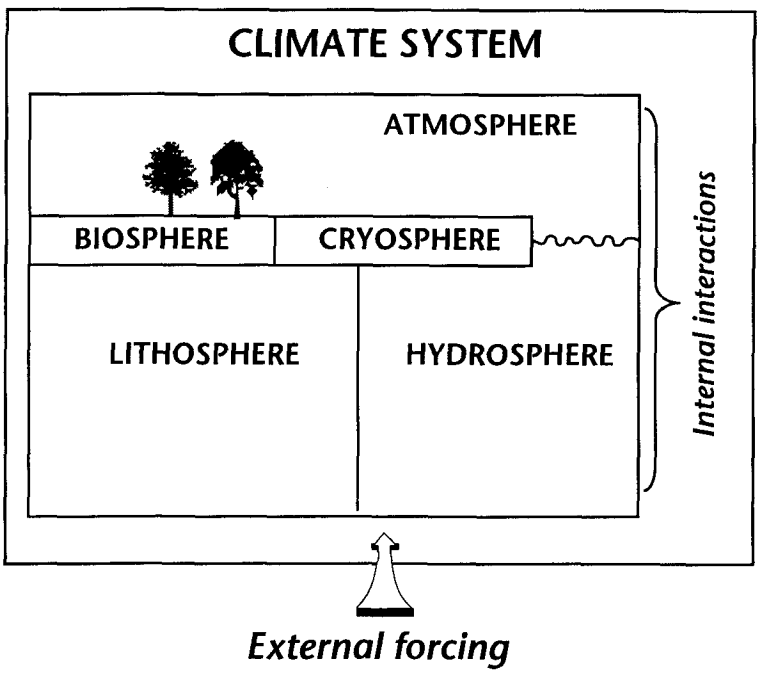

Figure 1.1.1 Schematic overview on the climate system (translated fromSchönwiese 1994).

of the atmosphere, but the atmosphere is not an isolated system, it is connected with all other systems of the earth. Therefore, it is more appropriate to talk about the *climate system*. Schönwiese (1979) defines it as the consequence of the interaction between the *atmosphere*, the *lithosphere*, the *hydrosphere*, the *cryosphere* and the *biosphere* of the earth. Flohn (1989) also talks about a climate system, whose subsystems are mutually connected, often in a non-linear way, and which have different characteristical time and space scales. Besides the interaction between the different earth systems, other external factors also influence the evolution of climate. These are, for example, solar variability, earth-orbital changes, volcanic eruptions and various human influences on the environment, and are also called external forcing mechanisms (Mitchell 1976). Figure 1.1.1 summarises all these phenomena.

1.2 Causes of climate change

The expression *climate change* is very general. It just expresses some kind of change with respect to an earlier situation. But climate can change in different ways, with different consequences on life on earth. A change of mean values of parameters like temperature and precipitation, without any change in variability, could cause a shift of the climatic regions and a spreading or retreat of ice cover. A change in variability (standard deviation) at constant mean values might leave the climatic regions unchanged but at the same time cause extreme events which make some areas much more dangerous to live in. Obviously, the contemporary occurrence of changes of mean values and variability cannot be excluded neither, in which case a prediction of the consequences is even more difficult.

Most of the studies on climate change carried out up to the present concern changes of mean values, probably because such changes are easier to be simulated with models. But as a variation in the occurrence of extreme events can also cause important changes to human activities, the interactions between the climate system and extreme events have also to be considered in climate research.

The climate system is a dynamical system in continuous evolution. Schönwiese (1979) compared the climate system to a huge machine. This machine is composed of many gearwheels, corresponding to the different phenomena of the climate system, and these gearwheels are all linked by connecting rods, which represent the physical laws governing the system. It is mainly driven by solar

energy. The output of the machine depends on the connections between the gearwheels and consists of a great number of effects of very different characteristical times and spatial dimensions. One major problem of this climate machine is that the position of many connecting rods is unknown or only partially known and therefore the output cannot be completely described.

The example of the climate machine shows how no single process will be found adequate to account for all the variability that is observed on any given time scale of variation. Mitchell (1976). groups all potential sources of climatic variability in three categories: *internal stochastic* mechanisms, *external forcing* mechanisms and some form of resonance between internal modes of climatic system behaviour and external forcing of a repetitive or cyclical character.

The following phenomena act as external forcing mechanisms on the climate system:

Variations in radiative balance (radiative forcing). In a climate system in equilibrium the absorbed solar energy is exactly balanced by radiation emitted to space by the earth and atmosphere. Any factor that is able to perturb this balance , and thus potentially alter the climate, is called a radiative forcing agent.

Variations of the earth's orbit parameters (Milankovitch and modified Milankovitch theory). This theory attributes the onset of an ice age to a variation of some elements of the earth's orbit and rotation (Hutter et al. 1990).

Sea floor-spreading and continental drift. This geologic phenomenon causes a continuous change of the earth's surface shape (mountain chains, distribution of the oceans, etc.) (Press and Siever 1986) and thereby exerts an influence over the global climate. A different distribution of the continents than the one we observe today can be connected with a different atmospheric and oceanic circulation (Ruddiman and Kutzbach 1991). Also *volcanic activity*, which can have a (rather short-term) influence on climate (Dutton and Christy 1992; Böhme 1993), is connected with the continental drift.

Anthropogenic forcing. The emission of greenhouse gases into the atmosphere seems to be the strongest forcing mechanism caused by mankind. The increased concentration of these gases (mainly CO_2 and CH_4) inhibits the radiative emission of

infrared radiation from the earth's surface into space, causing a stronger warming of the atmosphere.

The internal interaction mechanisms of the climate system are very numerous and a complete description would go beyond the aim of this work. We will just mention two phenomena which have caught the attention of many climatologists in the nearer past.

El Niño / Southern Oscillation (ENSO). The single most prominent signal in year to year climate variability is the Southern Oscillation, which is associated with fluctuations in atmospheric pressure at sea level in the tropics, monsoon rainfall, and wintertime circulation over North America and other parts of the extratropics. Although meteorologists have known about the Southern Oscillation for more than a half century, its relation to the oceanic El Niño phenomenon was not recognised until the late 1960's, and a theoretical understanding of these relations has begun to emerge only during the last few years. The El Niño phenomenon causes an anomalously high sea surface temperature in the tropical and the southern subtropical eastern Pacific. The primary manifestation of the Southern Oscillation is a seesaw in atmospheric pressure at sea level between the Southeast Pacific subtropical high and the region of low pressure stretching across the Indian Ocean from Africa to northern Australia (Rasmusson and Wallace 1983).

North Atlantic Oscillation (NAO). It is defined as the meridional pressure gradient (zonal index) between Ponta Delgada (Azores) and Stykkisholmur (Island) (Houghton et al. 1990; Schönwiese 1994). This pressure gradient was found to have weakened between 1900 and 1960, while it is following an increasing tendency since then.

Some climatic theories base on the assumption that, given the physical properties of the atmosphere and of the underlying ocean and land, specified environmental parameters (e.g. solar heating) determine a unique climate and that climatic changes therefore result from changes in the environment. Lorenz (1968, 1976) considers the possibility that no such unique climate exists and that nondeterministic factors are wholly or partly responsible for long period fluctuations of the climate system . In this context he defines three kinds of system:

the *transitive system,* whose statistics taken over infinite time intervals are uniquely determined by the governing laws and

the environmental conditions (i.e. a system for which only one climate is physically possible).

the *intransitive system*, which has the property that there are two or more distinct sets of statistics, any one of which could constitute the climate of the system without violating any physical laws. The particular climate that prevails then depends upon the conditions which happened to exist when the system first became established.

the *almost intransitive system*, for which two particular time-dependent solutions may appear to have considerably different sets of statistics if the solutions are extended over only a moderate time span, i.e., the system may appear to be intransitive. However, when the time span is made sufficiently long, the solutions will be found to have similar statistics. This means also that a single solution will exhibit different statistical properties within different segments of a long time span.

Lorenz suggests that the earth's climate system is the most likely to be an almost intransitive system and says that almost intransitivity might favour persistence throughout a season, but not from one year to another.

1.3 Analysis and forecast of climate change

Climate on a global scale can be studied by means of deterministic models or with statistical methods.

Deterministic models are used to study physical and physico-chemical processes of today's climate or to simulate the climate in a past or future state. The most important kind of models used for climate simulations are the general circulation models (GCM's), which are three dimensional models of the atmospheric (or oceanic) circulation. The atmospheric GCM's have the same structure as the models used for weather prediction: both are based on the so-called primitive equations (the basic equations that govern the time evolution of the large-scale atmospheric motion field). While weather predictions are made only with the help of atmospheric circulation models, climate studies and predictions are nowadays made with coupled atmosphere-ocean circulation models. Such coupled circulation models have the following advantages:

they give a three dimensional insight into the physical and physico-chemical processes of the climate system.

they consider linking-up features and non-linearities, including feedback's.

additionally to the temperature field they supply also information on the wind field, on precipitation and on cloud cover.

However, there are also some serious shortcomings connected with these models:

their description of the hydrological cycle is insufficient. This causes important uncertainties in the information on cloud cover and precipitation.

some problems with the simulation of the sea ice-cover are not yet solved.

the biosphere is not considered in these models.

their resolution is still to broad to allow simulations of regional climates.

they require powerful computers and very large amounts of computer time.

Climate can also be studied with the help of *statistical methods*. *Statistical models*, for example multiple regressions, are based on measurements or records derived from some kind of observation. Among their main advantages we mention the following ones:

they do not need much computer time.

they are strictly based on records.

additionally to the state and trends of past climates, they can also simulate (transient) fluctuations.

they enable extrapolations into the future and comparisons with the results obtained with deterministic models.

Important disadvantages:

they do not base on physical and physico-chemical principles.

long time series of data are needed in order to obtain meaningful results.

The results obtained with deterministic models are not representative on a regional scale (smaller than ~ 1'000 km); on the other hand, statistical models usually are not available on a global scale because of the lack of complete data sets. Therefore, regional climate scenarios can only be defined with the help of high

resolution-measurements or with regional climate models. Several techniques have been developed to link (*scale down*) global predictions with regional ones. These techniques can be classified in four groups: empirical, semi-empirical, statistic-dynamical and dynamical methods.

The *empirical method* infers future climatic scenarios from past ones. These past scenarios can be paleoclimatological scenarios (a few thousand to a few million of years ago) reconstructed with the help of paleo-environmental records or neo-climatological scenarios (up to about 200 years ago) defined with direct measurements.

The *semi-empirical* method is based on results of global climate simulations as well as on high resolution-measurements. The most simple way of combining simulations with measurements is to add the differences between the scenario and the control run to the measured values of the single stations.

The *statistical-dynamical* method defines a statistical link between global and regional model simulations. An example of this method is described in Frey - Buness (1993), where multi-annual global climate simulations are used to define large scale weather classes. In the following step, to determine the typical regional climate induced by complex orography and small scale surface characteristics, model simulations with a three dimensional mesoscale model for each weather class are performed.

The *dynamical method* embeds a regional high resolution model into a general circulation model. This method is particularly useful for areas with complex orography.

1.4 Past climate change

Climate varies naturally on all time scales from hundreds of millions of years to a few years. Prominent in recent earth's history have been the 100'000 year Pleistocene glacial-interglacial cycles when climate was mostly cooler than at present. There is growing evidence that the last period in which temperatures (particularly summer temperatures) were higher than at present is the mid-Holocene (especially 5'000 - 6'000 BP) . However, as the present work is not dealing with paleoclimatological data, we will not go further into detail on this subject.

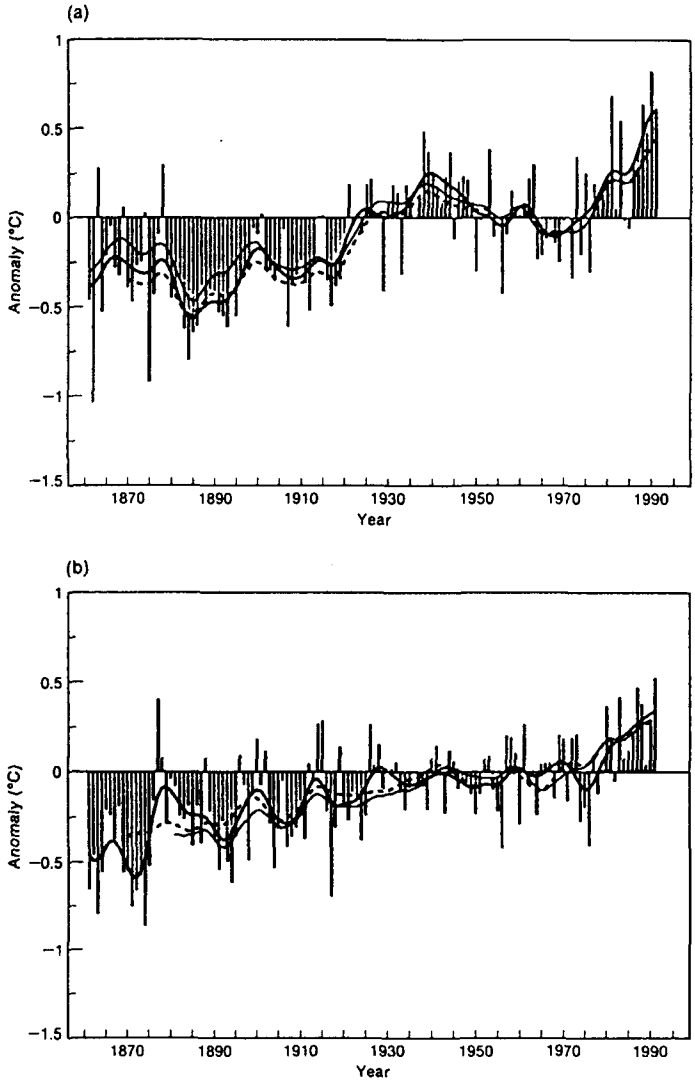

Figure 1.4.1 *Land air temperature anomalies, relative to 1951 - 1980.* Annual values from (Jones 1988), updated); thick solid line: Jones (1988, updated) (1861 - 1991); dashed line: (Hansen and Lebedeff 1988),updated) (1870 - 1991); thin solid line (Vinnikov et al. 1990),updated) (1861 - 1990 NH and 1881 - 1990 SH). **(a)** Northern hemisphere, **(b)** Southern hemisphere. (from Houghton 1992)

Although the era of instrumental measurements has begun in 17th century, useful climatological records are available only since the end of the 18th century.

The instrumental record of surface temperatures over the land and oceans remains sparse until after the middle of the 19th century. The record suggests a global (combined land and ocean) average warming of 0.45 ± 0.15 °C since the late 19th century, with an estimated small (less than 0.05 °C) exaggeration due to urbanisation in the land component.

The greater part of the global temperature increase was measured prior to the mid-1940s. A marked retreat of mountain glaciers in all parts of the world since the end of the 19th century provides further evidence of warming .The temperature record of the last 100 years shows significant differences in behaviour between the Northern and the Southern hemispheres, as can be seen in Figures 1.4.1 a) and 1.4.1 b) (taken from (Houghton et al. 1992)).

The temperature time series shown in Figure 1.4.1 are given by values averaged over whole hemispheres. In reality, on a regional scale the situation can look very different. This is illustrated in Figure 1.4.2, where isolines of the linear trends calculated for the summer land air temperature between 1891 and 1990 are drawn for the European continent (from Schönwiese et al. 1993).

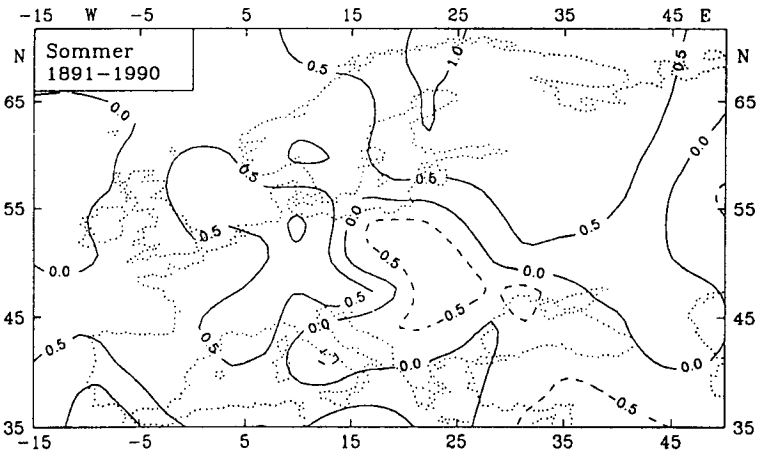

Figure 1.4.2 Linear trends 1891 - 1990 in K of the land air temperature in summer over Europe (Schönwiese et al. 1993).

1.5 The IPCC and the NFP31

Great theoretical and experimental efforts have been made to study the climate system and to determine the reasons of climatic variability and change. In spite of this, the understanding of the climate system is not yet complete enough for reliable predictions of the future evolution, so that a lot of additional work still has to be done. The scientific community concerned with the anthropogenic greenhouse enhancing is growing steadily, causing increasing communication and coordination problems. In order to rationalise the research efforts and to avoid unnecessary doubling of the work as much as possible, the *Intergovernmental Panel on Climate Change* (IPCC) was created.

The IPCC was jointly established by the World Meteorological Organization (WMO) and the United Nations Environment Programme (UNEP) in 1988. The Panel established three working groups to:

I) assess available scientific information on climate change

II) assess environmental and socio-economic impacts of climate change

III) formulate response strategies

In the present study we will refer mainly to the findings of Working Group I, which are gathered together in the final report (Houghton et al. 1990), and completed by a supplementary report (Houghton et al. 1992). The first three points of the judgement written in the executive summary of Working Group I look as follows:

> Global-mean surface air temperature has increased by 0.3 °C to 0.6 °C over the last 100 years, with the five global-average warmest years being in the 1980's. Over the same period global sea level has increased by 10-20 cm. These increases have not been smooth with time, nor uniform over the globe.
>
> The size of this warming is broadly consistent with predictions of climate models, but it is also of the same magnitude as natural climate variability. Thus the observed increase could be largely due to this natural variability; alternatively this variability and other human factors could have offset a still larger human-induced greenhouse warming. The unequivocal detection of the enhanced greenhouse effect from observations is not likely for a decade or more.

> There is no firm evidence that climate has become more variable over the last few decades. However, with an increase in the mean temperature, episodes of high temperatures will most likely become more frequent in the future, and cold episodes less frequent.

Furthermore, the IPCC states that it is relatively easy to determine the direct effect of the increased radiative forcing due to the increases in greenhouse gases. However, as climate begins to warm, various processes act to amplify (through positive feedbacks) or to reduce (through negative feedbacks) the warming. The main feedbacks which have been identified are due to changes in water vapour, sea-ice, clouds and oceans. The best available tools which take these feedbacks into account (but do not include greenhouse gas feedbacks) are three dimensional models of the climate system (atmosphere-ocean-ice-land), known as General Circulation Models (GCMs). However, in their current state of development, the description of many of the processes involved are comparatively crude.

For the prediction of the future climate evolution, the IPCC defines four scenarios depending on the future anthropogenic emissions. These scenarios are defined as follows:

> Scenario **A**: Business as usual. The energy supply is coal intensive and on the demand side only modest efficiency increases are achieved. Carbon monoxide controls are modest, deforestation continues until the tropical forests are depleted and agricultural emissions of methane and nitrous oxide are uncontrolled. For CFCs the Montreal Protocol is implemented albeit with only partial participation.
>
> Scenario **B**: The energy supply mix shifts toward lower carbon fuels. Large efficiency increases are achieved. Carbon monoxide controls are stringent, deforestation is reversed and the Montreal Protocol implemented with full participation.
>
> Scenario **C**: A shift toward renewable and nuclear energy takes place in the second half of the next century. CFCs are now phased out and agricultural emissions limited.
>
> Scenario **D**: A shift to renewables and nuclear in the first half of the next century reduces the emissions of carbon dioxide, initially more or less stabilising emissions in the industrialised countries.

The present study was carried out within the scope of the *National Research Foundation-Programme n. 31* (NFP31). The aim of this programme is to coordinate a number of 40 research groups working on the general subject *Climate changes and natural hazards.* In order to assure a certain internal and international comparability of the results obtained by these research groups, the NFP31 has suggested to base all forecasts of the future climatic evolution on two internationally defined scenarios: the IPCC-scenarios A and C. Starting from these two scenarios (which are defined for the whole Southern-European area) climatological scenarios for the Alpine regions have been established in the context of investigations carried out by the EPOCH / FUTURALP Project and by reinsurance companies. The temperature and precipitation forecasts obtained in connection with the scenarios mentioned above for the Swiss Mittelland are summarised in Table 1.2.1 (all changes are given for the time span between ~ 1800 and 2030, respectively 2100; the values for 2100 are the result of a linear extrapolation from the model results obtained until 2030). We were given these scenarios without any indication of the uncertainties (see NFP31, Info 6, December 1994).

Scenario	Temperature (°C)				Precipitation (%)			
	Winter		Summer		Winter		Summer	
	2030	2100	2030	2100	2030	2100	2030	2100
A	+ 1.9	+ 3.9	+ 2.7	+ 4.9	+ 5	+ 10	- 12.5	- 15
C	+ 1.5	+ 2.2	+ 2.3	+ 3.2	0	+ 5	- 7.5	- 12.5

Table 1.2.1 Scenarios suggested by the NFP31 (Changes between ~1800 and 2030, respectively 2100).

The IPCC statements mentioned up to now and the description of the subset of scenarios suggested by the NFP31 are very general. Does the IPCC also state some findings that regard mesoscale phenomena like mid-latitude storms and thunderstorms? One rather general statement can be found in the executive summary: Mid-latitude storms, such as those which track across the North Atlantic and North Pacific, are driven by the equator-to-pole temperature contrast. As this contrast will probably be weakened in a warmer world (at least in the Northern Hemisphere), it might be argued that mid-latitude storms will also weaken or change their tracks, and there is some indication of a general reduction in day-

to-day variability in the mid-latitude storm tracks in winter in model simulations, though the pattern of changes varies from model to model. Present models do not resolve smaller scale disturbances, so it will not be possible to assess changes in storminess until results from higher resolution models become available in the next few years. In fact, neither models with resolutions of 300 - 1'000 km nor current numerical weather prediction models simulate individual thunderstorms, which are controlled by mesoscale dynamical processes. However, they do simulate variables that are related to the probability and intensity of severe weather such as thunderstorms, hail, wind gusts and tornadoes. If the appropriate variables are saved from a climate model, it should therefore be possible to determine whether the frequency and intensity of severe convective storms will change in an altered climate.

These are the only statements of the report that deal directly with thunderstorms. The method suggested in the last statement is not put into practice in any of the described works. This means that, unless we find some very recent publication on the variation of thunderstorm frequency with climate change, we will not be able to compare the results of our work with other studies.

To the best of our knowledge, up to the present days no investigation has been published which make a precise forecast of the evolution of the future thunderstorm frequency and intensity. Some publications can be found on the connection between climate change and hurricanes (Shapiro 1982; Shapiro 1982; Emanuel 1987; Idso et al. 1990), probably also because the economic interest in a prediction of the future hurricane activity is larger than the one of thunderstorm activity. However, the results of the described investigations are sometimes diverging and no common statement on the future evolution can be found.

1.6 Thunderstorm theory

The understanding of the climatological evolution of thunderstorm frequency and intensity is only possible if the morphology and dynamics of thunderstorms are known. On the other hand, there are enough books and publications which describe the basics and the details of thunderstorm science as to justify the following reduced summary. In this section we limit the description of this atmospheric phenomenon to the essential features and to the definition of atmospheric parameters used in

the following chapters of this work. For further details the reader is referred to reviews on thunderstorm and hail science and to specialised books (e.g. Foote and Knight 1977; Kessler 1986; Houze 1993), from which a large part of this summary was also taken.

Local ascent of warm buoyant air parcels in a conditionally unstable environment produces convective clouds which can develop into thunderstorms. Convective clouds are also called with the Latin name *cumulus* (*cumulus humilis*, *cumulus congestus* and *cumulonimbus*, in increasing order of development), meaning heap or pile. Most of the cumulonimbus clouds, particularly at mid-latitudes, contain ice which in certain favourable conditions can reach the ground in form of graupel or hail.

The dynamical building block of a thunderstorm is the *cell*. A cell is a compact region of relatively strong vertical air motion (up to 30 m/s). The usual way of identifying the overall extent of cells is by visual observations of cumuliform turrets during early stages of their evolution before the development of precipitation and, thereafter, by RADAR observations of the associated volume of precipitation. Cells defined visually and by RADAR are not always co-located, and it is often necessary to make clear which is being referred to. The majority of convective storms, and indeed many of those that produce hail, are composed of ordinary cells. Ordinary cells are short-lived units of convection and most storms at any given time consist of a succession of them at different stages of evolution. Byers and Braham (1949) identified three stages in the evolution of an ordinary cell: the cumulus stage (with updraft alone), the mature stage (with updraft and downdraft together), and the dissipating stage (with downdraft alone). The mature stage lasts only 15 to 30 min.

The *single cell thunderstorm* may actually be the most common type of thunderstorm, but its significance in terms of precipitation or storm damage (other than lightning) is relatively small. The single cell of cumulonimbus takes on more importance when it serves as a building block of a larger *multicell thunderstorm*. Such a storm ordinarily consists of a pattern of cells in various stages of development: while some of the cells consist only of a vigorous updraft in which hydrometeors are growing rapidly, other ones have reached the mature stage or are even already decaying and consist only of a gradually weakening downdraft. Thus, the pattern of cells within the multicell thunderstorm is continually changing and the lifetime of the overall aggregate of cells can exceed considerably that of an individual cell (order of magnitude of hours). In some multicell thunderstorms the cells group in clusters,

in other cases they are aligned perpendicularly to the storm motion.

Another basic type of cumulonimbus structure is the *supercell thunderstorm*, which is far rarer and much more violent. Supercell thunderstorms are notorious for producing damaging hail and tornadoes. The name supercell refers to the fact that, although this type of storm is about the same size as a multicell thunderstorm, its cloud structure, air motions, and precipitation processes are dominated by a single storm-scale circulation consisting of one giant updraft - downdraft pair. Supercell thunderstorms can reach lifetimes of more than one hour to several hours.

The best way to define the type of a thunderstorm is to measure it by RADAR. Hail damage left by a hailstorm at the ground can give an idea of the storm motion and of the extent of the whole storm, but it does not reveal anything about the structure of the system. Therefore, occasionally it can happen that two or more RADAR cells are interpreted as one single cell at the ground. For this reason we will not be able to complete the hailstorm climatology composed in this study with details concerning the structure of the damaging storms.

The diameter of a thunderstorm cell ranges from one (in the case of a small single cell) to ten or more kilometres (supercell). In the vertical, thunderstorms often reach the tropopause (between 10 and 16 km), occasionally they even penetrate into the stratosphere. The updraft velocities usually exceed 10 m/s, while the horizontal displacement of the cell can attain velocities of 25 m/s.

The severity of a thunderstorm can be described by its dynamical intensity, which can be expressed in terms of the strength and lateral dimensions of the vertical drafts. Related to these criteria are other factors, such as the maximum height of the updraft, the strength of the surface winds, and to some extent, the maximum hail size. Surface rainfall is not always well correlated with dynamical intensity, nor is lightning frequency. Large hail is often produced by big cells (mostly supercells) which reach a long lasting steadiness. This means that they propagate continuously and at a uniform velocity with only minor fluctuations in dimensions and intensity over periods long compared with the time taken for air to pass through them. This steadiness promotes a dynamically efficient circulation which enables the hailstones to remain for a longer time in that area of the upper thundercloud where further ice deposition causes their growth.

Severe thunderstorms are favoured by:

- strong convective instability (resulting from cold air aloft and air with high wet-bulb potential temperature θ_w at low levels)
- abundant moisture at low levels,
- strong wind shear, usually veering considerably with height,
- a dynamical lifting mechanism that can release the instability.

The buoyant instability of the environment can be represented by the *convective available potential energy* (CAPE), which is given by

$$CAPE = g \int \frac{\Theta(z) - \overline{\Theta}(z)}{\overline{\Theta}(z)} \, dz$$

where the dimensions of CAPE are J kg^{-1} and the constant g is the gravitational acceleration (9.81 m / s^2). $\Theta(z)$ defines the moist adiabatic ascent of a representative surface parcel and the integral is taken over the vertical interval where the lifted parcel is warmer than its environment (positive area on a Skew T - log p diagram). $\overline{\Theta}(z)$ is the potential temperature of the environment (Weisman and Klemp 1982). Thermal buoyancy (i.e. high CAPE) is a primary contributor to strong updraft, which in turn is a necessary ingredient for the development of large hail (Johns and Doswell III 1992).

The condensation level necessary for the computation of the CAPE is calculated in different ways, depending on how the air parcel is brought to condensation. If the convection is triggered thermally (which leads to what we call airmass thunderstorms) the condensation level is called *convective condensation level* (CCL). In this case it is assumed that a well-mixed boundary layer will become the subcloud layer. Therefore the mean water-vapour mixing ratio which will be reached by the well-mixed layer has to be estimated. Often this is done by finding the mean mixing ratio in the lowest perhaps 500 or 1'000 m (50 or 100 hPa) of the morning radiosonde moisture profile. That mean mixing ratio is equal to the saturation mixing ratio at some level on the temperature profile, and this level is the CCL (Banta 1990).

If the vertical displacement is caused by dynamically forced lifting, e.g. by the passage of a cold front, saturation will be reached at the *lifting condensation level* (LCL). During lifting the mixing ratio w of the air and its potential temperature remain constant, but the saturation mixing ratio w_s decreases until it becomes equal to w at

the LCL. Therefore, the lifting condensation level is located at the intersection of the potential temperature line passing through the temperature T and the pressure p of the parcel of air, and the w_s line which passes through the pressure p and the dew point T_d of the air parcel (Wallace and Hobbs 1977).

The (density weighted) vertical shear of the mean horizontal wind is given in m / s and can be expressed as follows:

$$S = \frac{\int_0^{6\text{km}} \rho(z) \cdot |v(z)| \cdot dz}{\int_0^{6\text{km}} \rho(z) \cdot dz} - \frac{1}{2} |v(0) + v(0.5\ \text{km})|$$

where $v(z)$ is the wind velocity at level z. The choice of the integral limits (0 to 6 km) is based on the work by (Weisman and Klemp 1982), who found that, for their experiments, the storm motion in the direction of the shear was most comparable to a mean taken over the lowest 6 km of the shear profile. The wind shear used in the analysis of chapter 6 was computed in this way.

Figure 1.6.1 shows typical wind hodographs characterising the environment of three different kinds of storms, as derived by Chisholm and Renick (1972) on the basis of their experience in Alberta. The weak sheared hodograph (a) is associated with short-lived thunderstorms consisting of a single ordinary cell. It is also probably representative of poorly organised multicell storms that do not become intense. The two strong-shear hodographs (b and c) are both characteristic of severe hail-producing thunderstorms, hodograph b representing well-organised multicell storms and hodograph c representing the more nearly steady-state supercells. The most significant differences in the wind profile associated with supercell and multicell storms seem to be in the strength of the subcloud winds and the amount of veering with height, especially at low levels (Browning 1986).

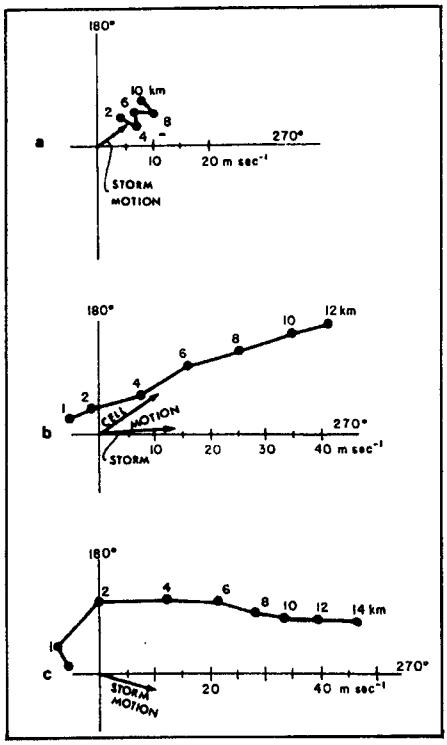

Figure 1.6.1 Typical wind hodographs representing environmental conditions accompanying different classes of Alberta hailstorms. Hodographs are representative of **(a)** ordinary single-cell storms producing very little hail, **(b)** well-organised multicell hailstorms, and **(c)** supercell storms (Chisholm and Renick 1972)

Hailstones

Hailstones are lumps of ice or ice and water, with air inclusions and diameters > 5 mm. Partially or completely opaque, they exhibit mostly layered, shell-like arrangement of air bubbles. Shapes are usually roughly spherical, conical, ellipsoidal or irregular with small or large protuberances. The density of hailstones is mostly between 850 and 917 kg/m^3, but somewhat less when there are large interior air cavities.

Hail formation generally takes place in a cloud of supercooled water droplets that originated from condensation on cloud condensation nuclei (CCN). Ice requires not only a temperature below 0 °C but also a catalyst to trigger the phase transition. Hailstones grow by

accretion of supercooled water droplets or drops, starting mainly from small ice particles. Sometimes frozen drops may be recognisable as embryos. Small hail is a transitory stage that, after densification of the original graupel is completed, automatically leads to a resumption of the volumetric growth. The growth of the various hailstone layers may be described as *dry* or *wet* depending on whether or not all of the accreted supercooled droplets can be frozen by the forced ventilation processes of heat conduction and evaporation from the hailstone surface. The nature of the ice deposited depends on the particular regime in which the layer was formed. In the wet growth regime, it is usual for the excess unfrozen water to be incorporated in the ice structure to form a *spongy* hail (Macklin 1977). The major growth stages of hail are summarised in Figure 1.3.2 (List 1986).

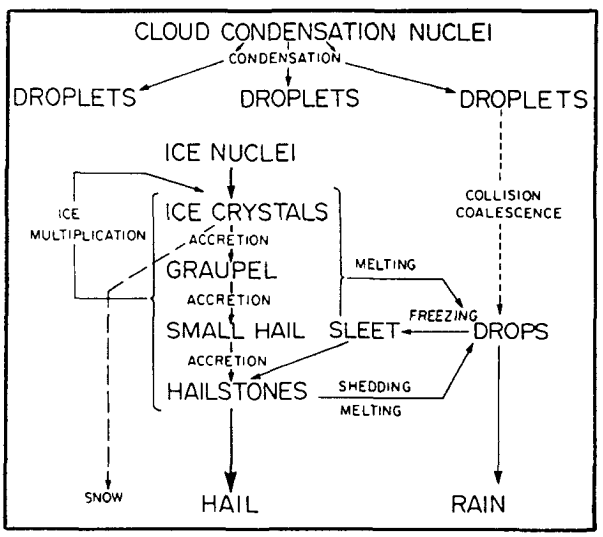

Figure 1.6.2 Major growth stages of hail in a cloud of supercooled droplets (List 1986).

The question of what is truly the largest hailstone ever to fall remains unanswered. Approaching credibility is the hailstone that fell in 1925 in Germany and was reported to have measured 26 x 14 x 12 cm. Its weight was estimated from its dimensions as 2.04 kg. In the USA the largest hailstone ever recorded fell in 1970 in Coffeyville (Kansas). It weighed 766 g and had a circumference of 44 cm (Morgan and Summers 1986).

1.7 Earlier studies based on damage claims

Meteorological and climatological studies based on damage records of hail insurance companies are not very numerous. Hail damage records are not direct meteorological measurements, their meteorological meaning has to be found on an indirect way which depends on the structure of the damage claims and on the additional data available (e.g. radiosoundings, weather maps, etc.). The studies described in the following of this section serve as an introduction to the discussion of the usefulness of insurance data to climatological studies.

Changnon and Stout (1967) derive empirical measures of hail intensity from crop-insurance data for 19 major grain producing states in the central and north-western United States. The insurance data represent approximately 75 % of all crop-hail insurance cover in the United States and were recorded during the time period between 1957 and 1964. The analysis is limited to wheat and corn crops and nothing is said about the absolute insurance cover. In each state and for each month a *median storm day loss cost value* was determined for either corn or wheat or both, and these were defined as intensity indices.

The time span covered by the data is too short as to enable climatological evaluations. Furthermore, the derived intensity indices are strongly influenced by the regional and temporal variation of the crop susceptibility (the analysed area includes different climatological regions and has a large latitudinal extension). This causes some difficulties in the comparison of the results. In spite of these problems, they find that in general, the regional comparison of the maximum monthly wheat indices suggests that, on the average, the hailstorms in the more mountainous states are much more intense at a point than those in the central plains and in the Northwest. A comparison between hail-day frequencies and hail intensity indices shows that the average hail-day values explain 79 % of the variation in the hail intensity (i.e. areas with more frequent hailstorms often experience also more intense hailstorms).

A second paper by Changnon and Changnon (1992) treats the more general topic of storm catastrophes in the United States. As in the previous study, the analysis is based on the amount of insured losses (adjusted to 1991 economic and insurance exposure conditions) available from statistical records of the insurance industry between 1950 and 1989. The analysis focused on their temporal fluctuations (on a regional and national basis). The

catastrophic storms were subdivided in four classes: hurricanes, winter storms, thunderstorm-related conditions (tornadoes, heavy rains, lightning, winds and hail) and windstorms. Much of the temporal analysis of the storms was done using values for eight pentads, those from 1950-54 through 1985-89, rather than annual values.

The distributions of all four storm types were generally similar in that they were all relatively high in the 1950's, high in the 80's, and had minimum's in 1970-74. Fluctuations found in the thunderstorm catastrophes, when analysed on a regional basis, revealed considerable inter-regional similarity during most pentads. The 1980's peak in thunderstorm induced catastrophes was not present in the amount of thunderstorm caused-losses, indicating that a relatively large number of storms occurred in these years but they were of lesser intensity than in prior years. The time distributions of these storms across the continental United States agreed well with the temporal distribution of surface and 500 hPa level cyclone activity, suggesting that the magnitude of North American cyclone activity may be a useful index for estimating the frequency of catastrophic storms but not storm intensity or extent.

Another hailstorm study based on nine years (1979-'87) of crop-hail insurance data recorded in Saskatchewan, Canada, is written by Paul (1991). In Saskatchewan grain farming dominates, spring wheat is the most common crop and the vast majority of farmers purchase at least some hail insurance. The land is surveyed into townships that contain 36 numbered sections 1.6 km square, each of which in its turn is subdivided into four quarter sections. Because of the limitation of the cultures to a few kinds of grain crops the hail-damage season for crops is shorter than the hail season. The method employed for this study does not consider the dollar amount paid for the loss but just the fact that the damage has been reimbursed. This avoids conversions to eliminate errors given by the varying harvest values or by different culture densities within the test area. The paper focuses on the geographic extent of damaging hailfall and particularly on the lengths of the hailswaths on the most severe thunderstorm days.

76 examples of damaging hailswaths 150 km or more in length are known to have occurred during the 9 summers studied, and an average of two or three per year were longer than 250 km. Time indications from the insurance data set itself and from other meteorological observations enabled the estimation of the storm lifetimes, which were found to be of at least 3 hours. More than half

of the thunderstorms persisted for 5 hours and more, a few as long as 8 to 10 hours.

The results of our study presented in Chapter 5 (Figure 5.2.4) show that the lengths of the hail clusters found in the Swiss Mittelland are mostly smaller than those found by Paul in Saskatchewan. On the one hand this might be due to the different morphology of the terrain in the two test areas. Saskatchewan is a fairly extended flat country. Once a thunderstorm is triggered, its further existence is favoured by a regular moisture supply and its dynamics is not disturbed by mountain induced changes of the environmental flow. On the other hand, our test area is rather small and, in case of storms entering or leaving the test area, we have no information on the remaining part of the tracks.

The most recent work on the subject of hailstorm climatology and insurance data has been published in 1994 as an extended abstract for a WMO conference (Dessens 1994). With a 47 - year time series of hail losses and of minimum temperatures, Dessens finds a significant year - to - year correlation between warm nights and severe hail. The storm severity index is expressed by the dimensionless loss - to - risk ratio, which has been calculated with hail insurance data of all hail insurance companies of France in the form of annual values. The minimum temperature has been computed as a mean of all minimum temperatures between June and August of 9 stations scattered in the hailed areas. The minimum temperature has been chosen for this comparison because it is a rough estimation of the wet bulb potential temperature, Θ_w, in the lowest kilometre of the atmosphere for the following day, and this latter is a measure of the available potential energy. A high value of Θ_w is usually associated with a large potential energy, and therefore, high minimum temperatures should be connected with a higher hailstorm activity. In fact Dessens finds a correlation between minimum temperature and log(1 + R) of 0.491 (R is the storm severity index). The results obtained with this comparison are interesting but still too uncertain. Although it is stated that the same study has been repeated on a smaller scale, it is not clear if this has been done with more precise data.

The following summarising remarks can be made on the papers presented up to now:

most of the studies are based on loss costs rather than on the mere appearance of the damage. This makes the results more

dependent on economical factors which are only partly quantifiable, and on how the crops are planted.

none of the studies mentions a quality test of the employed insurance data.

most of the studies are carried out in areas where cultures are limited to a few species. This reduces the susceptibility to hail damage to a short period during the hail season. Furthermore, a large hailstorm causes a longer lasting reduction of the susceptibility in monoculture areas than in areas with a larger variety of cultures.

many studies concern a rather short time span (around ten years), which does not enable climatological statements.

To the best of our knowledge, the only climatological hailstorm study based on hail insurance data recorded in Switzerland was published by Bider (1954). He analysed the same data of the Schweizerische Hagel Versicherung (in the following abbreviated with SHV) employed in the present work, but for the years 1895 - 1950. However, his data set is given in the form of *number of claiming communities per Canton*, without any information of the geographical position of the single communities. Therefore, also the results have a broader resolution (between 200 and 7'000 km^2, depending on the area of the considered Canton), and are extended to the whole Swiss territory. For this reason these results cannot be directly compared with those obtained in our study.

Although he mentions the fact that such an analysis is meaningful only for areas with intense agricultural exploitation, he does not limit the data processing to some test area where this condition is satisfied. An overview of the number of haildays and of claiming communities per decade shows a big difference between the data before and those after 1920. Bider judged the data between 1921 and 1950 to be fairly homogeneous and decided to base all further analyses on this time period.

He found a mean annual number of haildays (i.e. days with at least one damage claim) of 78.7. Considering that hail mainly falls between May and September, this means that on approximately 50 % of the days during the hail season some communities were hit by hail. Almost all cases with a large number of claims were connected with frontal passages, while on haildays with a smaller amount of claims the weather conditions were mostly typical for local airmass hailstorms. The maximum frequency of the number of haildays was found in June and July, whereas the most extensive

storms were observed in July and August. The seasonal evolution of hailstorm frequency varies from region to region. The origin of the most hail favouring air is mainly maritime tropical.

The Hess-Brezowsky weather types HM (high pressure over central Europe) and HNZ (high pressure over the North Sea / Iceland, cyclonic flow) are often connected with hailstorms in the northern Prealps and in the alpine Cantons (the Hess-Brezowsky weather classification is described in Chapter 6, Table 6.1.2). HNZ is the weather class with the highest relative number of haildays. The situation WS (southern westerly flow) leads to a reduced hailstorm tendency on the northern side of the Alps but favours hailstorms in Ticino and in the alpine region.

Additionally to the comparison of the Hess-Brezowsky weather classification with haildays, Bider also carried out an evaluation of the main meteorological features observed during the day before and the day of a hailstorm. His main findings were that the pressure did not necessarily drop during the time preceding a hailstorm and that the dew point temperature almost always was higher than normal. At the time of Bider's analysis radiosoundings were not yet operational, so that all the discussed observations were made at the ground level.

1.8 Aim and overview of this study

The aim of this work is to investigate the climatological aspects of hailstorm occurrence and intensity and to find out if the detected climatic variation (mainly temperature change) of the last decades coincides with some change in hailstorm frequency or intensity.

Hailstorms (and thunderstorms) are complicated phenomena, which cannot be clearly described with one or two parameters like temperature or pressure, and it is very difficult to find a data set covering a long time span which describes the spatial distribution of hailstorms. Information on the frequency of occurrence of thunderstorms can be taken from the lightning observations, which have been collected since 1978 by the Swiss Meteorological Institute (SMA: Schweizerische Meteorologische Anstalt), but lightning does not give a direct information about the number of thunderstorm-cells and their size. The best way to determine the size of a thunderstorm is to measure it by RADAR, which can also give an information about the intensity of the storm. Unfortunately, meteorological RADAR measurements are made since a relatively

short time, specially those which are carried out on a regular time step. The SMA has been producing composit pictures of the RADAR echoes measured with two RADARs on the northern side of the Alps since 1983.

The longest continuously available data set on severe thunderstorms in Switzerland is given by the hail damage claims collected by the SHV, which enable a spatial analysis of hailstorm events since 1949. As not every thunderstorm produces hail which reaches the ground, a climatology based on these data is a hailstorm climatology, which is a subset of a thunderstorm climatology.

In Chapter 2 the hail insurance data are presented and their usefulness for climatological purposes is tested with agricultural and insurance statistics. Chapter 3 is dedicated to the description of the data processing and to the obtained data set. The definition of a test area (TA) and a test season guarantees the comparability of the annual number of hailstorms and of their extent (Sections 3.1 and 3.2). A short description of the cartographic representation of the damage claims (Section 3.3) and the definition of their temporal and spatial resolution (Section 3.4) complete the introduction to the method with which the data were processed to obtain the surfaces of the single hailswaths (Section 3.5). Potential damage surfaces are obtained joining the damage claims. From these surfaces only those with an elongated shape most probably connected with one or more hailcells and exceeding a length of 25 km are selected and called clusters. For every cluster its length, area and orientation is stored, together with other meteorological information concerning the observed day, in a data set which is described in Section 3.6.

In Chapter 4 we discuss the analysis of the damage data. In a first step we analyse the raw data, i.e. the damage claims, in relation to their temporal evolution (Section 4.1). A similar analysis is carried out in Section 4.2 with the cluster data (particularly with the annual number and area), together with an evaluation of the geographical distribution within the season and in time steps of five years.

In Chapter 5 the damage data are analysed in connection with climatological parameters like airflow and frontal activity, maximum and minimum temperatures at ground level, weather classifications and radio soundings. Searching for parameters which have a separating effect on hailstorm days with respect to fair weather days, all days considered for the analyses are divided in four classes. These classes are defined basing on the increasing

number of damage claims and on the detection of clusters (which points to the presence of larger organised thunderstorm cells).

The RADAR measurements mentioned previously in this section cannot be used to put together a longer hailstorm climatology but can nevertheless be used to calibrate the damage cluster-data. This is done in Chapter 6 with two kinds of comparison. In the first one the RADAR echoes of the first two highest reflectivity levels measured on two particular days are related to the hail damage-pattern detected at the ground (Section 6.3). In Section 6.4 the swaths of all RADAR cells between 1983 and 1993 satisfying a certain criterion are compared to the hail damage-swaths.

Chapter 7 concludes the work with a summarising discussion and some statements on the possible future evolution of hailstorms under consideration of the NFP31-scenarios (see Section 1.5). The outlook in Chapter 8 describes the work that could be done to complete or continue the project described in this dissertation.

2 The hail insurance data and their usefulness to hail climatology

2.1 The damage claims

In the description of the aim of this work (Section 1.8) we explained why we decided to base our hailstorm climatology on damage claims of the hail insurance company. As it is rather unusual to use insurance data for meteorological purposes it is appropriate to briefly describe this data set.

The damage claims are strictly limited to hail damage (without windstorms, floods or other natural hazards) caused to crops and the SHV is the only insurance company in whole Switzerland that insures cultivated land. Between 1876 and 1932 a second insurance company ensuring only grapevines existed in the Canton Neuchâtel, and in 1929 a third company was founded in the Canton Vaud, but it survived only until 1943. A few more details can be found in Appendix B.

Figure 2.1.1 was published in the *Hagel Kurier* nr. 129 (winter 1987/88, adapted by Schiesser 1988) and shows the SHV insurance participation in percent of the number of farms. It is probably based on data of 1976, as that is the last year for which such statistics were recorded.

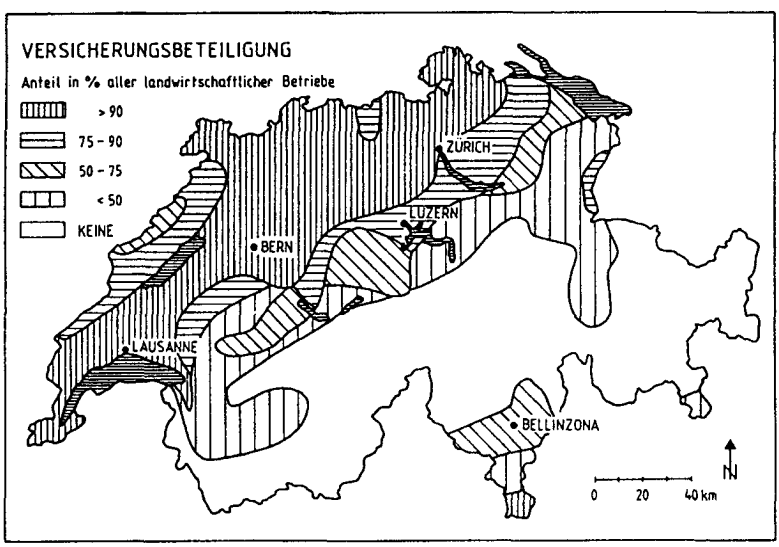

Figure 2.1.1 SHV insurance participation in percent of the number of farms.

The SHV supplied the damage claims collected since 1947, but the data of 1948 are not complete, so that a continuous climatology is possible since 1949. Therefore, the observation period (OP) is defined as the time span between 1949 and 1993.

The damage claims have a very simple structure. This is probably an advantage, as more detailed information might complicate unnecessarily the data processing without attaining a better quality of the results. For every Swiss community it is known on which days at least one hail-damage claim has been registered; the extent of the damage and its position in the community itself are unknown.

A reduced data set, indicating only the number of damage claims per day without any geographical information, was obtained from the annals of the SMI for the years between 1920 and 1947. A short evaluation of the resulting 74 year-time series will be shown in Chapter 5.

2.2 Adequacy of the hail damage claims for climatological applications

The adequacy of the hail damage claims used in this work for a climatological study has to be checked since these data were not collected for this purpose. The quality of these data depends on the variety of the cultures, on their homogeneous distribution over the test area and on the insurance participation in this area.

- In an area with a large *variety of crops* being hail-sensitive at different phases of the hail season the period of time in which damage claims can be recorded is longer than in an area with single-crop farming.
- A *homogeneous distribution* of every kind of culture over the whole test area is important to guarantee the same degree of hail-sensitivity everywhere, in order to be able to compare the hail damage in different parts of the test area.
- The *agricultural areas* should have stayed possibly *constant* during the observation period (OP) considered for the climatology.
- The *insurance participation* has to be *high* in the whole test area and *approximately constant* during the whole period considered for the climatology, otherwise the damaged areas would not be comparable in space and time.

The following sections of this chapter are dedicated to the verification of the conditions mentioned above.

It was decided that it would be more reasonable to first check whether the data can be used for the predetermined goal and then, with the help of the results found in this first step, define the method of data processing. For this reason the discussion of the test area (TA) and the test season (TS) follows in Chapter 3. However, as they are repeatedly mentioned already in the following sections, we define them in advance. The TS is defined as the time span between the 20th of May and the 10th of September (included) and the TA is illustrated in Figure 2.2.1.

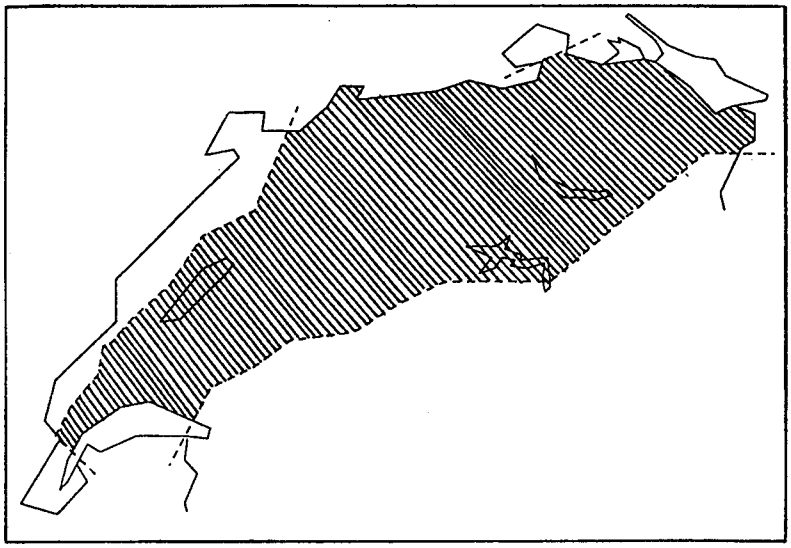

Figure 2.2.1 Test area of the present study (the reason of this choice is discussed in Chapter 4).

2.3 Distribution of crops in Switzerland

Switzerland covers a total area of 41'293 km^2, 28 % of which are exploited for agriculture, 21 % as pasture-land and 26 % for forestry (Bundesamt für Statistik 1990). For the TA the portion of agricultural productive land is much larger, because the alpine region, which does not include much productive land, is not included. The borders between the different areas are not sharply defined. 60 % of the agricultural land are meadows and 40 % (roughly 400'000 ha) are cultivated land (mainly arable land, cultivated grasslands and orchards). The following short analysis of the agricultural situation in

Switzerland will consider only the cultivated land, which is also the area pertinent for hail insurance.

Swiss agriculture has a big variety of cultures distributed in relatively little patches (the average size of a wheat field is of 1 - 3 ha, i.e.0.01 - 0.03 km^2) over the whole agricultural area which is mainly limited to the Mittelland (see map in Appendix C and Figure 3.1.2). This is the flattest part of Switzerland between the Alps and the Jura mountains. As can be seen from Figure 2.1.1, the Mittelland is also the area with the highest insurance participation. These facts are important for the choice of the TA, which will be described in Section 3.1.

Figures 2.3.1 and 2.3.2 show the distribution of the areas used as arable land and of those cultivated with grass. The arable land is generally well distributed over the Mittelland, while the grasslands show a higher density in the Canton Bern. As grasslands are not very hail-sensitive and only a small part of them is insured, their irregular distribution should not have a detectable influence on the homogeneity of the damage claims.

The distribution of the most widespread cultures in 1985 is illustrated in Appendix D. The most homogeneously distributed crops are cereals and maize, whereas the largest areas are covered by wheat and barley. The grapevine is the most unevenly distributed culture, as it almost only appears in the south-western and scarcely

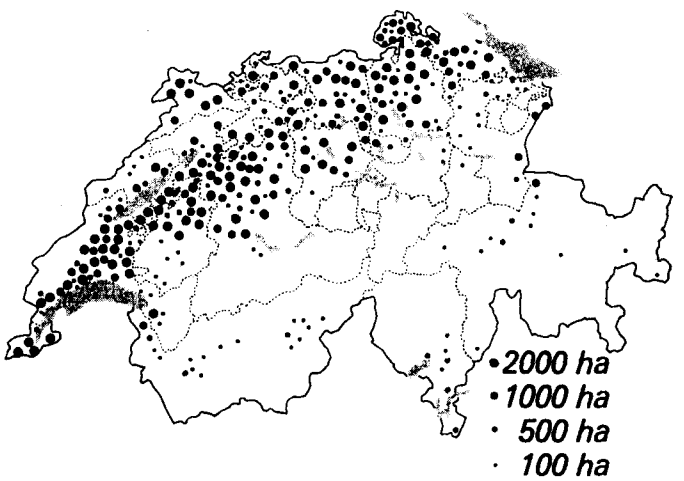

Figure 2.3.1 Arable land (Kipfer 1988).

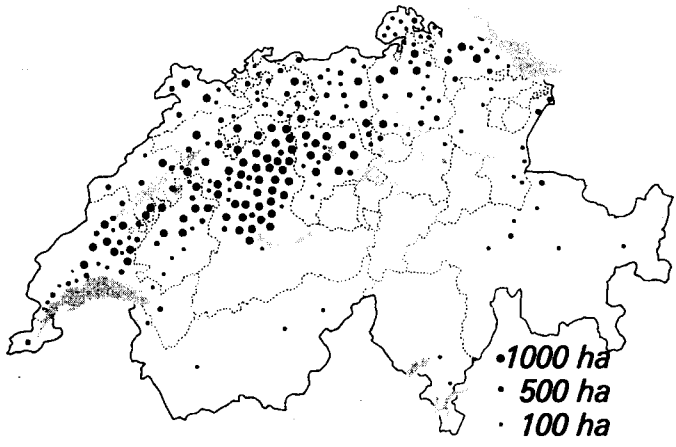

Figure 2.3.2 Grassland (Kipfer 1988).

in the northern part of the Mittelland. Altogether, the most widespread cultures are distributed quite uniformly on the Mittelland.

Basing on the information on the distribution and type of crops showed here and in Appendix D we judge that the first two conditions mentioned at the beginning of this chapter are fairly well satisfied. Consequently we assume that a given hailstorm has the same damaging potential in the whole area. This enables to record and compare, besides the mere occurrence of the storms, also the dimensions of every hail swath.

2.4 Variations in agriculture since 1955 in Switzerland

The structure of Swiss agriculture has changed markedly in the last thirty years. The number of farms has decreased, whereas the mechanisation has increased, leading to an almost three times larger productivity. The arable farmland showed an increase of 38'000 ha between 1965 and 1985, mainly because part of the grasslands were substituted with silo maize and because some farms in the lower areas gave up the stock breeding in favour of some kind of cultivation. The area of cereal cultivation increased thanks to federal subventions. Also the technology for intensive farming improved, making more attractive above all the cultivation of sugar beets. A further development of the sugar beet-area was stopped by a public referendum on the 28th of September 1986. The strong decrease of

the potato areas is mainly due to the increased productivity and to the dropping demand (Bundesamt für Statistik 1990).

The examples of the cereal- and the sugar beet-cultures show how the development of the Swiss agriculture not only depends on the rules of the market economy but also on the measures taken by the government and on the public decisions.

Nevertheless, the total agricultural area has not been influenced much by the structural changes during the years between 1955 and 1985 (the values for 1995 are not yet available): the largest decrease of this area compared to 1955 amounts to 5 % was recorded in 1975, as can be seen in Table 2.4.1.

Year	Total area (ha)	Relative to 1955
1955	1'109'304	100 %
1965	1'080'429	97.4 %
1975	1'055'627	95.2 %
1985	1'076'339	97.0 %

Table 2.4.1 Agricultural area in Switzerland between 1955 and 1985.

Figure 2.4.1 shows that in the same time span the arable land increased by 10 % while 20 % of the grasslands disappeared. The area of the grassland amounts to about one half of the arable land.

The distribution of the main categories of cultures illustrated in Figure 2.4.2 shows that cereals occupy most of the agricultural area (in 1965 even almost double as much as all other cultures together) and that their total area remained fairly constant during the considered time period. The grapevine area remained almost unchanged and represents only a small part of the agricultural surface. Also orchards cover only a little part of the total, although they have gained some importance.

On a national basis, the agricultural features which have an influence on the quality of the hailstorm time series analysed in this work show a satisfying constancy. However, these statements concern the Swiss country in general, while the insurance-damage claims might be influenced by small scale changes not detected by such a large scale statistics.

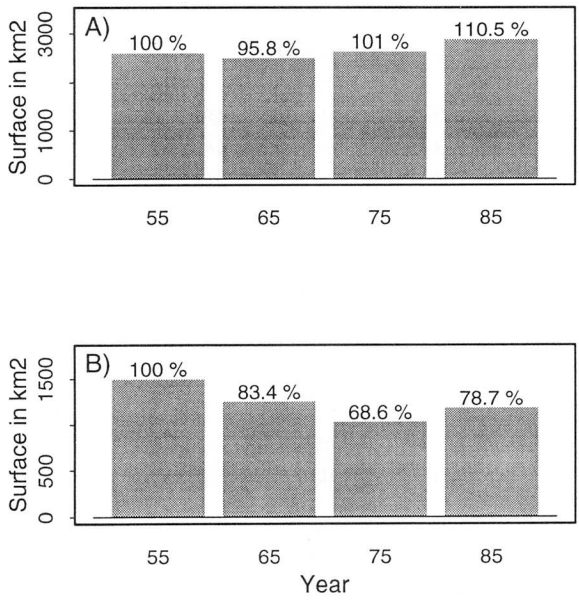

Figure 2.4.1 Evolution of the arable land (A) and grassland (B) areas between 1955 and 1985. The percentages are referred to the total of the respective culture in 1955 (Bundesamt für Statistik 1990).

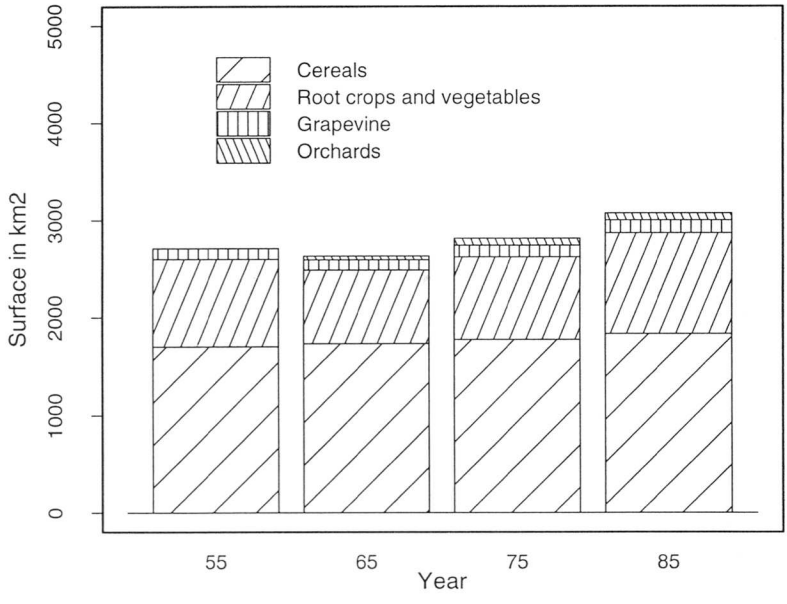

Figure 2.4.2 Total area of the main categories of cultures between 1955 and 1985.

2.5 Regional variations in agriculture

Some useful additional information can also be obtained with a regional evaluation limited to the area of interest on Cantonal base (for more details on the Swiss geography see Appendix C).

Figure 2.5.1 illustrates the portion of agricultural productive land per Canton for the years 1955, 1969 and 1990. In most of the Cantons the productive area occupies between 35 and 55 % of the total area. Exceptions are given by the Cantons of Nidwalden, Obwalden and Schwyz (30 %), which have large mountainous areas and partly belong to the border area of the TA, and by Basel-Stadt, which is mainly an urban area. The areas indicated in Figure 2.5.1 can be defined as *potentially damageable* areas, while the insured portion of these areas corresponds to the *detectable* hail area .

For practical reasons, in the following figures the Canton Jura has been included in Canton Bern (in the years after the separation of these two Cantons). The data for these diagrams were taken from the Swiss statistical annals (Eidg. Statistisches Amt 1959; Bundesamt für Statistik 1970; Bundesamt für Statistik 1990).

As has been shown in Section 2.3 and 2.4, the biggest part of the agricultural productive land is occupied by arable land, which therefore plays an important role in this work. For this reason we take a closer look at the temporal evolution of the surfaces of arable land per Canton.

Figure 2.5.2 shows that between 1955 and 1969 the area of arable land per Canton stayed fairly constant or even decreased, whereas in the following 20 years they increased in most of the Cantons. The largest relative increases observed in 1990 with respect to 1955 were recorded in Zürich, Zug, Aargau, Thurgau, Vaud and Neuchâtel, ranging from 23 to 35 %. Two Cantons recorded a decrease: Luzern (–4 %) and Schwyz (–23 %). However, the absolute changes play a more decisive role on the quality of the hailstorm time series. In fact, a 20 % - change in a Canton with a total arable land of 600 km^2 has more important repercussions on the detection of hail damage than in a Canton with 60 km^2.

The cereal cultures, of which the largest part of arable land is constituted, show a similar time evolution as in Figure 2.5.2. As can be seen in Figure 2.5.3, the Cantons in the flatter areas registered the largest increases whereas the mountainous Cantons show a rather

stable or even decreasing tendency (like in Figure 2.5.2, those with less than 1 km^2 cereal cultures are omitted again).

In Appendix D (Table D1) the areas of the most important cultures are listed for every Canton. The data related to the cereals are represented in Figure 2.5.3. The areas cultivated with vegetables show a considerable decrease everywhere, except for the Canton Aargau, while those cultivated with tubers and root crops decreased in 1969, but by 1990 they increased to values in some cases higher than in 1955. The grapevine areas (not included in the table) are generally very small and irregularly distributed, only three Cantons have areas larger than 500 hectares (Neuchâtel, Vaud and Zürich) and only one of them (Vaud) recorded remarkable increases. The orchards show a general increasing tendency but, except for Thurgau and Vaud, they occupy only very small areas. The general increase of arable land observed in Figures 2.4.1 and 2.4.2 is mainly caused by the growth of the cereal and of the tuber and root cultivation's, which are the most widespread ones. This growth might have a perceptible influence on the damage claim-potential in the whole TA. However, the decrease of vegetable cultivation's has a damping effect on the increase of the damage claim potential.

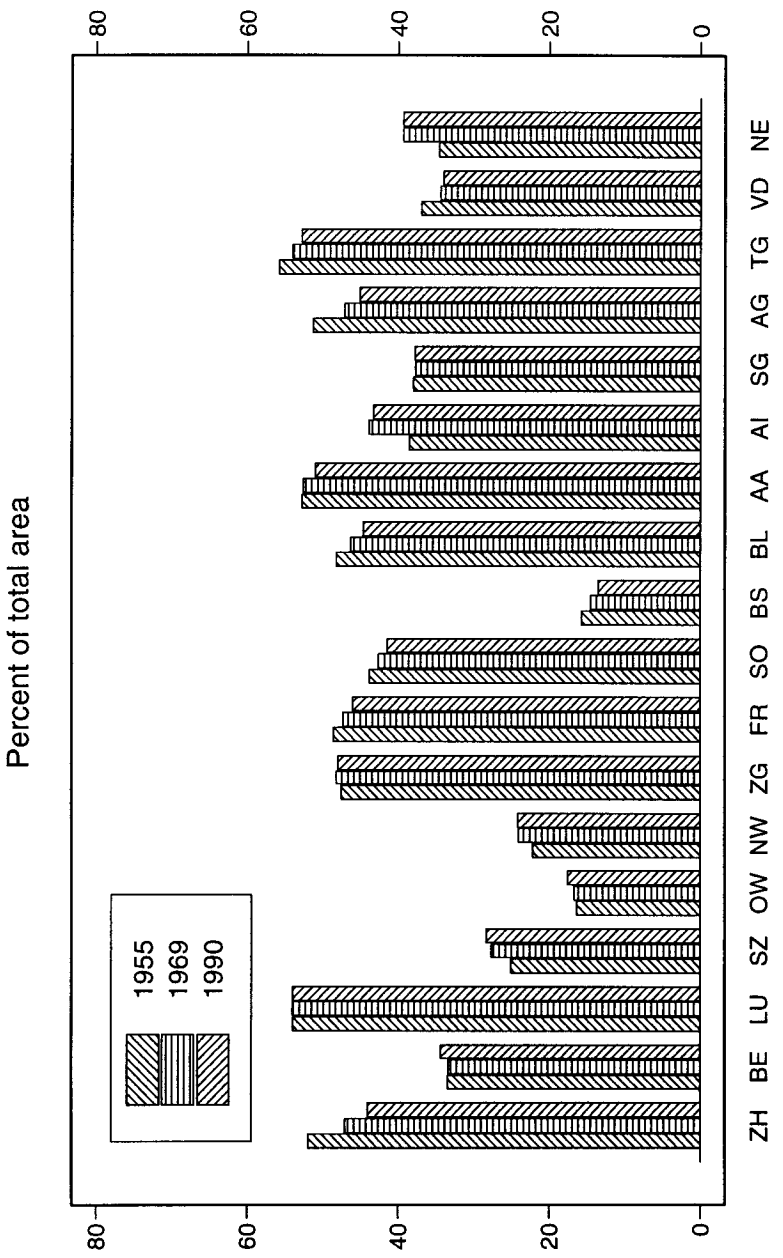

Figure 2.5.1 Portion of agricultural productive land per Canton for the years 1955, 1969 and 1990.

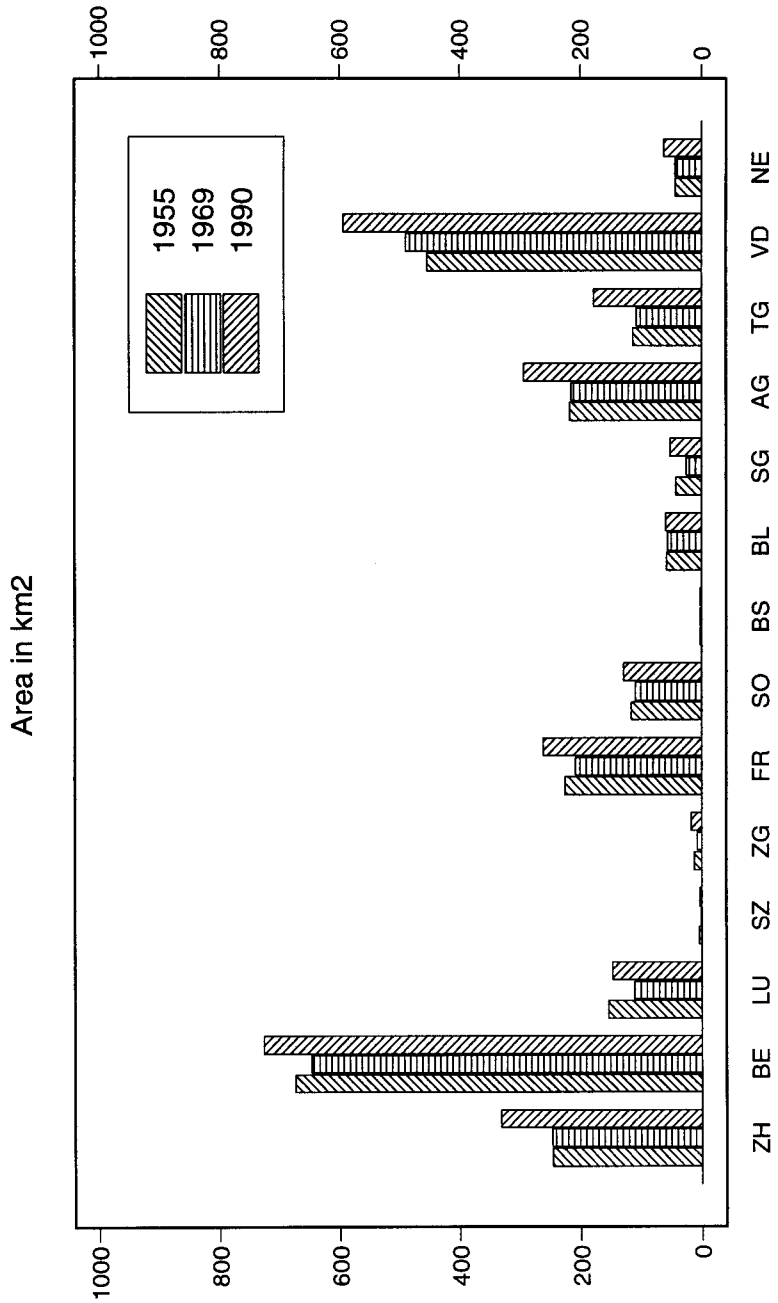

Figure 2.5.2 Arable land per Canton in hectares for the years 1955, 1969 and 1990 (only Cantons with more than 1 km^2 arable land).

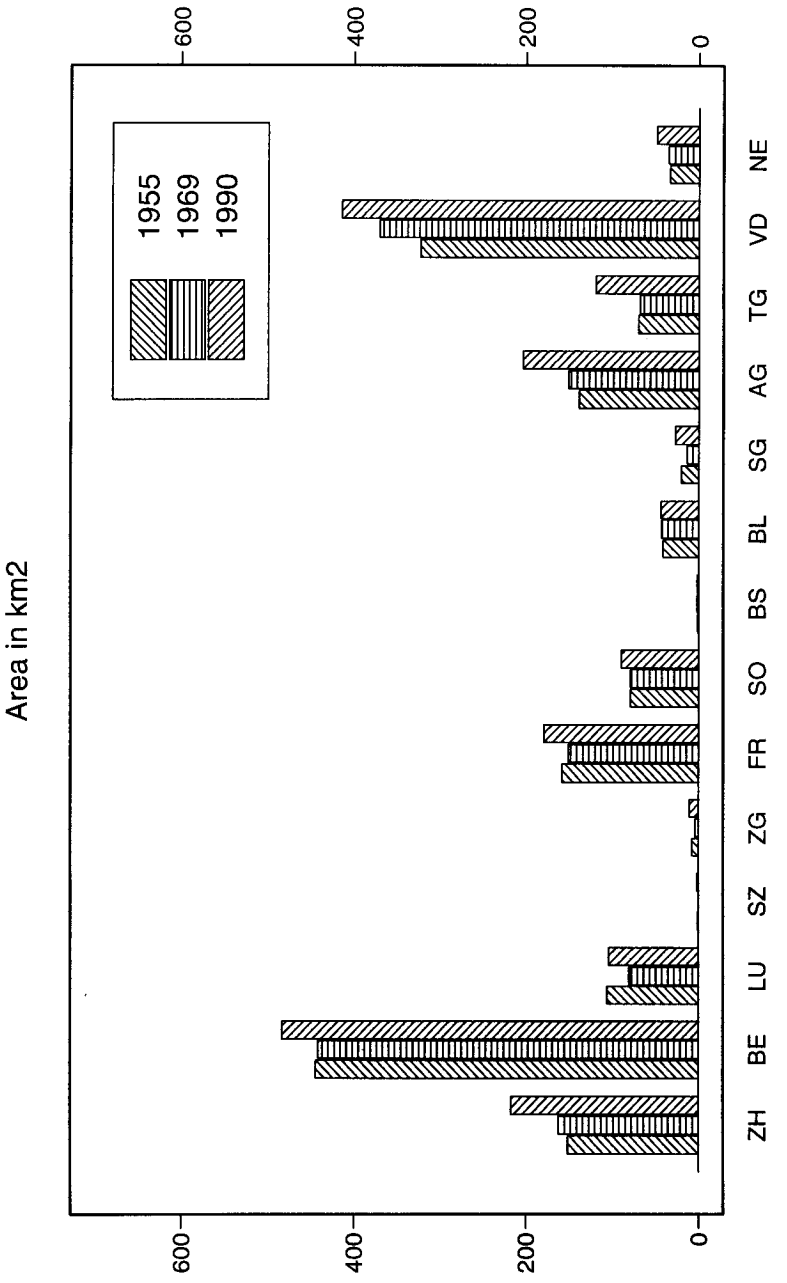

Figure 2.5.3 Cereal cultures per Canton in hectares for the years 1955, 1969 and 1990 (only Cantons with more than 1 km^2 cereal cultures).

2.6 Variations of the insured areas between 1951 and 1976

Following the definition of the potentially damageable areas we want to examine these detectable hail areas that are insured areas.

Insurance participation during the last 45 years is not documented very well. The SHV could deliver only statistics of the insured areas for the years 1951 and 1976, which means that for the second half of the hail climatology we can only derive estimates.

Figure 2.6.1 gives an overview on the changes of the insured agricultural areas per Canton without distinguishing the kind of culture. Among the larger Cantons the biggest changes took place in Aargau (~ + 45 %), in Zürich (~ + 70 %) and in Luzern (~ - 40 %), therefore these Cantons will be given particular attention in the summary of the discussion in Chapter 3.5.

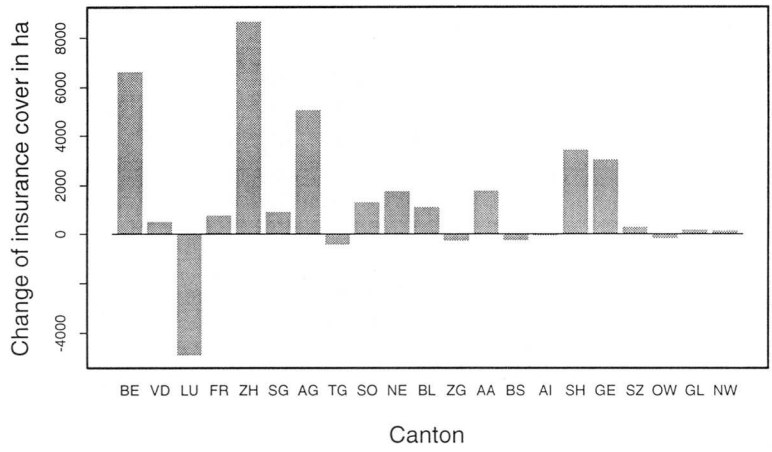

Figure 2.6.1 Variations of the insured areas between 1951 and 1976.

Table D2 in Appendix D shows which part of the cereal-, maize-, rape-, root crop- and vegetable-cultures was insured per Canton in 1951 and in 1976. Among the eight Cantons with the largest areas of cereal cultivation's two show a large relative change between 1951 and 1976: Vaud recorded a decrease of 20 %, Zürich an increase of 12 % (see Table 2.6.1). Except for St. Gallen, all Cantons growing large amounts of cereals have a hail insurance policy on at least 50 % of the areas.

Canton	Total culture area (ha, in 1976)	Relative change of the insured area 1951-1976
Bern	38'924	+ 1 %
Vaud	32'895	- 20 %
Zürich	15'236	+ 12 %
Aargau	14'088	+ 4 %
Fribourg	13'644	+ 3 %
Solothurn	7'348	+ 2 %
Luzern	6'383	± 0 %

Table 2.6.1 Cereals

The insured maize areas are known only for 1976. Except for Vaud, all Cantons with large maize cultures have an insurance cover of at least 45 %.

The rape cultures begin to be hail sensitive already in April and in most Cantons at least 60 % of them are covered by hail insurance. During these 25 years the most important relative changes in insurance cover were observed in Fribourg, Thurgau and Zürich, showing a decrease between 22 and 29 %.

Canton	Total culture area (ha, in 1976)	Relative change of the insured area 1951-1976
Vaud	2'200	+ 1 %
Bern	1'821	- 8 %
Zürich	1'144	- 22 %
Fribourg	621	- 29 %
Solothurn	418	+ 3 %
Thurgau	390	- 23 %

Table 2.6.2 Rape.

The insurance cover of the root crops is clearly lower than for the cultures shown above. Between 1951 and 1976 all larger root crop producers recorded an increase of the insured areas of at least 10 %, but in 1976 only the Canton Zürich insured more than 40 % of the total surface. Tables D1 (Appendix D) and 2.6.3 illustrate these facts.

Canton	Total culture area (ha, in 1976)	Relative change of the insured area 1951-1976
Bern	13'351	+ 9 %
Vaud	6'511	+ 22 %
Zürich	3'851	+ 34 %
Fribourg	3'557	+ 18 %
Aargau	2'476	+ 21 %
Thurgau	2'112	+ 18 %
Solothurn	1'674	+ 14 %
Luzern	1'298	+ 11 %

Table 2.6.3 Root crops.

The vegetable cultivation's, which occupy a surface between two and ten times smaller than the root crop-areas, recorded an increase in insurance cover in 19 of the 21 considered Cantons. The largest increases concern the Canton Vaud.

Canton	Total culture area (ha, in 1976)	Relative change of the insured area 1951-1976
Bern	1'526	+ 8 %
Zürich	1'208	+ 22 %
Thurgau	933	- 18 %
Aargau	691	+ 19 %
Vaud	588	+ 37 %
Fribourg	541	+ 14 %

Table 2.6.4 Vegetables.

The grapevine cultivation's are distributed very irregularly over the TA and only three Cantons have areas larger than 400 ha, which are the ones listed in Table 2.6.5. The only two Cantons that are completely in the TA, and therefore could have an influence on the damage claim potential, are Vaud and Zürich.

Canton	Total culture area (ha, in 1976)	Relative change of the insured area 1951-1976
Vaud	2'994	- 6 %
Neuchâtel	487	- 11 %
Zürich	429	+ 15 %

Table 2.6.5 Grapevine.

Up to 1976, in the TA the part of the grasslands covered by the hail insurance was, on average, only 4 %, while in the alpine area almost no grasslands were insured. In 1977 a new comprehensive insurance on the grasslands was introduced. The consequent increase of insurance cover cannot be quantified, but is estimated not to exceed a few percent, which would have a very small influence on our analyses.

2.7 The *claim potential*, a summarising discussion

The damage claim-potential, or in abbreviated form, the **claim potential** (CP), is an expression for the probability that the damage caused by a given hailstorm is reported to the insurance company. For a given culture, this claim potential can be expressed as a combination of probabilities as follows:

$$CP^i = P_1^i * P_2^i * P_3^i$$

where CP^i = claim potential

$P_1{}^i$ = probability, that falling hail hits a field

= total area of the culture / total considered area

$P_2{}^i$ = probability, that the field is hail sensitive

= total period of sensitivity of the culture / test period

$P_3{}^i$ = probability, that a field is insured

= insured area of the culture / total area of the culture

The total claim potential is given by the sum of the culture-claim potentials:

$$CP = \sum_i CP^i$$

The available data enable the computation of CP^i only in a few cases and only approximately. Consequently, the calculation of CP does

not lead to meaningful values. The main reasons for this limitation are:

- The insured areas are known only for the years 1951 and 1976, so that we do not know anything about the time in between these two years and about the second half of the observation period.
- All values are on a Cantonal base. In some cases a part of the Canton lies in the border area and is mainly mountainous, which leads to a too small value of the CP for those parts included in the TA.
- The agricultural and the insurance statistics are not given for the same years.
- As the agricultural and the insurance statistics are given for groups of cultures and not for single cultures, the hail sensitivity period also has to be defined for the same groups. This leads to errors, particularly in the case of heterogeneous groups like vegetables.

In order to obtain a useful set of CP values, we would need a complete set of agricultural and insurance statistics with a time step not longer than two or three years, on a community basis rather than on a Cantonal basis.

However, to estimate of the order of magnitude of a CP^i, we will make a few examples for cereal cultures at the beginning of the 50's. The probability that a cereal field is hail sensitive is the same for every Canton: cereals are hail sensitive on roughly 93 days of the 114-day test season, which means that $P_2{}^i$ is 0.81 or 81 %. Canton Vaud has a total area of 3'218 km^2, a total area of cereal cultures of 322.2 km^2 (1955) and a total insured cereal area of 312.5 km^2 (1951). This leads to a $P_1{}^i$ value of 0.1 (10 %) and a $P_3{}^i$ value of 0.97 (97 %), which yields a CP^i of 0.08 or 8 %. The same calculations for the Cantons Thurgau and Bern yield a CP^i value of ~ 4 % and for the Canton Zürich ~ 5 %. On the base of these results we estimate the total claim potential CP per Canton to oscillate between 5 and 15 %. The CP for the single communities probably shows a larger variability.

Additionally to the factors appearing in $P_1{}^i$, $P_2{}^i$ and $P_3{}^i$, there are others which influence the CP but cannot be quantified in the present study. A change of the crop sensitivity to hail can be due to the cultivation of a more or less sensitive kind of plants, but also to some kind of illness or to a density change of the cultivation (more densely planted plants sustain and protect each other better).

Owing to the fact that a quantitative estimation of the CP is difficult with the available data, a qualitative rough estimation was made of the net effect of the changes of the Swiss agricultural and insured areas on the CP. The results are summarised in Table 2.7.1, where the Cantons are ordered by decreasing size of their territory inside the TA. Only the territories of the Cantons Thurgau, Aargau, Appenzell, Solothurn, Zug, Zürich, Basel-Land and Basel-Stadt are located completely within the TA. The assessed increases of the CP are indicated with "(+)", "+" or "++" and decreases with "(–)", "–" or "– – ", depending on their strength. In the first three columns, that relate agricultural statistics, the indication to the left of the comma is related to the development between 1955 and 1969 and the one to the right is for the time span between 1969 and 1990 (e.g. 0,+). The signs in the fourth and the fifth column refer to the insurance cover and pertain only to the time period between 1951 and 1976 as no other data are available. The estimated net effect on the CP caused by the changes described in columns 1 - 5 is displayed in the last column. The assessment is made for the first half of the observation period and extrapolated into the second half. I. e. it is assumed that the insurance participation continues to follow approximately the same trend .The CP evolution is mostly indicated by a range (e.g. [0,(+)]), which expresses the uncertainty given by a possible change of trend during the second part of the period. The evaluations in the first 5 columns are based on absolute changes as these are the ones that influence directly the claim potential (the indication of relative changes does not tell anything about the extension of the changes). For the first two (agricultural and arable land) and the fourth column (insured cultures) a "0" indicates a change within the range of ± 500 ha, "(–)" and "(+)" a change between ± 500 and ±1'500 ha, "–" and "+" a change between ±1'500 and ±10'000 ha and "– –" and "++" more than ± 10'000 ha. For the third and the fifth column (cereals and insured cereals) the respective thresholds are (± 300, ± 1'000 and ± 8'000 ha).

The estimation summarised in Table 2.7.1 does not show any clear tendency common to all Cantons for the first half of the observed period. Among the larger Cantons in the TA Luzern and Thurgau seem to have experienced a non-negligible decrease of the claim potential, while the decrease of culture land seems to counterbalance the higher insurance cover in Aargau and Zürich. In the last 15 years the agricultural development and the general increase of arable land could have caused a rise of the claim potential, but without better statistical information of the SHV this supposition cannot be confirmed.

Canton	Agricult land	Arable land	Cereals	Insured cultures	Insured cereals	Net effect
Bern (BE)	0,+	–,+	(–),+	+	–	[0 , (+)]
Vaud (VD)	–,(–)	+,++	+,+	0	–	[0 , (+)]
Luzern (LU)	0,0	–,+	–,+	–	–	[– , 0]
Fribourg (FR)	–,–	–,+	(–),+	(+)	(–)	[(–) , 0]
Zürich (ZH)	–,–	0,+	+,+	+	+	[0 , (+)]
St. Gallen (SG)	(–),0	–,+	(–),+	(+)	(–)	[(–) , (+)]
Aargau (AG)	–,–	0,+	+,+	+	(+)	[0 , (+)]
Thurgau (TG)	–,(–)	(–),+	0,+	0	–	[– , 0]
Solothurn (SO)	(–),(–)	(–),+	0,+	(+)	0	[0 , (+)]
Neuchâtel (NE)	+,0	0,+	0,+	+	(+)	[(+) , +]
Basel-Land (BS)	(–),(–)	0,0	0,0	(+)	0	[(–) , 0]
Zug (ZG)	0,0	(–),(+)	(–),(+)	0	(–)	[(–) , (+)]
Appenzell A. (AA)	0,0	0,0	0,0	+	0	[0 , (+)]
Basel-Stadt (BS)	0,0	0,0	0,0	0	0	0
Appenzell I. (AI)	(+),0	0,0	0,0	0	0	0
Schwyz (SZ)	+,(+)	0,0	0,0	0	0	[0 , (+)]
Obwalden (OW)	0,(+)	0,0	0,0	0	0	0
Nidwalden (NW)	(+),0	0,0	0,0	0	0	0

Legend:
– – / ++ : important decrease / increase
– / + : moderate decrease / increase
(–) / (+) : small decrease / increase
0 : negligible change

Table 2.7.1 Estimation of the net effect of the changes of the agricultural and insured areas on the claim potential. Absolute values are given in the text.

This information will not be available in its short term, and thus an attempt was made to calculate the insurance cover indirectly by dividing the sum insured by the harvest value for the years 1977 to 1993. This computation is not as simple as it might seem, the insured sum is given for different cultures together and the contribution of a single crop to this sum is not indicated. Furthermore, the sum insured of the comprehensive insurance is composed by the contributions of cultures with very different harvest values. Cereals turn out to be the only culture for which such a calculation might be of some use, although a quantitative interpretation is probably not possible. A comparison of the computed insured areas with the corresponding arable land-areas gave an insurance cover of over

100 % after 1980, which is, of course, absurd. Qualitatively, the larger Cantons seem to have experienced some increase in insurance cover (particularly Bern and Vaud) whereas the smaller ones don't show important changes.

A closer look at the development of the single cultivation's shows, among other things, that the rape areas in 1985 were about four times as large as in 1955 (Bundesamt für Statistik 1987). Figure 4.2.1 shows that the rape cultures become hail sensitive already in the last third of April, that means at least three weeks earlier than most other cultures. Therefore, the claim potential might have become higher during the first two weeks of May, but this does not have any influence on our evaluation as this study is based on a TS which begins on the 20th of May.

The whole discussion on the agricultural and insured areas presented in this chapter is based on total surfaces and the smallest unity is the area per Canton. We should not forget, however, that a variation of these areas does not appear in form of one single big additional patch or hole, but it is distributed in many little patches or holes whose influence on the claim potential decreases with the increasing size of a hailstorm. As this climatological work is aimed mainly at larger hailstorms, the use of the SHV data for a first evaluation of the past hailstorm activity appears to be justified.

3 Methods of analysis.

The discussion of Chapter 3 has shown that the damage claims of the SHV, subject to some restrictions, are suitable for the compilation of a climatology of hailstorms.

In order to guarantee the comparability of data from different years, we need to define a *test area* and a *test season* . Thereafter, a method must be designed for the quantification of the information contained in the geographic distribution of damaged communities.

3.1 The test area (TA).

The selection of the test area (abbreviated with TA in the following) constitutes an important step in this work. The meaningfulness of the hailstorm climatology depends for a great deal on this selection, which was carried out under the consideration of the following factors:

- **Insurance participation and distribution of the cultures.**

  These two factors are tightly interconnected and cannot be treated separately. Although the cultivated areas are not always proportional to insured areas, it is quite obvious that the insurance participation is high only when the cultivated areas are large enough.

  The SHV ensures agricultural areas all over Switzerland, but these are distributed very inhomogeneously: in the Alpine region there are almost no important cultures and therefore less insured areas. As can be seen in Figure 2.1.1, the highest insurance participation is recorded in the Mittelland, where almost all of the most important Swiss cultures are concentrated. An other area with well insured cultures is situated in the southern part of Ticino, but for our purpose it is too small and too distant to be included in the TA.

  It is quite obvious that a climatology based on insurance data can only be created for relatively large regions with a high insurance participation. This condition is satisfied only in the Mittelland and, partly, in the Jura as well as in the Prealpine regions. Therefore the TA will be limited to the Mittelland, while the latter two regions will be used as border areas. An exception is the region between the Vierwaldstättersee and the Lake of Zürich, which is a part of the Prealpine region that shows also good conditions for

the collection of hail damage-data (high insurance cover and community participation), and therefore it has been included in the TA.

- **Political borders.**

  The Swiss border has a very irregular shape, smaller regions like Schaffhausen and Geneva are connected to the rest of the Swiss territory only by a narrow land strip. When a hailstorm hits these areas, the interpretation of the resulting damage distribution is very difficult: as no damage claim-information from the adjacent countries is available, it is not possible to find out if it is a local event or if the damaging hailstorm continued its track into the neighbouring country. For this reason these regions are considered border areas, even if geographically and climatologically they belong to the Mittelland and their cultures are well insured. On the other hand, the eastern part of Jura has been included in the TA because its insurance cover is high enough and it does not compromise the compactness of the TA.

- **Distribution and size of the communities.**

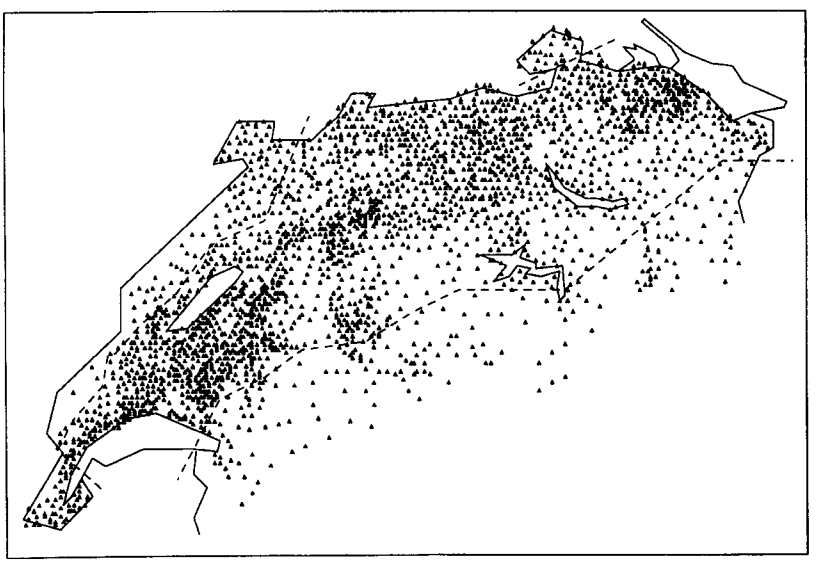

Figure 3.1.1 Geographic distribution of the 2'420 communities considered for the damage claim recording.

Figure 3.1.1 shows the distribution of the 2'420 communities whose damage claims were used for this climatological work. The centre of every community is indicated by a triangle. In the Prealps and in the western Jura the surface of the single communities is larger causing a decrease of density and therefore a smaller resolution of the damage claim-data. Although the community density of the TA is still somewhat irregular, it is high enough to guarantee the detection of all larger hailstorms.

- **Climatic regions of Switzerland.**

  Although Switzerland is a small country, it is divided in many climatic regions because of the presence of the Alps and of the Jura mountains. Figure 3.1.2 illustrates these regions as defined by the SMA in its annals (e.g.(SMA 1991), and shows how the Mittelland-climatic region coincides fairly well with the TA (except for the eastern Jura and the central Prealps, which were added for the reasons described above). This fact should guarantee that a given culture is hail sensitive more or less at the same time everywhere in the TA.

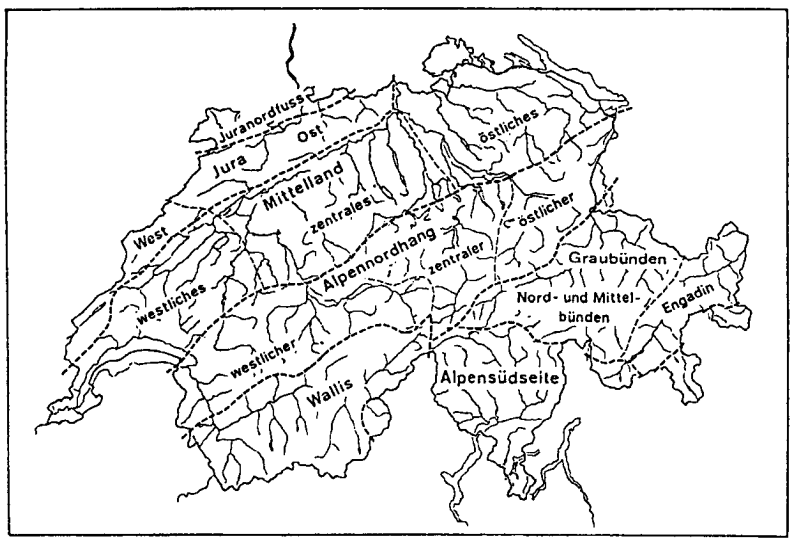

Figure 3.1.2 Climatic regions of Switzerland (from (SMA 1991))

- **Border areas**

  The damage claims of the border areas will not be considered directly for the hailstorm climatology, but in case of hailstorms entering, exiting or crossing the TA these data can be useful to

determine whether the storm was produced *in situ* or moved into the TA, and wheter it stopped at the border or left the TA.

Finally, under consideration of all points mentioned above, the TA for the hailstorm climatology was designed as represented in Figure 2.2.1.

3.2 The test season (TS)

The variety of culture species is large enough to ensure the presence of at least a few hail-sensitive crops during almost the whole hailstorm season.

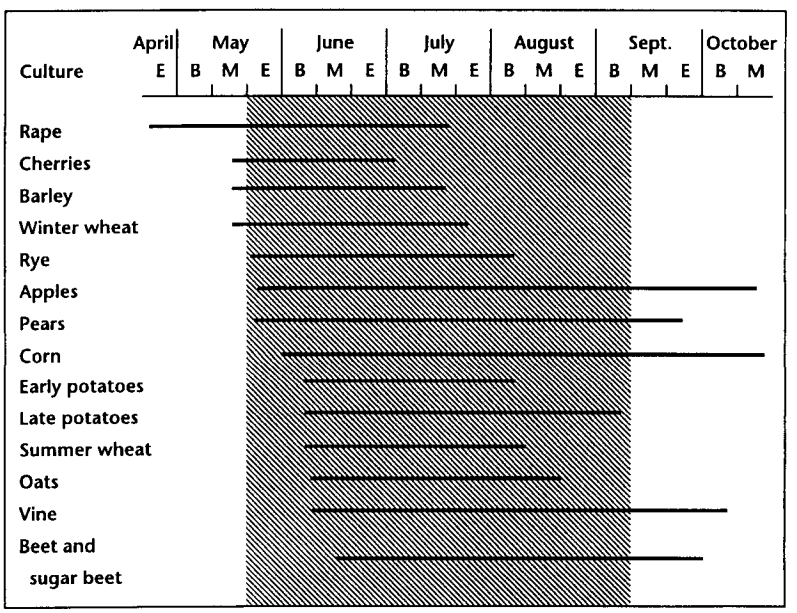

Figure 3.2.1 Time interval per culture during which crop loss is possible

This fact is illustrated in Figure 3.2.1 where the time interval of hail sensitivity is drawn for the most common cultures. This figure was put together with the help of damage curves which the SHV has defined for most of the cultures (SHV 1972; SHV 1975; SHV 1979; SHV 1981; SHV 1982; SHV 1982; SHV 1984) and with Figure 3.12 of the study by Schiesser (1988). Examples of such damage curves are given in Figure 3.2.2. The highest *sensitivity density* is observed during

the months of June and July, but even during the longer time period between the 20th of May and the 10th of September there are always a few hail sensitive crops. As during this period the probability of crop loss is always larger than zero it is fairly well guaranteed that every bigger hailstorm appearing during that time can be detected, so that we decided to choose it as the *test season* (TS) for all the data analyses carried out in this work.

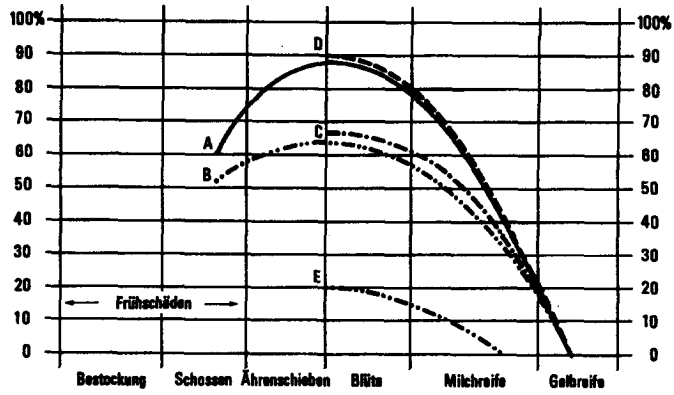

Körnerverluste in Prozenten (inklusive Qualitätsverlust aber ohne Ernteverlust), verursacht durch Halmknickungen an Getreide. Senkrechte: % Körnerverlust; Waagrechte: Stadium, in welchem die Knickung erfolgte.

Kurve A: untere und mittlere Knickung: Weizen, Korn, Gerste, Roggen
Kurve B: untere und mittlere Knickung: Hafer
Kurve C: obere Knickung: Weizen, Korn, Gerste
Kurve D: obere Knickung: Roggen
Kurve E: obere Knickung: Hafer

Figure 3.2.2 Damage curve for different kinds of cereals.

3.3 Cartographic representation of the damage claims.

A geographic representation of the hail damaged communities enables a quantification of the hail swaths left by the storms and a direct comparison with RADAR measurements. Figure 3.3.1 is an example of such a representation: every triangle is the centre of a community which claimed hail damage on the 23rd of July 1983.

A comparison with RADAR measurements can be done qualitatively by overlaying the damage distribution and the RADAR echo or, indirectly, by comparing some measure of the single swaths with a measure of the corresponding RADAR echo. Such comparisons,

which are mainly carried out for calibration purposes, will be described in Chapter 7.

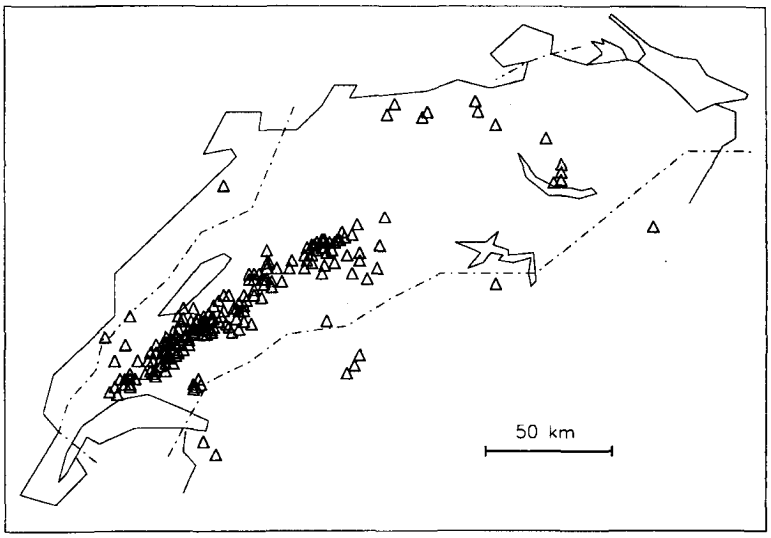

Figure 3.3.1 Damage claims on the 23rd of July 1983.

A strong hailstorm leaves a swath of damaged cultures, which in this representation is made visible by a cluster of triangles; the above picture shows clearly the swath left by a storm which crossed the Mittelland from the Lake of Geneva to Bern. As we can imagine, this is not always the case: on days with widespread local, mostly smaller hailstorms it becomes more difficult to determine the single swaths. On the other hand it can also happen that with the passage of a squall line a few larger cells leave overlapping swaths, which are difficult to be kept apart in a geographical representation with a time resolution of one day. Fortunately, such cases happen far less often than the first ones. For this reason, if these data are to be used only for the evaluation of larger hailstorms, the problem can be neglected. Swaths like the one shown in Figure 3.3.1 will be called *hail damage clusters* or short *clusters*.

3.4 Temporal and spatial resolution.

The temporal resolution of the damage claims is one day, except for those cases where the time of approximate appearance could be

defined with the help of annals and thunderstorm observation charts of the SMA. This was possible in 75 % of the cases.

The spatial resolution depends on the size of the communities and therefore it can be defined only approximately. To find an average distance between the centres of the communities it was assumed that these are circular, so that the mean radius could be calculated starting from the area, which is known for every community. This radius amounts to 1.6 km (which corresponds to a surface of roughly 8 km^2), whereas the smallest one measures 0.3 km and the largest 7.9 km, with a standard deviation of 0.9 km. A comparison of this approximate resolution of 8 km^2 can be made with the resolution of the SMA-RADAR pictures, which amounts to 4 km^2.

3.5 Hailstorm data-collection with the program HAAN.

With the analysis of the SHV data we want to obtain a time series of damage clusters which can be compared with other climatological time series. For this purpose we need some measures characterising the single hail swaths, like length, area and direction of movement, and an indication on the meteorological environment in which the storm developed.

The Program HAAN.

The program HAAN ("hail analysis" oder "Hagel Analyse") has been written especially for the evaluation of the damage claim-data. It has been written in PV-WAVE CL (command language), which is a visual data analysis software system. Its commands, which include also complex graphical and mathematical functions, can be entered and executed interactively or combined to form whole programs.

In the first step the damage claims are joined into potential damage surfaces (*potential* because we are not sure that the whole community represented by the triangle has been hit by hail). These surfaces can be obtained by constructing a *damage mountain*-topography and by representing it as a contour plot. To this purpose the program creates a three-dimensional matrix with the horizontal coordinates of all the 2'420 communities and a third dimension z which contains the information of the hail damage. For a given day, z = 1 for all communities recording damage and z = 0 for the others. This matrix of irregular points is then transformed in a regular grid with a PV-WAVE routine called GTGrid.

The GTGrid routine transforms three-dimensional data sets described by x- , y- and z vectors in a 2 dimensional array with the z-values connected to a regular x-y grid. For the computation of this grid four methods are available, but the numerical routines used for these methods are not described in the manual. In the present case the method *Cluster*, which uses the *Radial search for clustered or linear data* algorithm, gave the most satisfying results. In fact it is said to be suitable for randomly distributed noisy data with or without discontinuities.

Besides with the choice of the method, the computation of the grid can also be controlled with a number of keywords. For the program HAAN the distance of the grid points was fixed at 2 km, which corresponds to the resolution of the SMA-RADAR pictures. The *Radius* keyword specifies the distance over which the interpolation is performed and can be interpreted as the distance at which the covariance function goes to zero. In HAAN this radius was chosen to be of roughly 5 km, so that the interpolation is computed only with the nearest surrounding communities and possible *damage free* holes become visible.

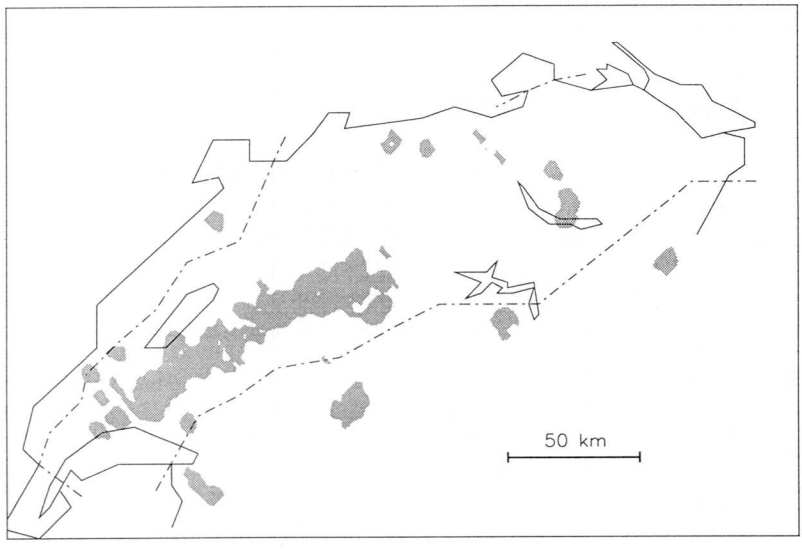

Figure 3.5.1 Potential damage areas as computed by the program HAAN.

After the indication of the date of the day for which the damage surfaces have to be computed, the program requests some meteorological data which can be useful for the interpretation of the

damage contour-plots and for the analysis of the cluster-data set (which will be described in more detail in the next section).

This introductory part is followed by the interactive choice of the clusters which will be recorded in the data set. This choice is carried out on a plot which shows only the 0.2 contours of the damage surfaces (see Figure 3.5.1). The clusters have to satisfy some conditions which are described in the next section together with the data set.

3.6 The obtained data set.

The data analysis with HAAN was carried out under the following conditions:

- To avoid the recording of small local hailstorms, which we are not interested in, a minimum cluster length of 25 km was defined.
- To enable a better comparability in time and space of the recorded clusters, their length has been measured only within the TA, even if the potential hail surface continued in the border area.
- Only days with at least 30 damage claims were taken into consideration for the evaluation (596 such days were counted during the 5'130 days of the 45 year-observation period). This decision was taken after a test run with a smaller number of claims which showed that in most of the cases the damaged communities are scattered all over the TA and no cluster was recognisable. In the few cases where a cluster was found, its length hardly reached the minimum of 25 km.

On 61 % of all days with at least 30 claims 651 clusters satisfied the conditions described above. The final data set was loaded on the Oracle data base-system available at the Institute of Atmospheric Science of ETH (abbreviated LAPETH) and published in an internal report (LAPETH 1995).

The full data set is described below:

- Date
- Frontal, prefrontal or airmass day: frontal (fr) if a cold front crossed the TA on the same day, prefrontal (pf) if the front reached the TA the following day and airmass (ai) if no front was in sight.
- Frontal passage in the morning (fm) or in the afternoon (fa).

- Origin of airflow: maritime polar and maritime tropical, continental polar and continental tropical.
- Number of the cluster (within the given day).
- Code that specifies the position of the cluster with regard to the TA: 1 = cluster completely in the TA; 2 = begin outside, end inside the TA; 3 = begin inside, end outside the TA; 4 = the cluster crosses the TA, beginning and ending outside of it.
- Area of the cluster (only the part within the TA).
- Length of the cluster (only the part within the TA).
- Coordinates of the beginning- and end-points (in accordance with the Swiss coordinate system).
- Direction of movement of the cell producing the damage cluster (defined with the help of radiosoundings and synoptic charts)
- Approximate time of appearance (for those cases which could be recognised on daily thunderstorm-observation charts of the SMA)

4 Damage claims and damage clusters

4.1 Time series of damage claims

Before continuing with the analysis of the data set obtained with the program HAAN (Chapter 4), we consider the original data, viz. the damage claims themselves. One damage claim is defined as one damage reporting community. Information on the number of damage claims, without the geographical indication of the claiming communities, is available since 1920, which enables us to look at a time series of 74 years. However, the lack of information on the history of the insurance participation causes some uncertainties in the interpretation of the data.

Between 1920 and 1993, during the TS, the total number of days amounts to 8'436 (5'130 since 1949) and on 52 % (57 %) of these days at least one damage claim was recorded (such a day is called a *hailday*). On 927 days (21 % of the haildays) at least 30 communities were hit by hail (since 1949 it were 596 days, corresponding to 20 % of the haildays). The number of days with only one damage claim is 3.5 % higher during the period 1949 - '93 than during the period 1920 - '49.

Bider (1954), who published an analysis of the same data for the time span 1895 - 1950, found that after 1921 the number of haildays stayed fairly constant, while the number of *hail communities* still increased. He judged the period 1921 - 1950 to be homogeneous enough for a statistical analysis of the hail frequency

The annual sum of haildays (defined as days with at least, respectively, 1, 30 or 100 damage claims) in Figure 4.1.1 and the annual sum of damage claims in Figure 4.1.2 do not really confirm Bider's statement. Both plots show the annual anomalies of these sums, while the average of every series is indicated in the left upper corner. Bider found an average number of 78.7 haildays per year, but this value is not directly comparable with our values because they are computed for a smaller time span (TS) and a smaller test area (not whole Switzerland).

During the first five years of the considered period the annual sum of haildays (Figure 4.1.1 a)) shows a larger negative anomaly than the sum of damage claims (Figure 4.1.2 b)). This could be interpreted as an increase of haildays, observable particularly during the last 20 years. Although the number of damage claims shows also a slightly

increasing trend, its annual sum seems to oscillate more randomly around the mean.

Table 4.1.1 summarises the main features of the time series illustrated in Figures 4.1.1 and 4.1.2. The computation of the trend values was carried out with the method applied by Schönwiese et al. (1993). ‹x› is the mean value of the series and s is the standard deviation.

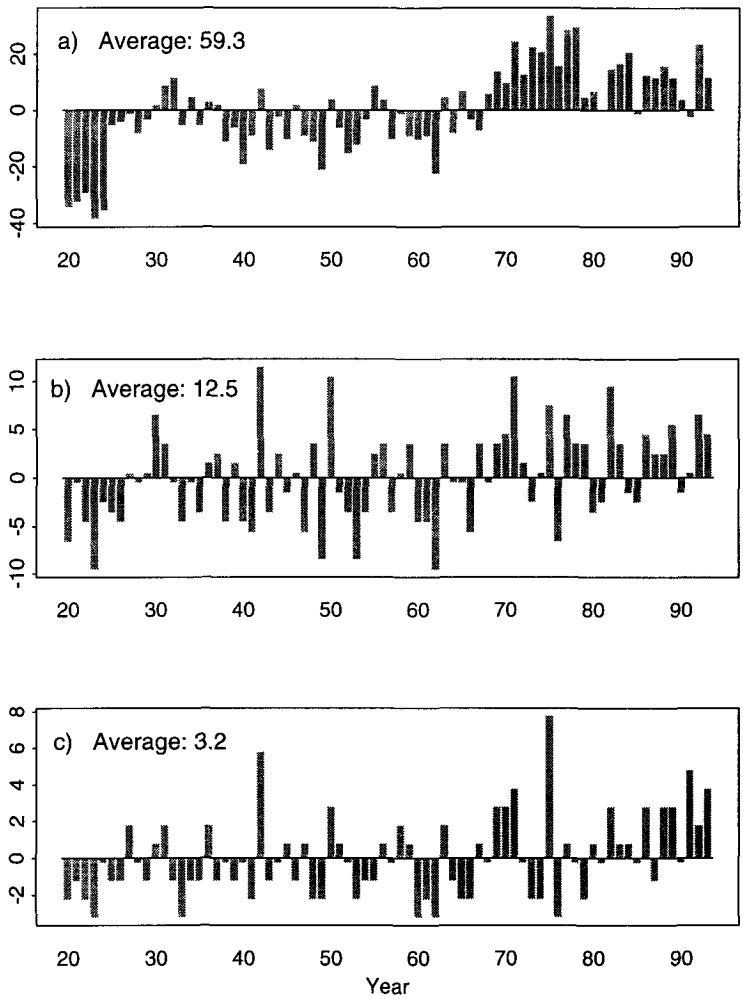

Figure 4.1.1 Anomalies of the *annual sum of haildays* for the test area and the test season. a): days with at least 1 damage claim; b): days with at least 30 damage claims; c): days with at least 100 damage claims

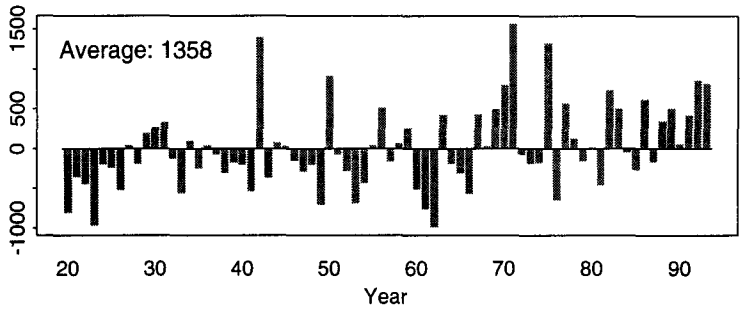

Figure 4.1.2 Anomalies of the *annual sum of damage claims* for the test area and the test season.

The trend is given as number of claims, respectively as number of haildays per year and was computed with a least square fit. T is the difference between the trend value at the end of the time series and the one at the beginning (expressed in total number of days) and T / s is the trend to noise ratio. *signif.* is the corresponding significance, while s / ‹x› is the relative standard deviation.

	Sum of damage claims	Sum of haildays (≥ 1 claim)	Sum of haildays (≥ 30 claims)	Sum of haildays (≥ 100 claims)
‹x›	1'358	59.3	12.5	3.2
s	525.2	15.3	4.7	2.2
trend	9.17	0.46	0.07	0.04
T	669.4	33.6	3.2	2.6
T / s	1.27	2.20	0.67	1.19
signif.	≈ 80 %	> 95 %	< 60 %	≈ 75 %
s / ‹x›	38 %	26 %	38 %	69 %

Table 4.1.1 Statistical characteristics of the sum-time series (Figures 4.1.1 and 4.1.2)

The number of haildays with at least 1 damage claim shows a more significant trend than the number of days with at least 30, respectively 100 claims, which means that the number of days with a small number of claims (between 1 and 30) increased more than the *big* haildays. This is probably due to the fact that the number of

insured cultures increased, particularly during the 20's, causing a higher detection sensitivity in the case of smaller hailstorms.

The maximum number of damage claims recorded in one day, per year, oscillates quite steadily around 230 claims until the end of the 80's, with an absolute maximum for the whole time series of 703 in 1971 (see Figure 4.1.3). Only at the end of the series an uninterrupted row of four fairly high values catches the eye: it might be an oscillation which is a little bit stronger than the previous ones, but it could also be the beginning of an increase of the maximum number of damage claims per day. For this reason the low pass filtering was not completed at the beginning and at the end of the series with some numerical procedure.

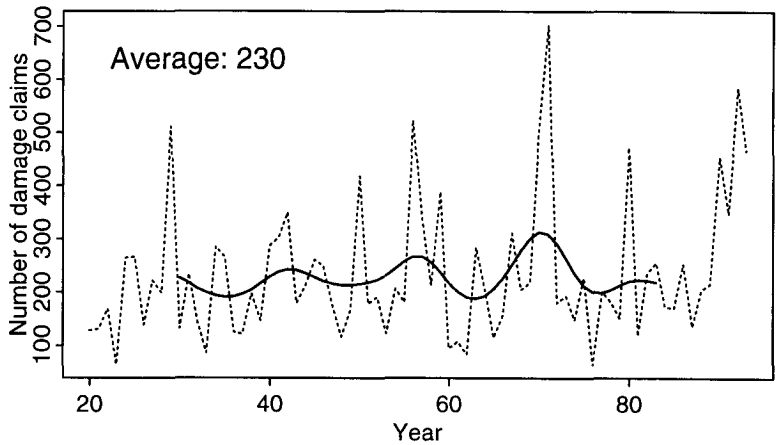

Figure 4.1.3 Maximum number of damage claims recorded in one day, per year. The dotted line is the original time series, the thick continuous line is a 21 point Gaussian low-pass filter (theory on low-pass filtering: Schönwiese (1992)).

The mean number of damage claims recorded in one day, per year, amounts to 23.1 claims for the whole time period, with a standard deviation of 7.1 (Figure 4.1.4). Except for the peak around 1970, a smoothing of the curve shows a slightly decreasing tendency until the beginning of the 80's, while the annual mean of daily claims of the last decade climb to values similar to the ones observed during the 40's. An explanation to the decreasing trend might be found in the increased detection sensitivity mentioned above: a higher number of haildays with a small amount of damage claims lowers the mean value of daily claims. Of course it cannot be excluded that at the same time the extension of the hailstorms decreased.

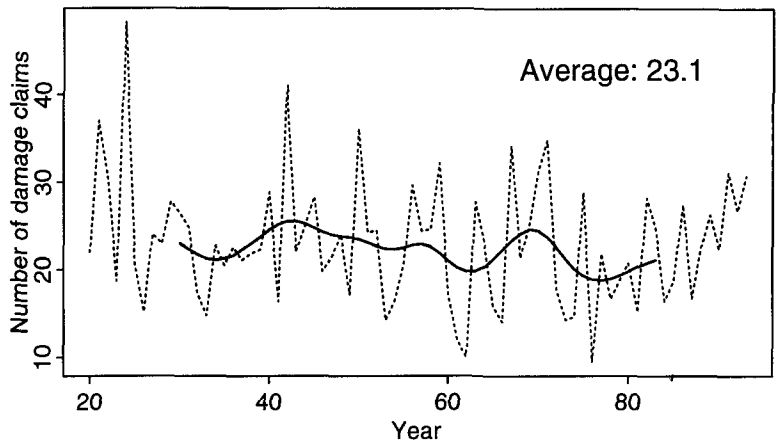

Figure 4.1.4 Mean number of damage claims recorded in one day, per year. The dotted line is the original time series, the thick continuous line is a 21 point Gaussian low-pass filter.

Figure 4.1.5 illustrates the monthly number of damage claims for the 5 months of the test period. For the months of May and September only the days included in the TS were considered. No particularly striking feature can be observed in either one of the plots, the smoothed curves show a fairly flat course. A slight increase during the 70's and the 80's is visible, particularly in August.

Concluding this first overview on the evolution of the damage claims, it seems that the insurance participation has stabilised after the 30's and that further oscillations of the insurance cover influence mainly the *smaller* haildays, which have only a negligible influence on the climatology of strong hailstorms. As the geographical position of the damage claims is only known for the data after 1948, further analyses will concentrate mainly on this shorter time span, so that the uncertainties on the insurance cover during the 20's and the 30's will not have any effect on these analyses.

In general, the annual number of claims and the annual number of haildays show an increasing tendency during the last two decades. As it is assumed that the insurance participation has not changed much during these years, this increase could effectively be due to natural factors, but it is too early to interpret it as the beginning of a climate change: it could also be the upslope part of a stronger peak.

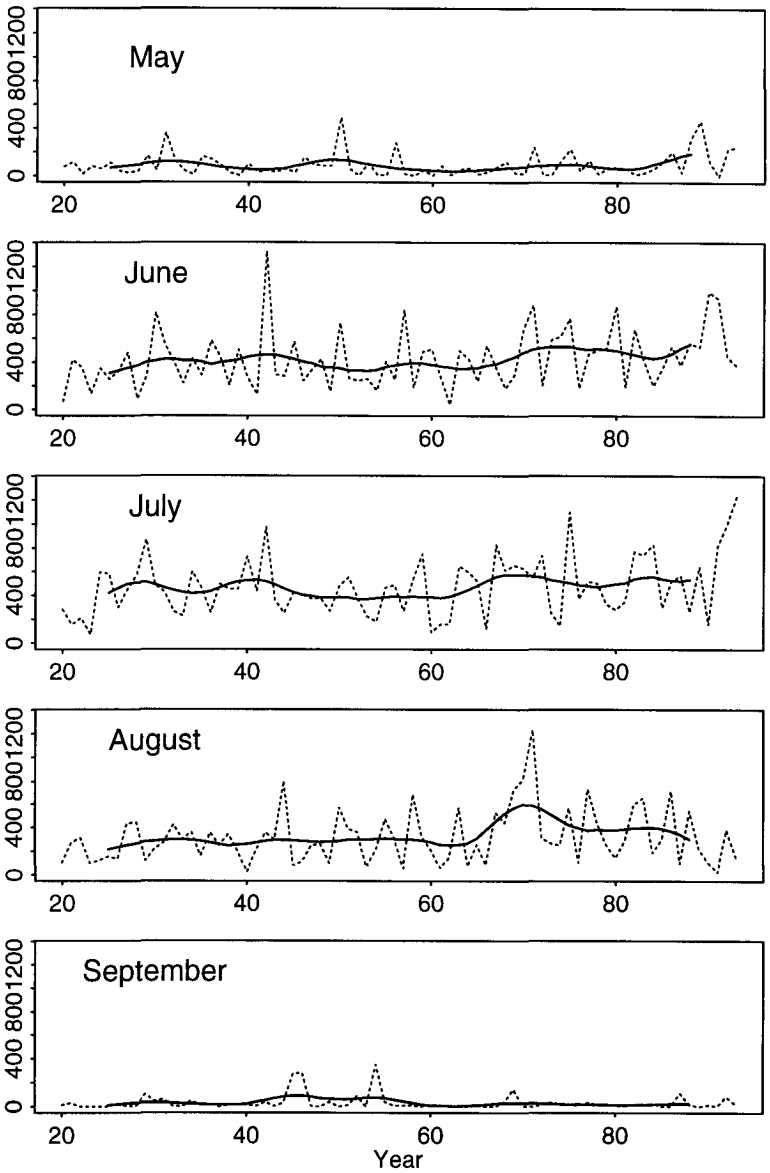

Figure 4.1.5 Monthly number of damage claims for the 5 months of the TS. The dotted lines are the original time series, the thick continuous lines are 11 point Gaussian low-pass filters. For the months of May and September only the days included in the TS are considered.

4.2 Time series of damage clusters and their spatial distribution

The damage claim-statistics illustrated in the previous section give an idea of the hailfall frequency during the last 74 years but no information on the size and the position of the storms that caused the hail. The method described in Chapter 3 makes it possible to localise and separate the larger hailstorms from the local ones. This was done with all the 596 days during the TS between 1949 and 1993 on which at least 30 damage claims were recorded.

The original cluster-time series (the data base is described in Section 3.6) is given on a daily basis, which makes it a very irregular series, as there are many days without clusters. For further evaluations it will be transformed in a yearly time series, but let us first take a look at a representation of the *raw* data. Figure 4.2.1 shows the daily sum of the cluster areas for the whole time span of 45 years, divided in five lines for reasons of space and readability. To avoid long empty spaces between two summers, the winter seasons (October until March included) have been omitted from the time scale. Although this kind of representation does not allow a trend evaluation, it gives an idea of the distribution of the clusters within the single seasons. In many cases the clusters are bundled in periods of a few days, showing that favourable conditions for thunderstorms often last longer than just one or two days and that such a period of longer hailstorm activity can be enough to define a summer season as a strong hail season, even if the rest of the summer is dry and hot.

The same data set plotted as a time series of annual values is given in Figure 4.2.2. The dotted line represents the original data, the thicker continuous line is an 11 point Gaussian low-pass filter. The computation of a linear regression is not very meaningful for a time series with such a high variability. Besides that, one might be tempted to extrapolate the trend into the future, which is even more meaningless. The higher number of damage claims around 1970 and the increasing tendency in the 80's (e.g. Figures 4.1.2 and 4.1.3) caused also a larger amount of clusters, but it is again not possible to say whether the observed trend during the last decade is the beginning of a long term climate change or if it is the left side of a local maximum like the one of 1970.

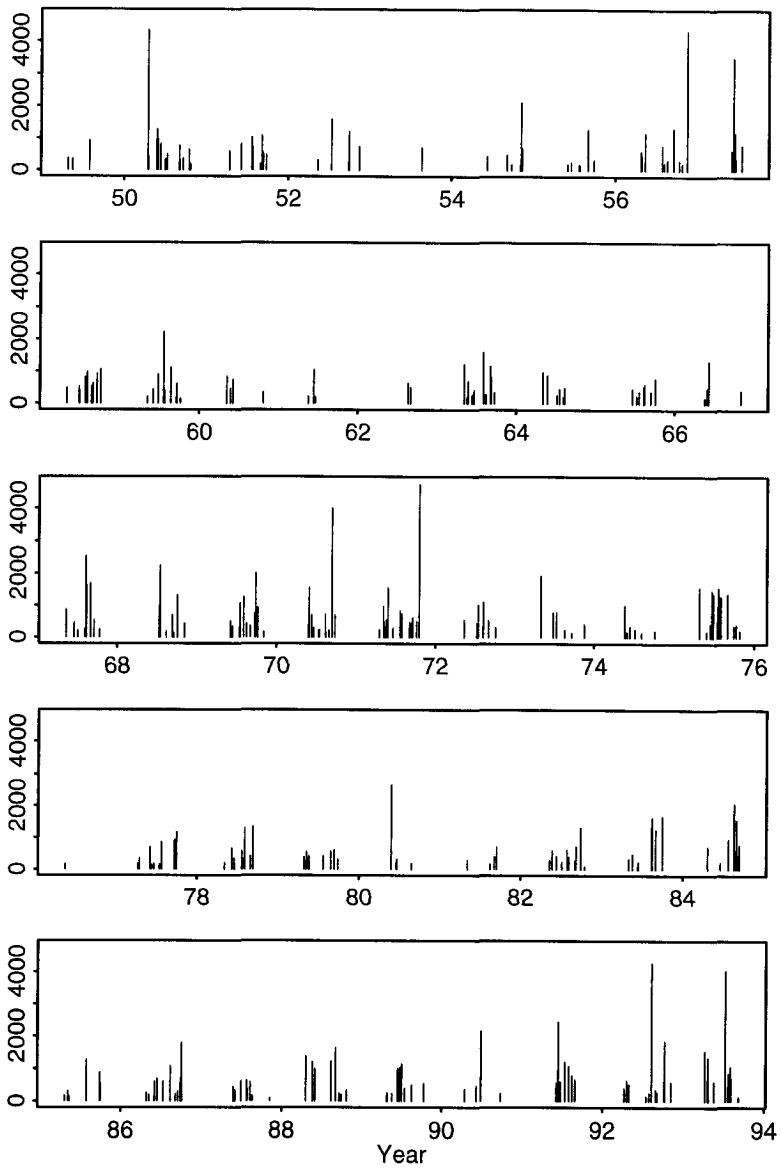

Figure 4.2.1 Daily sum of the cluster areas (in km^2) for the whole observation period of 45 years. Only the days belonging to the summer season are represented on the time scale.

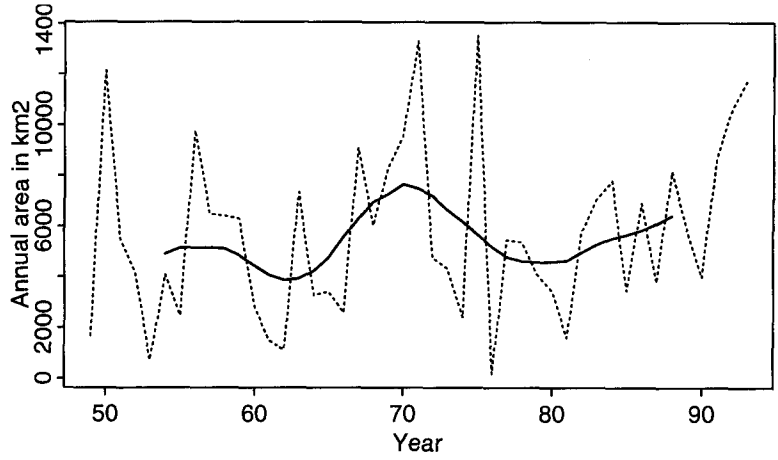

Figure 4.2.2 Annual sum of the cluster areas in km^2. The dotted line is given by the original data and the thick continuous line is an 11 point Gaussian low-pass filter.

Figure 4.2.3 illustrates the time series of the annual number of clusters. The similarity of this curve with the annual sum of the cluster areas points out to the fact that the mean cluster area did not change during this 45 year-time span. The mean annual number of clusters amounts to 14.5, the smallest number was recorded in 1976 with only 1 cluster, while the largest number was recorded in 1971 and in 1975 with 34 clusters.

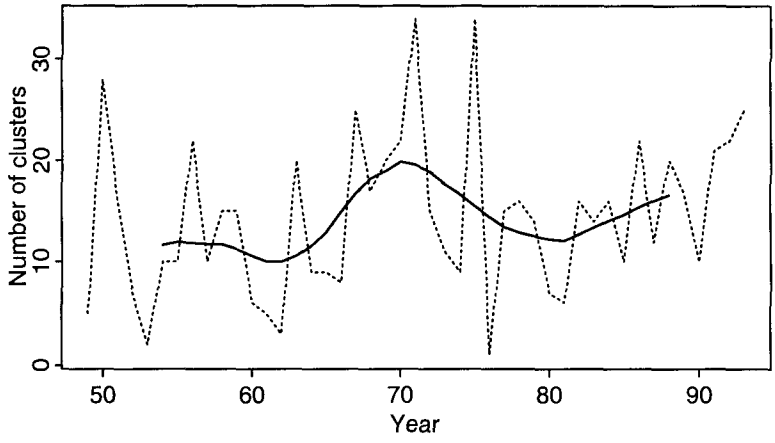

Figure 4.2.3 Annual number of clusters. The dotted line is given by the original data and the thick continuous line is the result of an 11 point Gaussian low-pass filter.

The distribution of the cluster lengths provided in Figure 4.2.4 shows that the majority of clusters do not reach 50 km. The mean length is found to be 42 km, the median (37 km) is smaller because of the right-skewed distribution, and the longest cluster has a length of 179 km. The distribution is cut at a length of 25 km on the left side because of the minimum condition defined for the analysis method (Section 3.6). If this evaluation is limited to the clusters that are completely in the TA (code = 1, 451 clusters), very similar results are found: the distribution has the same shape, the mean value is 41.1 km, the median 35 km and the longest cluster measures 153 km. This indicates that a large portion of the most severe hailstorms originates and decays in the TA.

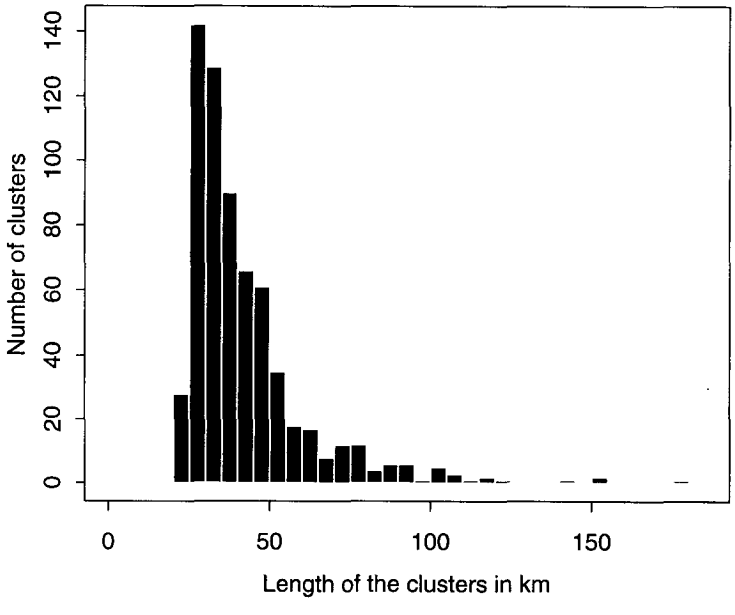

Figure 4.2.4 Distribution of the cluster lengths in km.

The time evolution of the cluster lengths does not reveal remarkable changes during the observed 45 years. Both the shorter clusters (between 25 and 39 km) and the longer ones (more than 39 km) show a large variability, as can be seen from their anomalies plotted in Figures 4.2.5 a) and b). The shorter ones are less frequent during the first 20 years, have a sudden period of positive anomalies around 1970 and finally oscillate around their mean value in the last 15 years. The net effect is a slight increase, which could be due to a real increase of hail swaths of that length as well as to other non-

meteorological factors like a change of the insurance participation or an increase of sensitivity of the crops. For hailstorms of this size a change of these factors might still have some influence on the detection probability. The larger hail swaths show a longer period with alternating positive and negative values lasting until 1981, and a period with predominant positive values during the last 12 years. The last 3 years recorded remarkable positive anomalies, whose interpretation remains very uncertain. The influence of the non-meteorological factors mentioned above on these larger hail clusters probably are reduced, therefore the variations illustrated in Figure 4.2.5 b) might be caused mainly by changes of the hailstorm activity. Once more it is impossible to tell if the more frequent positive anomalies of the last years are connected with a long term climate change or if they belong to one of the numerous shorter period oscillations.

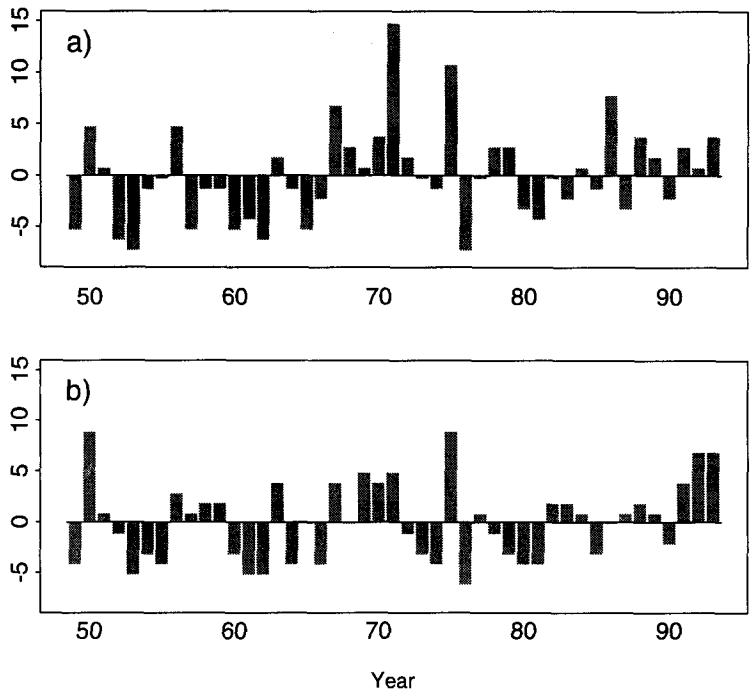

Figure 4.2.5 Annual number of clusters a) with a length between 25 and 39 km, b) longer than 39 km expressed as anomaly with regard to the mean value (a)=8.3, b)=5.1 clusters per year).

The geographical distribution of the hail swaths also experienced some changes during the 45 year-observation period, as can be seen

from the plot-series (a) to (i) of Figure 4.2.6. Each one of these plots illustrates the storm tracks recorded during the TS's of one pentad of the OP. The most outstanding features are:

1949 - 53: low number of swaths, quite well distributed over the whole test area.

1954 - 58: number of swaths slightly higher than during the previous pentad, concentration in the south-central and in the eastern part of the TA.

1959 - 63: pentad with the lowest number of hail swaths. Most of them are concentrated in the Napf-region (south-central part of the TA), the remaining ones are in the north-east.

1964 - 68: situation similar to the one in the second pentad.

1969 - 73: pentad with the highest total number of clusters and with the largest amount of very long (≥ 75 km) ones, too. The highest density is on the eastern side of the TA, but the western part also shows a density higher than usual. Only the Basel-region stayed fairly untouched (like in the previous pentad).

1974 - 78: situation similar to the one in the second pentad.

1979 - 83: number of hail swaths like the first pentad, but with a different distribution. This time the density is very small in the Napf-region but unusual high in the western Mittelland. The Luzern-area does not show remarkable anomalies.

1984 - 88: amount of clusters slightly above the mean value of 72 per pentad, with a distribution similar to the one in the second pentad, except for the higher density in the centre-northern area.

1989 - 93: second highest number of swaths, with a distribution similar to the previous one.

The number of very large clusters (with a length ≥ 75 km) shows a strong variability: during the period '59 - '63 only one cluster with a length between 75 and 100 km was observed, while during the pentad '69 - '73 12 very long clusters were recorded. The reasons for these differences from pentad to pentad will be investigated in the next section, where our data set will be compared with other climatological data sets.

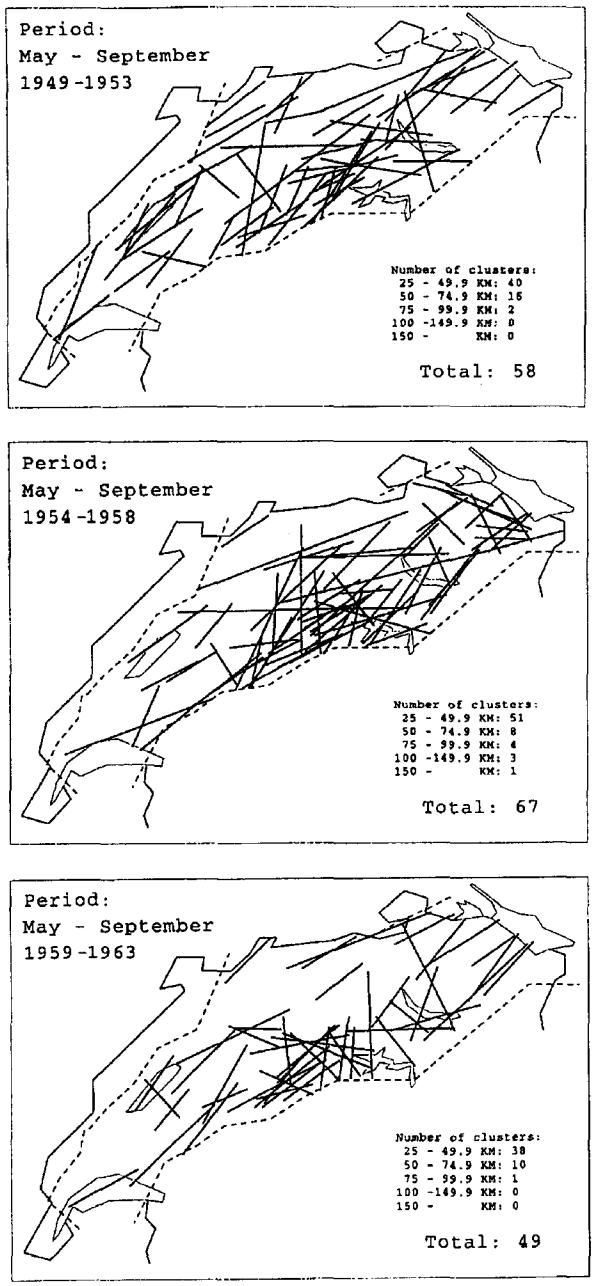

Figure 4.2.6 a Geographical distribution of the hail swaths for time intervals of five years: 1949 - 1953, 1954 - 1958, and 1959 - 1963.

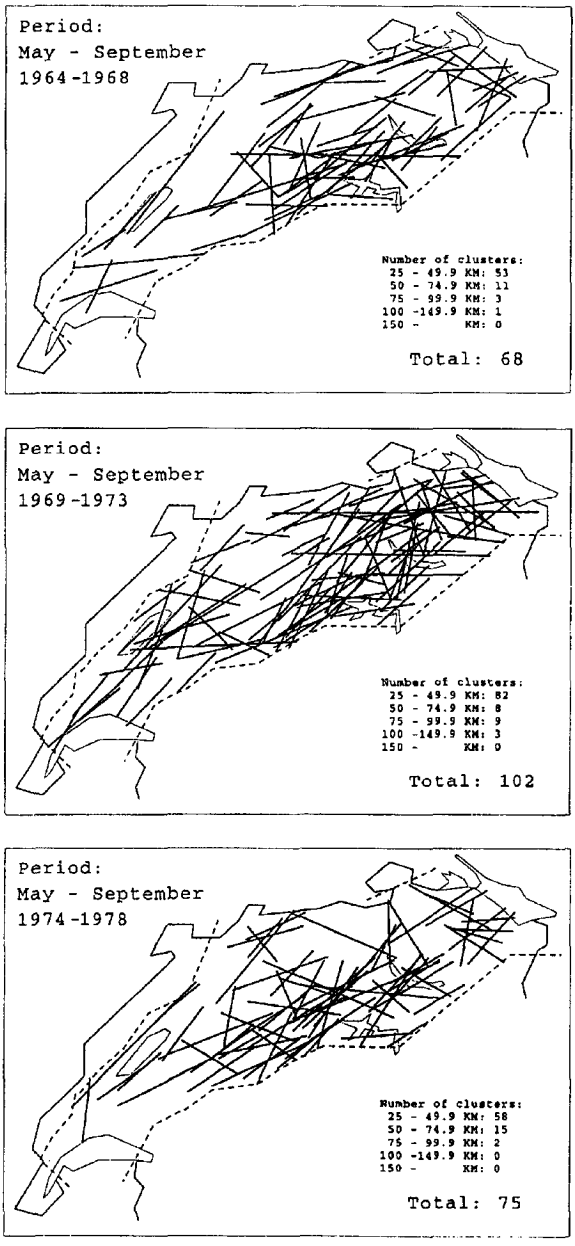

Figure 4.2.6 b Geographical distribution of the hail swaths for time intervals of five years: 1964 - 1968, 1969 - 1973, and 1974 - 1978.

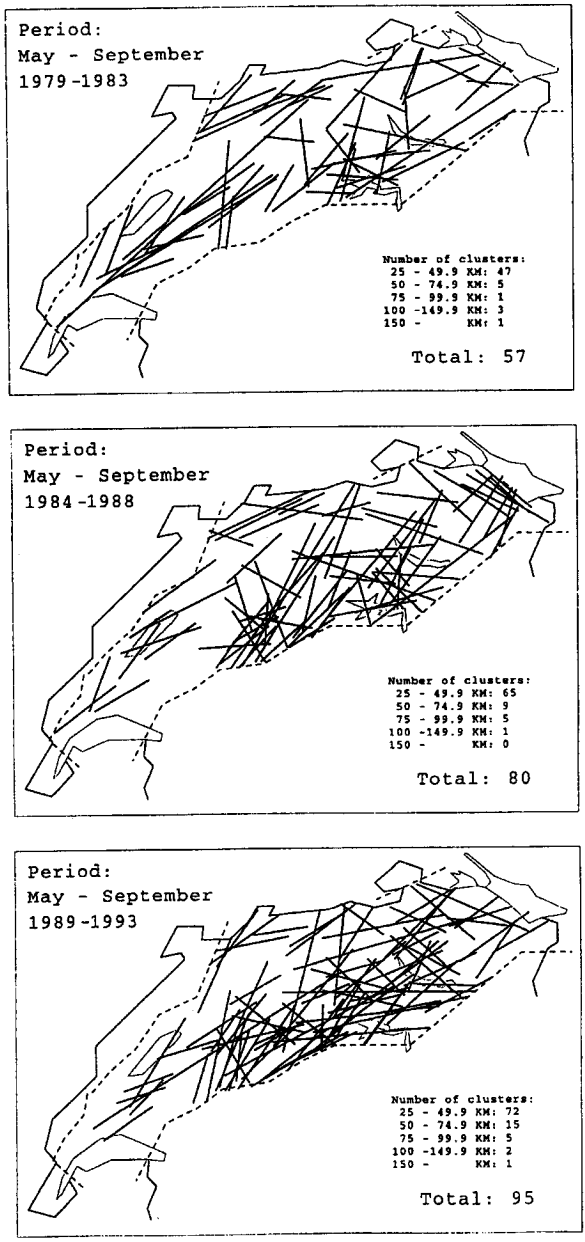

Figure 4.2.6 c Geographical distribution of the hail swaths for time intervals of five years: 1979 - 1983, 1984 - 1988, and 1989 - 1993.

Further interesting observations can be made on the seasonal evolution of the location of the hail clusters: in Figure 4.2.7 the swaths of the whole observation period are grouped by month. Again, for the months of May and September only the days during the TS were considered.

This illustration shows a quite striking *migration* with time of the hailstorms from the central Prealpine and the eastern areas to the rest of the TA.

May: hailstorms originate mainly in the Prealpine region, in airmass situations, and leave relatively short tracks.

June: tracks are found also in the north east and some longer ones cross the Mittelland.

July: month with the highest number of hail swaths (218), which now extend also into the western Mittelland. The region of Solothurn is still spared from swaths.

August: this month shows the most homogeneous distribution of the hail swaths over the whole TA, but their number shrunk compared to the two previous months.

September: the number of swaths for this month cannot be compared directly with the other ones (a multiplication by 3 to obtain the equivalent number for the whole month would probably overestimate the real number of clusters). However, one important feature that stands out quite clearly is the fact that the tracks recorded in September are distributed everywhere within the TA and are, on the average, very long.

Altogether, the best conditions for strong, long-lived hailstorms are reached in the second half of the hail season, probably because the frontal systems crossing the country in this period are connected with the most unstable conditions. In the first part of the season the most favourable conditions for the release of stronger hailstorms are met in the Prealpine areas, favoured by the upslope thermal wind and by the fact that the triggering temperature is usually reached faster and / or earlier than in the lower and flatter regions, but these hailstorms usually are not as long-lived as those triggered by frontal systems.

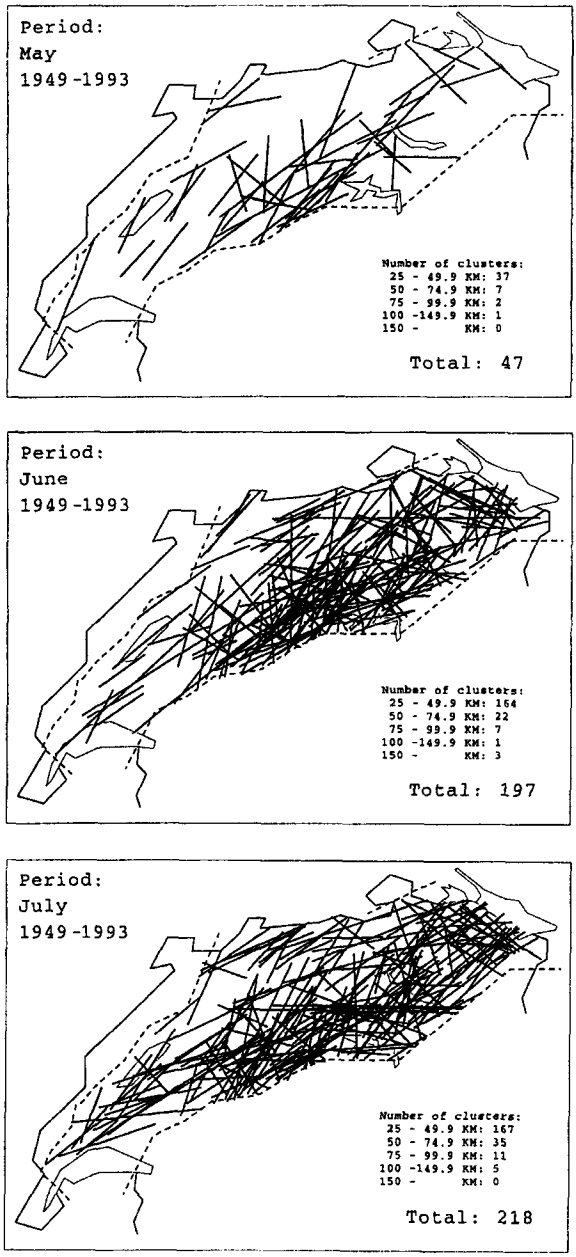

Figure 4.2.7 a Geographical distribution of the hail swaths for every month of the TS (for the months of May and September only the last 12, resp. the first 10 days were considered): May, June and July.

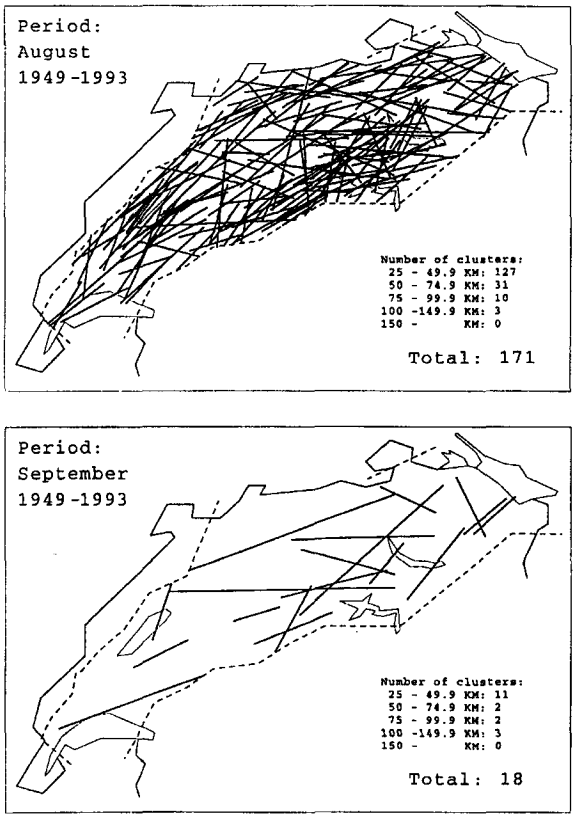

Figure 4.2.7 b Geographical distribution of the hail swaths for every month of the TS (for the months of May and September only the last 12, resp. the first 10 days were considered): August and September.

The last figure of the *geographical series* (Figure 4.2.8) gives an overview of the whole 45 year-observation period. Many of the single swaths are not recognisable any more, but the most frequent paths of these hailstorms can still be seen. Essentially three areas show a surprising lower density of tracks: beginning from the lower left corner, the first one is the Moléson region (coordinates 570 / 160), which is quite a mountainous area with a lower density of crops. In this region the lower density of hail swaths could be an artefact. The second low density area, between Biel and Solothurn (610 / 235), is a region of intensive agricultural exploitation and therefore the lack of trajectories might be natural. The third area being crossed by an unusual low number of swaths is the hilly territory south of Wil (SG)

(coordinates 710 / 250), where agriculture is not as wide spread as in some other areas, but surely not less than in the Napf region , which is completely covered by hail swaths. For this reason this low density area is expected to be given, at least partly, by natural lack of hailstorms.

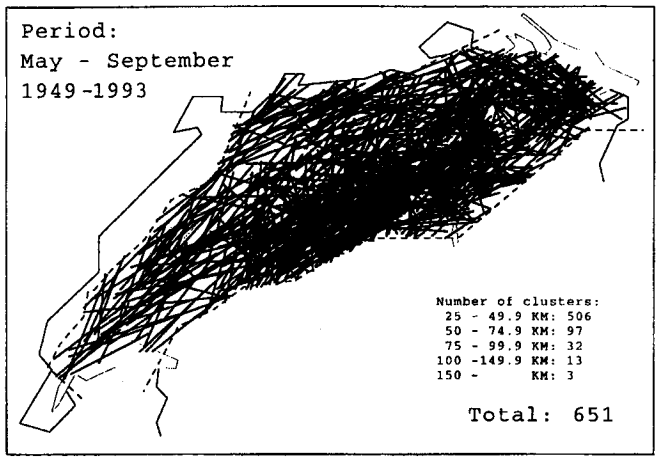

Figure 4.2.8 Tracks of all hail clusters recorded during the observation period of 45 years.

Some other regions with a low track density are observed along the borders of the TA, but these are mainly due to border effects, except for the southern border of the eastern area, which crosses mountainous regions without cultures. On the other hand, the hilly territory around the Napf with a rather low density of cultures, confirms its fame of *birthplace* of many hailstorms, as has been observed with RADAR measurements. This is a point in favour of the use of the hail insurance data.

Another feature that captures the attention in these figures is the orientation of the clusters, which corresponds roughly to the direction of movement of the hail cell. The longer the swaths are, the more they are oriented along the Southwest - Northeast axis. If this were an artefact caused by the shape and the orientation of the TA there would be many clusters crossing the TA in Northwest - Southeast direction, but this kind of clusters constitutes only 1 % of all recorded clusters. Furthermore, 78 % of the clusters entering or exiting the TA (code 2 and 3, 30 % of the total amount of clusters)

are oriented in a direction between 180° and 270°. In Figure 4.2.9 the orientation of each cluster is plotted against its length, showing that the predominant part of the clusters are located between 180° and 300°, and that the longest ones are concentrated in the SW to W sector.

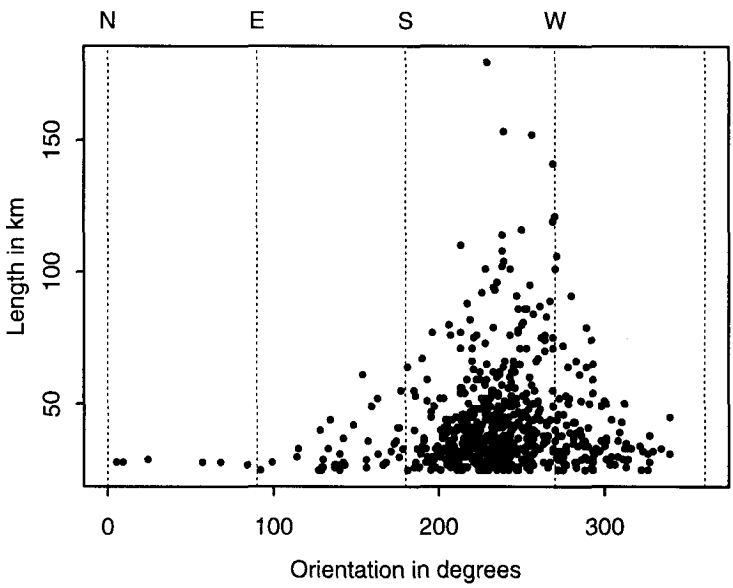

Figure 4.2.9 Orientation of the hail clusters compared to their length.

The mean direction of all clusters during the whole 45 - year period is of 238°, but the variability of the annual mean is quite strong, as can be seen from Figure 4.2.10. Although no clear trends or periods are visible, the largest deviations from the mean are found in the 70's. However, the interpretation of this figure needs some caution because some of the yearly means are computed with a very low number of clusters (particularly in 1976).

In 499 cases (out of 651) the time of appearance of the clusters could be defined approximately with the help of thunderstorm observation maps of the SMA. In these maps the time of every thunderstorm observation made by official observers is indicated on its approximate geographical position, so that particularly in the case of hail cells that have covered a longer distance, a kind of time track can be compared with the hail clusters. The time indicated in the data set corresponds approximately to the time found in the middle of the hailswath. Figure 4.2.11 illustrates the distribution of the

appearance time of the hail cells that produced the recorded clusters. Most of the hailstorms were active between 14 and 21 p.m. (12 - 19 UTC), some between 10 a.m. and 14 p.m. (8 - 12 UTC) and some in the later hours of the evening. Between midnight and 10 a.m. larger hailstorms were rather rare.

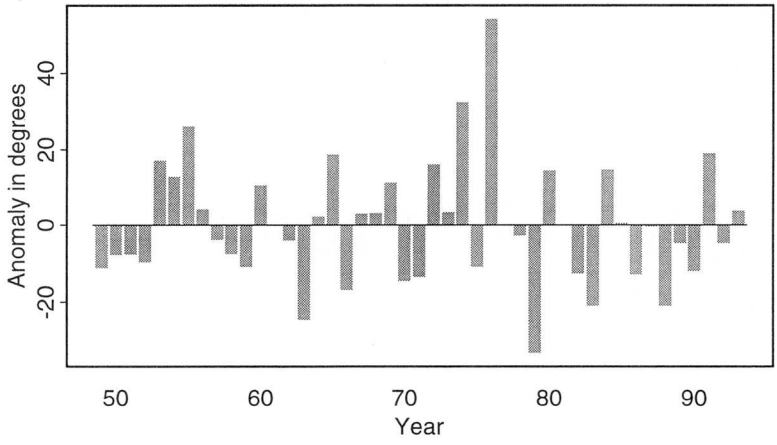

Figure 4.2.10 Annual mean orientation of the clusters (45 - year mean: 238°)

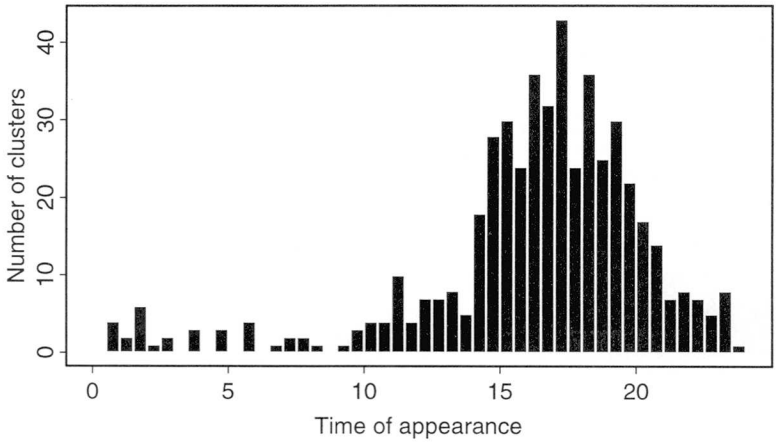

Figure 4.2.11 Distribution of the time of appearance of the hailstorms causing the recorded damage clusters.

This first part of the insurance data-analysis leads us to the conclusion that the variability of hailstorm activity is very large. The

signal to noise ratio is too small and the time series still too short as to enable speculations on the future evolution of hailstorm activity. For this reason we will continue our search for connections between hailstorm activity and climatic changes on an indirect way. In the next chapters we will try to define the meteorological environment of hailstorms and to describe a few possible future scenarios.

5 Connections between hail damage and meteorological data

The overview of the main features of the damage claim- and cluster-data sets presented in Chapter 4 is now followed by an analysis of the connections between these data sets and meteorological data sets. The aim of this chapter is to examine if strong haildays are characterised by meteorological features which distinguish them from fair weather-days.

5.1 Description of the available data sets

In the following the hailstorm days on which clusters were recorded will be referred to with *cluster days*.

A) Airflow and frontal activity

The origin of the air reaching the TA plays an important role on the triggering of hailstorms. Such information is available from the SMA annals, which indicate the origin of the airmass observed over Switzerland for every day of the year at noon in five classes:

aa arctic polar air

mp maritime polar air

cp continental polar air (or land-modified mp)

mt maritime tropical air (might also have cooled and aged)

ct continental tropical air (mt modified by föhn also possible)

The same SMA annals provide also the information on frontal passages. The frontal activity of every cluster day has been described with the following classification:

pf passage of the front during the next day (prefrontal)

fr passage of the front on the same day

ai no frontal activity (airmass day)

Although the most commonly used classification contains only two classes (frontal and airmass days), we decided to add the class **pf** for a better differentiation. Schiesser (1985) also describes the use of such a third class.

This information is available for every cluster day of the 45-year observation period and for every day of the May-September test period of the years '78 to '89.

B) Temperature

The temperature-data used in this work were taken from the Swiss Climate Data Base (SCDB) available at the SMA. Two time series of daily mean maximum and mean minimum temperatures (1920-92 and 1949-92) were calculated from stations distributed over the Mittelland, which were chosen with the following criteria:

- height above sea level of approximately 500 m
- temperature recording without interruptions during the whole time span
- equal number of stations for the western, the central and the eastern part of the TA

For the longer time series (since 1920) only three stations satisfied these criteria, i.e. Bern-Liebefeld, Neuchâtel and Zürich-SMA, while for the shorter ones (since 1949) three additional stations were available (Basel-Binningen, Luzern, Montreux-Clarens). Before the computation of the mean values the temperatures of every station were transformed, with the assumption of a lapse rate of a 0.6 °C / 100 m, into the corresponding values at the height of 500 m above sea level.

A comparison of the series calculated with three stations with the one calculated with six stations for the years 1949-92 showed that the differences are negligible.

The temperature data of the SCDB have already been used by other research groups for studies on regional climate change in Switzerland and in the Alpine area (Beniston et al. 1994; Weber et al. 1994). As they found that the data are of good quality and reliable enough for such studies we did not test them on homogeneity in further detail.

C) Weather classifications

Schüepp - classification (SC):

This weather classification was designed for the Swiss meteorological conditions, which are heavily influenced by the presence of the Alps. The main part of the classification has been done by Schüepp (1979). On the Swiss territory the mountain chain

of the Alps is oriented in a SW - NE direction, causing strong leeward and windward effects (e.g. Föhn) in situations of southerly or northerly flow, and is located roughly at the latitude of the polar front. Along the east - west axis, Switzerland lies in a transition zone from oceanic to continental climate, so that, depending on the origin of the airflow reaching the country, the features of both kinds of climate can be observed.

The whole classification is valid for a circular area with a radius corresponding to two degrees of latitude (222 km), centred in the middle of the Alps at 46.5° north and 9° east, i.e. near the Rheinwaldhorn. This circle encloses the whole Swiss territory and the adjacent border areas of France, Italy, Austria and Germany.

The SC is carried out according to the following three steps:

i) Definition of the predominant flow:

Vertical → **I**: convective situations

Horizontal → **II**: advective situations

Horizontal and vertical → **III**: mixed situations

ii) Specification of the direction of the predominant flow:

(I): **H**: high pressure; **F**: flat pressure distribution; **L**: low pressure (defined with respect to the average pressure at the 500 hPa level)

(II): **W**: westerly flow; **N**: northerly flow; **E**: easterly flow; **S**: southerly flow

(III): **Xx**: cyclonic situation; **Xj**; jetstream situation with weak surface flow; **Xø**: strong surface flow, weak upper level flow

iii) Specification of the non - predominant part of the flow and / or of other important features:

(I): generally weak surface winds combined with:

ø: weak upper level winds; **w**: westerly upper level flow; **n**: northerly upper level flow; **e**: easterly upper level flow; **s**: southerly upper level flow

(II): **j**: jet stream at the upper level; **+p**: upper level pressure above normal, upper and lower level flow parallel; **-p**: upper level pressure below normal, upper and lower level flow parallel; **+x**: upper level pressure above normal, rotation of the wind with height; **-x**: upper level pressure below normal, rotation of the wind with height

(III): (only for the classes Xj and Xø) +: upper level pressure above normal; -: upper level pressure below normal

Every weather class was assigned a number, indicated in Table 5.1.1 and used for the plot labelling.

Nr.	Class	Nr.	Class	Nr.	Class	Nr.	Class
1	$H_ø$	11	$L_ø$	21	N_j	31	S_j
2	H_w	12	L_w	22	$+N_p$	32	$+S_p$
3	H_n	13	L_n	23	$-N_p$	33	$-S_p$
4	H_e	14	L_e	24	$+N_x$	34	$+S_x$
5	H_s	15	L_s	25	$-N_x$	35	$-S_x$
6	$F_ø$	16	W_j	26	E_j	36	X_x
7	F_w	17	$+W_p$	27	$+E_p$	37	$+X_j$
8	F_n	18	$-W_p$	28	$-E_p$	38	$-X_j$
9	F_e	19	$+W_x$	29	$+E_x$	39	$+X_ø$
10	F_s	20	$-W_x$	30	$-E_x$	40	$-X_ø$

Table 5.1.1 SC: weather classes with their corresponding number.

Note that the four main wind sectors W, N, E and S do not contain the same number of 45° sectors (see Figure 5.1.1).

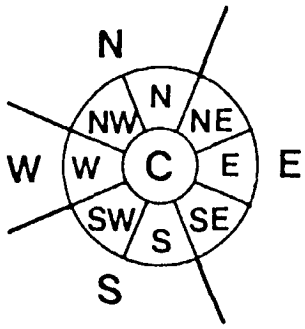

Figure 5.1.1 Assignment of the 45° sectors to the main wind sectors according to the Schüepp classification.

The most important consequence of this irregular subdivision for the present work is that flow indicated as southerly flow can have a more or less large westerly component, which on the northern part of the Alps leads to weather situations ranging from the thunderstorm inhibiting föhn situation to the thunderstorm favouring maritime tropical air-advection from the south-west.

Hess - Brezowsky classification (HBC):

Compared to the SC, the Hess-Brezowsky classification (in the following HBC), which was developed at the German weather service (DWD) includes a much larger area, i.e. all European countries, with Germany at the centre (Hess and Brezowsky 1952; Gerstengarbe and Werner 1993).

The 29 (+1) *Grosswetterlagen* are split into three subgroups, depending on the zonality / meridionality of the flow. Class number 30 was created to collect all cases that could not be classified using one of the 29 defined classes. No further division in subgroups was undertaken. The whole list of *Grosswetterlagen* is given in Table 5.1.2 with their short description. In the following the single weather situations will be indicated by their number as shown on the left of Table 5.1.2.

Nr.	Description	Code
A. Weather situations with zonal circulation		
1	westerly flow, anticyclonic	Wa
2	westerly flow, cyclonic	Wz
3	southern westerly flow	WS
4	"winkelförmige" westerly flow	WW
B. Weather situations with mixed circulation		
5	south - westerly flow, anticyclonic	SWa
6	south - westerly flow, cyclonic	SWz
7	north - westerly flow, anticyclonic	NWa
8	north - westerly flow, cyclonic	NWz
9	high pressure over central Europe	HM
10	high pressure bridge over central Europe	BM
11	low pressure over central Europe	TM

C. Weather situations with meridional circulation		
12	northerly flow, anticyclonic	Na
13	northerly flow, cyclonic	NZ
14	high over North Sea / Iceland, anti-cyclonic	HNa
15	high over North Sea / Iceland, cyclonic	HNz
16	high over the British Isles	HB
17	trough over central Europe	TRM
18	north - easterly flow, anticyclonic	NEa
19	north - easterly flow, cyclonic	NEz
20	high over Scandinavia, anticyclonic	HFa
21	high over Scandinavia, cyclonic	HFz
22	high over North Sea / Scandinavia, anticyclonic	HNFa
23	high over North Sea / Scandinavia, cyclonic	HNFz
24	south - easterly flow, anticyclonic	SEa
25	south - easterly flow, cyclonic	SEz
26	southerly flow, anticyclonic	Sa
27	southerly flow, cyclonic	Sz
28	low over British Isles	TB
29	trough over western Europe	TRW
30	not classified cases	–

Table 5.1.2 HBC: Grosswetterlagen and their corresponding number.

D) Radiosoundings

The SMA operates only one radiosonde station, which is located in Payerne (for its geographical position see Appendix C). The soundings are carried out twice a day, at noon (12 UTC) and at midnight (00 UTC), (UTC: universal time coordinated; local time is UTC + 1 h, local summertime +2 h).

The first soundings measured on a daily basis were made in 1954. Until 1956 the average number of measured levels oscillated between 13 and 14, then it gradually increased to 41 levels in 1982. In 1983 the sounding measurement system was changed and the resolution increased to about 170 data points per sounding, after 1990 this

number was doubled and in 1993 a number of 415 levels was reached.

The measured parameters are:

- Temperature
- Dew-point temperature
- Pressure
- Wind speed and direction
- Ozone concentration

The whole set of soundings with the raw data and some derived parameters is now available on the Oracle data base of the institute.

Most of the analyses in Section 5.5 are done with parameters derived from the original sounding measurements: convective available potential energy (CAPE), wind shear (S), convective condensation level (CCL), lifting condensation level (LCL) and 0 °C level.

The CAPE represents the buoyant instability of the environment and S is the density weighted mean of the wind shear of the layer between 0.5 and 6 km. Their computation is described in Chapter 1.

Also the CCL used here is a modified version of the standard CCL. It is computed with the mean dew point temperature of the layer between ground level and 850 hPa instead of the single dew point temperature at ground level (Federer et al. 1973; Mahrt 1976; Banta 1990). It has been found that such a mean value better represents the humidity conditions necessary for the calculation of the CCL than the mere ground level dew point temperature .

The LCL available from the institute's data base is a modified version of the one described in Chapter 1, which has been used in several works mentioned in literature (e.g. Marwitz, 1972, Fankhauser et al., 1976). Here the temperature and the dew point used as starting points are not the values found at ground level but the mean values of the lower 400 m (50 hPa).

Representativity of the sounding for hailstorm days in the Mittelland.

The airflow situation in the free atmosphere over a topographically complicated country like Switzerland can hardly be described with one vertical profile. Particularly the conditions over the Alpine region and the southern part of Switzerland usually are quite different from those over the Mittelland. However, as our test area is restricted to the Mittelland and the Jura mountains, i.e. north of the

Alps, the representativity of the Payerne sounding depends mainly on the dominant airflow. On days of south-westerly or westerly flow, the profile measured in Payerne is thought to be valid for the whole Mittelland. Similar assumptions were made by Schiesser (1985), who checked the representativity of the Payerne sounding with soundings carried out at a location 100 km farther north-east, and by Houze et al. (1993) in connection with the field measurements of Grossversuch IV. Since most of the larger hailstorms originate in southwesterly to westerly flows (see Chapter 4, Figure 4.2.9) the Payerne sounding is taken as representative for the environmental conditions in the free atmosphere, provided that the sounding precedes the appearance of the storm. On the other hand, on days with southerly flow, a sounding over eastern Switzerland would measure dryer conditions than those measured in Payerne. Therefore, on hailstorm-free days the representativity can be worse.

At the time the evaluations in Section 5.5 were carried out, only a reduced data set was available on the database, for this reason all analyses were made with the sounding data of the years 1978 to 1989 (included). The complete data set is available for 1'287 days out of the 1'368 days of the considered time span, and therefore all analyses of and comparisons with these data are made with this reduced number of days.

E) Stratification of the analysed days in four categories

For several evaluations all available days have been stratified in four categories as follows:

1 days without damage claims

2 days with a number of damage claims between 1 and 29

3 days with more than 29 claims but without clusters

4 days with clusters

The reason for the choice of the number 29 (damage claiming communities) is mentioned in Section 3.6.

5.2 Airflow and frontal activity

In this section we will consider three different classifications (described in Sections 6.1 A) and 6.1 E)) of the analysed days:

1. Airflow: aa, mp, cp, mt, ct.

2. Frontal activity: pf, fr, ai.

3. Number of damage claiming communities: categories 1 to 4.

The first comments consider mainly the connections between *cluster days* (category 4 of classification 3) and classifications 1 and 2.

The evaluation of the clusters (Chapter 4) show that most of the responsible hailstorms moved from SW to NE. In situations of south-westerly flow the air is mostly of maritime tropical (mt) origin. In fact, from all cluster days 213 (59 %) were mt-days, only 82 (23 %) mp-days, 55 (15 %) ct-days, 9 (2 %) cp-days and 4 (1 %) were aa-days. If we consider the frontal activity we find that 76 % of the prefrontal, 62 % of the frontal and 42 % of the airmass cluster days are connected with mt airflow. The distribution of airflow types is illustrated in Figure 5.2.1.

Figure 5.2.1 confirms the expectations of severe hailstorms in mt / frontal situations. The air ahead of a cold front, usually coming from the south-west, is mostly warm and moist. The convergence along the front causes it to be lifted above the cold and heavier air behind the front. This forced convective lifting results in the rapid condensation of abundant water vapor and consequently in strong precipitation, in summer often in the form of thunderstorms. This explains the fact that prefrontal clusters mostly appear in mt airflow; the exceptions are probably connected with cases where the influence of the approaching front was very weak and the dominating airflow still given by the previous weather situation (*prefrontal* means that the front reached the TA on the following day but does not say anything about its distance on the cluster day).

The relatively high frequency of mp airflow on frontal cluster days can be explained by the fact that the air behind a cold front usually is of maritime polar origin and even if it is cooler at lower levels it might be still unstable enough to trigger some larger thunderstorms. As the classification of the airflow is done at noon, in the case of a frontal passage in the morning it will record the airflow behind the front.

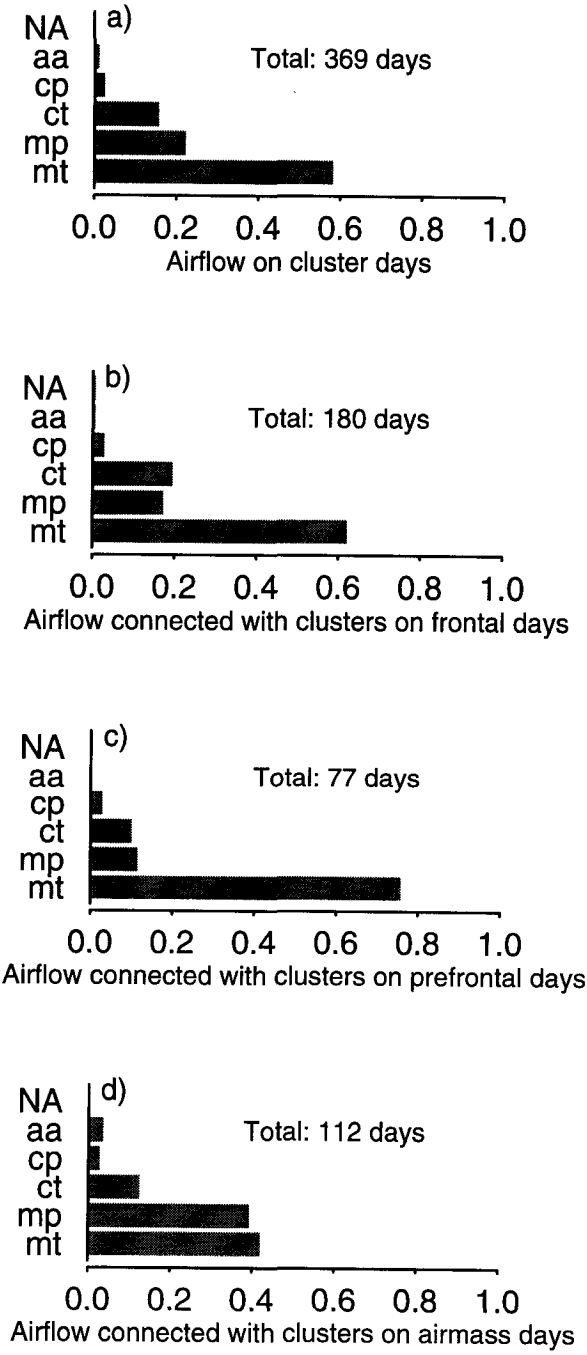

Figure 5.2.1 Distribution of airflow types on cluster days (NA means *not available*), a) on all cluster days b) on frontal, c) prefrontal and d) airmass days.

More surprising is that in a relatively high number of frontal cluster days the flow is classified as continental tropical, which is warm dryer air coming from the African continent or from the Middle East. The beginning points of the clusters on these days are fairly well distributed over the whole test area and not limited to the western part, as would be expected in föhn-situations.

All clusters developing in ct-airflow are oriented in a south-western direction, which probably means that the wind in the Mittelland is not directly connected with ct-airflow. Case studies of severe thunderstorm days under investigation at LAPETH (personal communication with H. Huntrieser) show that some larger hailstorms were triggered in flow situations where south-westerly winds were measured in the Mittelland and at the same time southerly winds were blowing over the Alps. An explanation for such a wind regime could be that strong advection from the south causes a local low pressure centre in the lee of the Alps which sucks the maritime tropical air ahead of the approaching front toward the Mittelland. This situation is sketched in Figure 5.2.2.

In cases where the low pressure system connected with the advancing cold front is located far south (over southern Spain or over the western Mediterranean), the air flowing into the warm sector on its right side is of continental tropical origin. In these cases the hailstorms are triggered at the passage of the front and not in the prefrontal region.

After these considerations on cluster days we will dedicate some attention to the complete data set (categories 1 to 4 of classification 3), which is available for the TS of 12 years ('78 - '89). During this time span the frequency of occurrence of the different airflow types shows the following distribution: 44 % mp-days, 33.7 % mt-days, 17 % ct-days, 5 % cp-days and 0.3 % aa-days. A comparison with the percentages mentioned at the beginning of this section evidences larger differences for the first two categories (21 % less mp-days and 25 % more mt-days on cluster days) and no remarkable difference for the remaining three categories.

Figure 5.2.3 evidences that the probability of hailstorm origin in mt airflow increases with its severity and its degree of organisation. The difference between category 3 and category 4 is mainly that in the latter one the damage claims are *organised* in larger clusters mostly connected to long living hail cells, while the claims on category 3 - days are distributed more randomly over the test area without forming remarkable clusters. mp-airflow seems to be more favourable

to smaller hailstorms, while cp-airflow inhibits larger hailstorms (categories 3 and 4).

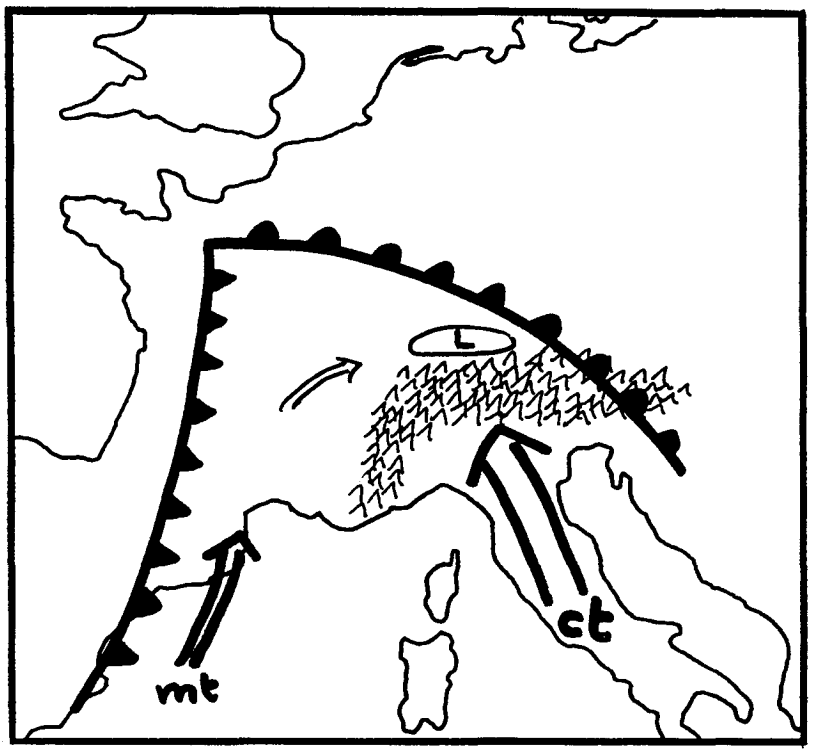

Figure 5.2.2 Synoptic situation on cluster days with continental tropical airflow.

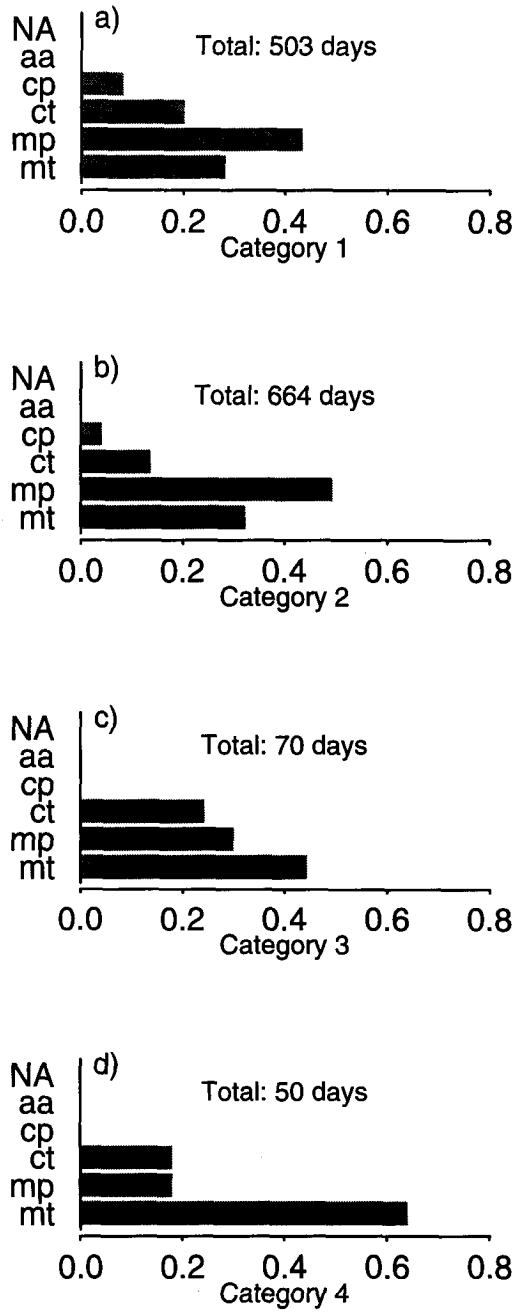

Figure 5.2.3 Distribution of the airflow types for the categories 1 - 4 described in section 5.1 E.

5.3 Temperature

All temperature-time series considered in this work are limited to the test season and therefore they are not directly comparable with temperature series of annual means published in other works. As the difference between the 1949 - 92 temperature series calculated with 6 stations and the 1920 - 92 series computed with 3 stations is negligible for the purpose of this work, it was decided to consider the longer series for a first analysis of the temperature data. Later on, for the comparison with the cluster data, the shorter series will be used.

The most traditional way of determining climate and climate change is to describe it in terms of mean values, whereas the importance of extreme values has gained the attention of climatologists only in the recent years. For a thunderstorm climatology the minimum and maximum temperatures are expected to be more meaningful than the mean temperature, therefore the present analysis will concentrate on the extreme values.

Figure 5.3.1 shows the seasonal average (over the 114 days of the TS) of the minimum, the mean and the maximum temperatures. The mean temperatures were computed as an average of the daily minimum and maximum. The dotted lines are the original data, the smoothed curves represented by the continuous lines were computed with an 11 point Gaussian low-pass filter, and the linear regression (dashed line) was calculated with a least square fit. The vertical dashed lines indicate the beginning of the cluster-time series (1949).

The same features observed in climatological analyses on a yearly basis (Beniston et al. 1994; Weber et al. 1994) are to be seen for the summer season. The minimum temperature follows an increasing trend, with maxima around 1950 and in the mid 70's, while the maximum temperature shows a slightly decreasing trend with one clear maximum around 1950, coinciding with the first one of the minimum temperature. The difference in variability between the minimum and maximum temperatures is quite remarkable (the size of the y-axis is the same for all three plots). The seasonal mean temperature does not follow any remarkable trend. A longer period of higher temperatures are found in the second half of the 40's and at the beginning of the 50's and the variability is generally fairly large.

The monthly mean minimum temperatures (Figure 5.3.2) show similar features particularly in July and August, while in May the two maxima are quite evident but no long lasting trend is observed. However, the curves for the months of May and September should be interpreted with caution, as they were computed only with that part

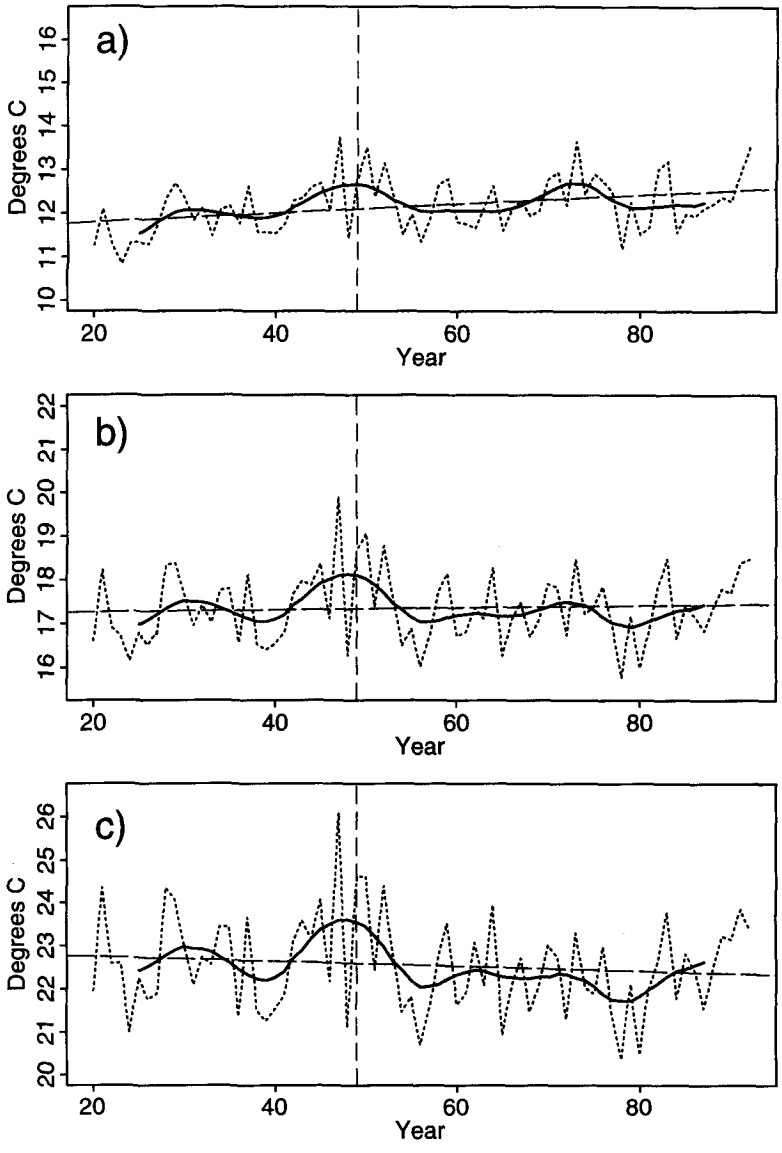

Figure 5.3.1 *Seasonal mean average minimum (a), mean (b) and maximum (c) temperatures since 1920. Smoothed curve: 11 point Gaussian low-pass filter; linear regression: least square fit. The vertical line at '49 indicates the beginning of the cluster-time series.*

of the monthly data that fits in the test period. In June the minimum temperature shows a larger variability during the first decade and smaller oscillations during the last one, but on the whole the variability is small and the linear regression has only a slight positive

slope which is mainly caused by the low values at the beginning of time series

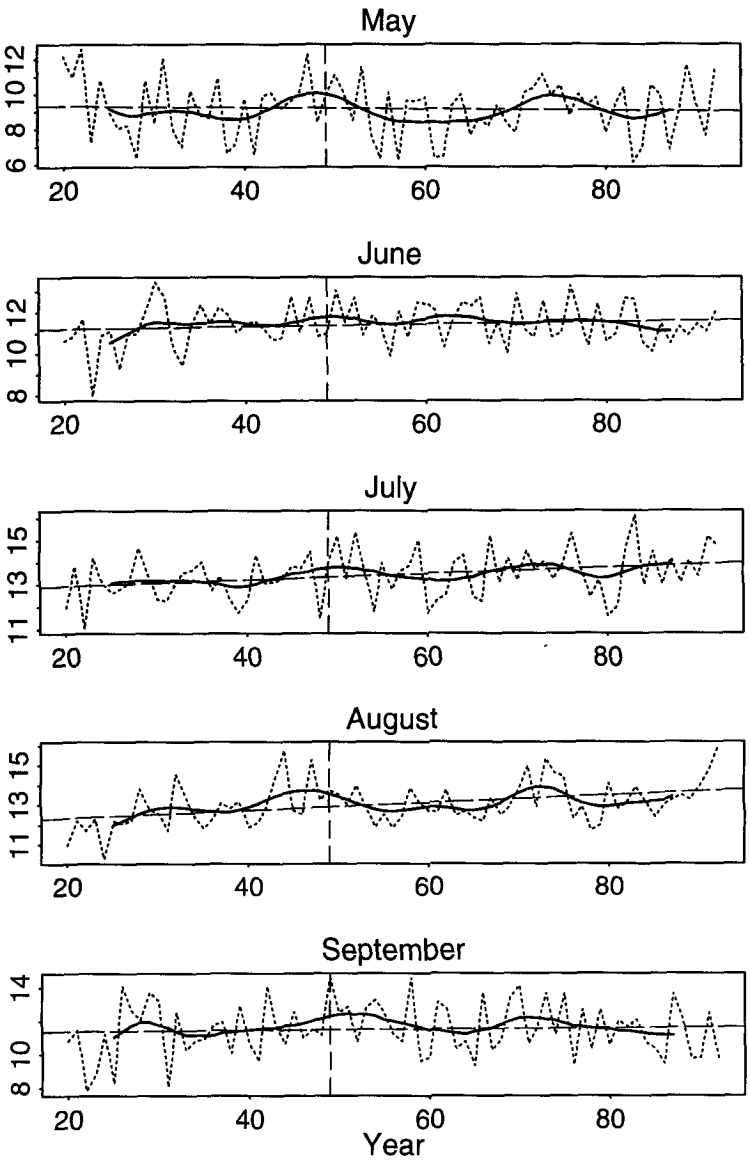

Figure 5.3.2 As Figure 5.3.1 but for the monthly mean average minimum temperature. The curves for the months of May and September were computed only with the days included in the test period.

The same kind of representation as for the monthly mean minimum was produced for the maximum temperatures and is represented in Figure 5.3.3.

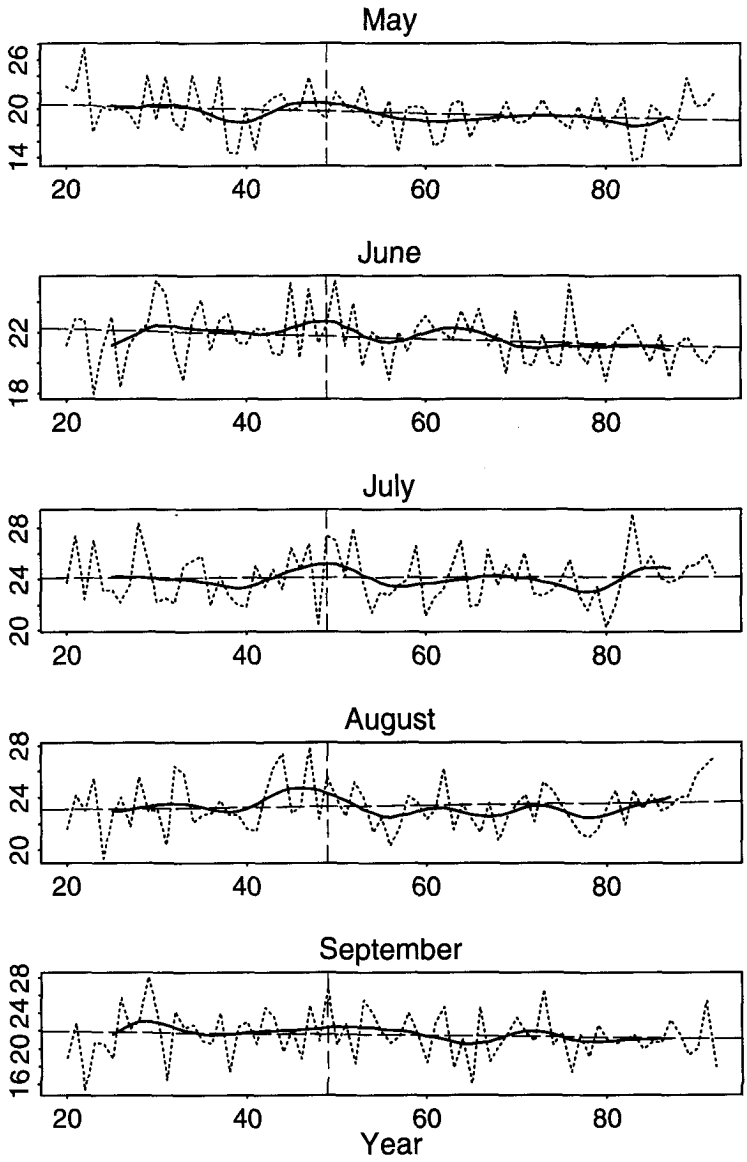

Figure 5.3.3 As Figure 5.3.2 but for the monthly mean average maximum temperature.

The large seasonal maximum around 1950 is clearly recognisable also in the main summer months, whereas the minimum around 1980 is originated mainly in July and August. On the other hand, the strongest general decreasing tendency is observed in June. May and September follow the general downward trend but do not show any pronounced maximum or minimum.

An increase of nocturnal temperatures and stable or decreasing daily maximum temperatures lead to a general decrease of the 24-hour temperature variations, as can be verified in Figure 5.3.4. A general increase of minimum temperatures and decrease of diurnal temperature ranges was found by Rind et al. (1989) and Karl et al. (1991). The large positive anomaly observed for the minimum as well as for the maximum temperatures around 1950 seems to cause also a temporal increase of the diurnal temperature range. The lowest diurnal range was reached at the end of the 70's, followed by an increase in the 80's which, however, does not rejoin the level of the first decades of the time series. The mean diurnal range per month shows that the general seasonal decrease is recognisable in every month.

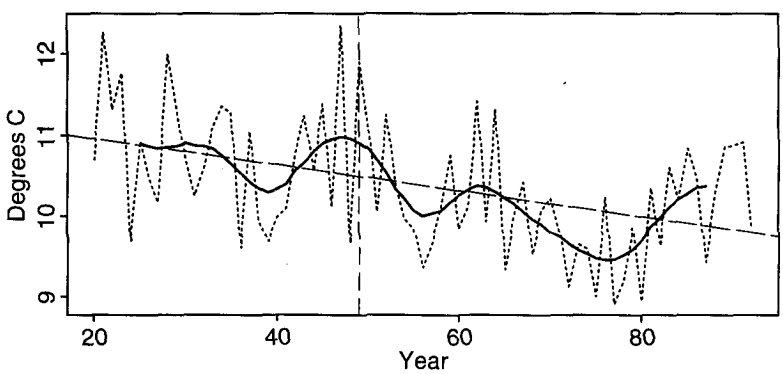

Figure 5.3.4 As Figure 5.3.1 but for the seasonal mean of the daily temperature range.

Summarising this first overview on the evolution of extreme temperatures, we can say that the main features characterising yearly temperature extremes in Switzerland observed in other publications are found also for our main hailstorm season.

In the remaining part of this section we search for connections between the temperature series and the damage and cluster data. A first, rather unsuccessful attempt was made with seasonal mean or total values. After having verified the approximate normal

distribution and the independency of the single data sets, correlation coefficients were calculated between the minimum, mean and maximum temperatures, the temperature range and the annual number of clusters, their total annual area and the mean daily number of damage claims per year. The best results were obtained with the minimum temperatures, with a correlation of 0.3 with both the annual number of cells and the square root of their total area. The same parameters yield a correlation coefficient of roughly – 0.2 with the temperature range and insignificant correlation's with the maximum temperatures. The plots of the annual number of clusters against the seasonal mean minimum, average and maximum temperatures in Figure 5.3.5 illustrate the weak relationship between these measures. The p-value of the linear regression (represented by the dotted line) is approximately 4 % (two-sided) in the case of the minimum temperature (in this case the linear model explains about 10 % of the variation). In the case of the mean and the maximum temperatures the p-value is of 37, respectively 80 %.

The correlation coefficients between the mean daily number of damage claims per year and the minimum, mean and maximum temperatures are all below 0.2. The only conclusion that can be drawn from this first comparison is that, as was found by Dessens (1994), higher minimum temperatures really seem to favour larger hailstorms. This could be explained as follows: the minimum temperature generally corresponds to the night-time temperature. A high minimum temperature during the night is usually reached when the water vapour content in the air is high, causing an inhibition of the cooling of the earth surface (by backscattering of the radiation). On the other hand, during the day, when convection starts, this moist air favours the triggering of thunderstorms.

A qualitative comparison between Figures 4.1.1 to 4.1.5 and 4.2.1 to 4.2.8 with the figures presented in this section show some similarities but also some discrepancies. The negative anomaly of the damage claim-time series during the first decade coincides fairly well with the low values of the minimum temperatures during that time period. The more regular appearance of large clusters during the 80's (Figures 4.2.2 and 4.2.3) matches with the increasing regularity of the minimum temperatures in June and July (Figure 5.3.2). On the other hand, the local maximum around 1970 found in the damage claim and in the cluster series cannot be connected with the maximum of the nocturnal temperatures in the mid-70's, and, similarly, the large peak observed in all temperature series around 1950 does not show up in the damage claim-series.

Also these observations lead to the conclusion that extreme events like thunderstorms have a rather loose connection to mean temperatures computed over longer time spans including thunderstorm-free days. For this reason the next comparison will move away from the time series and consider only the temperatures measured on days where clusters were observed. Figures 5.3.5 to 5.3.7 show the area of the clusters plotted against, respectively, the minimum and the maximum temperatures and the daily temperature range. Every data point is represented by a number indicating the frontal activity (Section 5.2) on the day the cluster was observed.

Clusters larger than approximately 900 km^2 appear only on days with minimum temperatures above ~ 9 °C, max. temperatures above ~ 17 °C and a diurnal temperature range between 8 and 15 °C. Severe hailstorm conditions producing clusters larger than 1'500 km^2 seem to need minimum temperatures around 15 and maximum temperatures around 25 °C. A general feature not connected with the temperature characteristics but valid for all three plots is the fact that the largest clusters originate mainly in connection with frontal passages. Furthermore, most of the clusters recorded on days with low minimum and maximum temperatures were produced by airmass thunderstorms.

The temperature features described for cluster days are valid only for these special days. For a discussion of future thunderstorm scenarios, we have to know how well these features separate cluster days or, more generally, severe thunderstorm days from fair weather-days. For this purpose we consider again the classification of all days of the observation period in four categories described in Section 5.1 E). The box plots in Figure 5.3.9 show the distribution of minimum and maximum temperatures for the four categories. The box widths are proportional to the square root of the number of observations for the box and the range covered by the box of one category contains 50 % of its data. The white line in the middle of the notches indicates the median and the whiskers are drawn to the nearest value not beyond 1.5 times the inter-quartile range (points beyond this span are drawn individually). If the notches on two boxes do not overlap, this indicates a difference in location at a rough 5 % significance level.

As the figures show, severe-hailstorm days cannot be separated from fair weather-days just by defining typical minimum and maximum temperatures. The possible range of these temperatures at which severe hailstorms can occur is smaller than the one found for days with little or no thunderstorm activity and temperatures on days of category 3 and 4 are significantly higher than those of category 1 and

2, particularly the minimum ones. Also the diurnal temperature variation is limited to a smaller range and is in general slightly smaller than on hailstorm-free days. However, the ranges covered by each one of the categories are completely overlapping, so that this evaluation enables only a one-directional statement: if temperatures are lower than certain values, no larger hailstorms are to be expected (the same is valid for maximum temperatures above ~ 30 °C). A statement in the opposite direction is not possible, because at a minimum temperature of ~ 14 °C or a maximum temperature of ~ 25 °C all kinds of weather are possible, even if there is a higher probability of hailstorms.

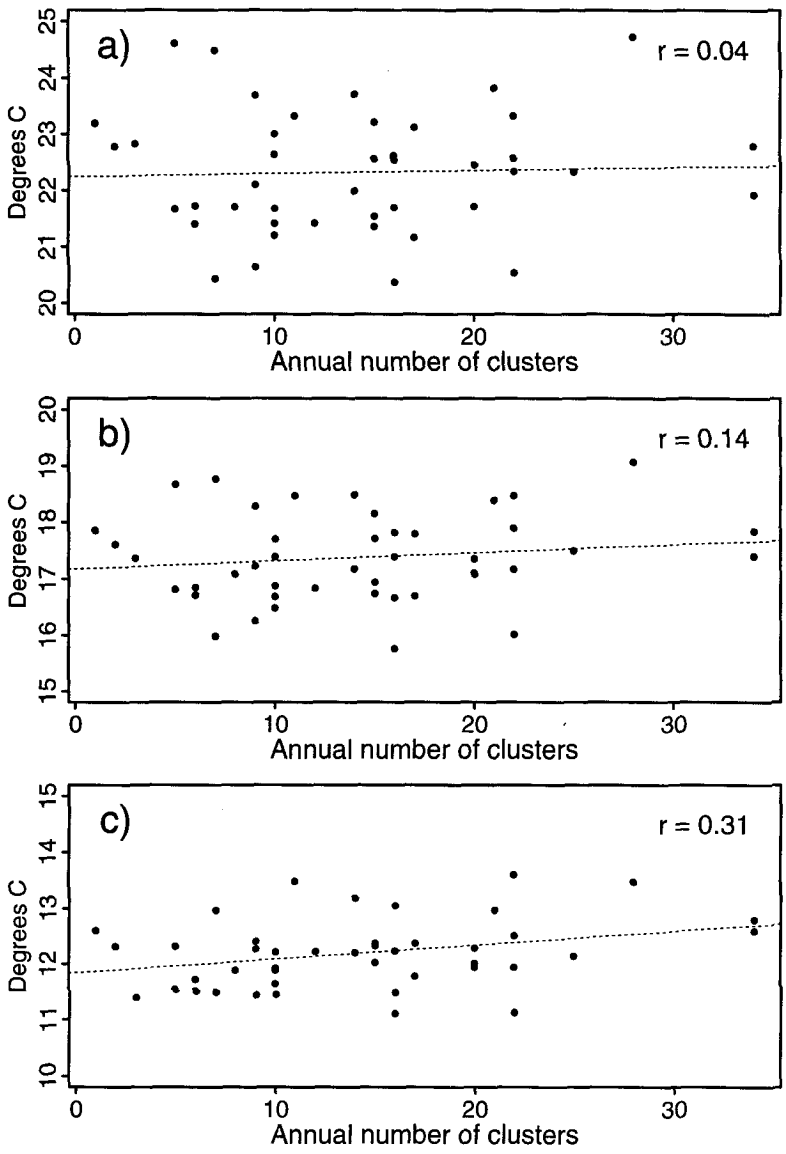

Figure 5.3.5 Annual number of clusters plotted against the seasonal mean a) maximum, b) average, c) minimum temperature.

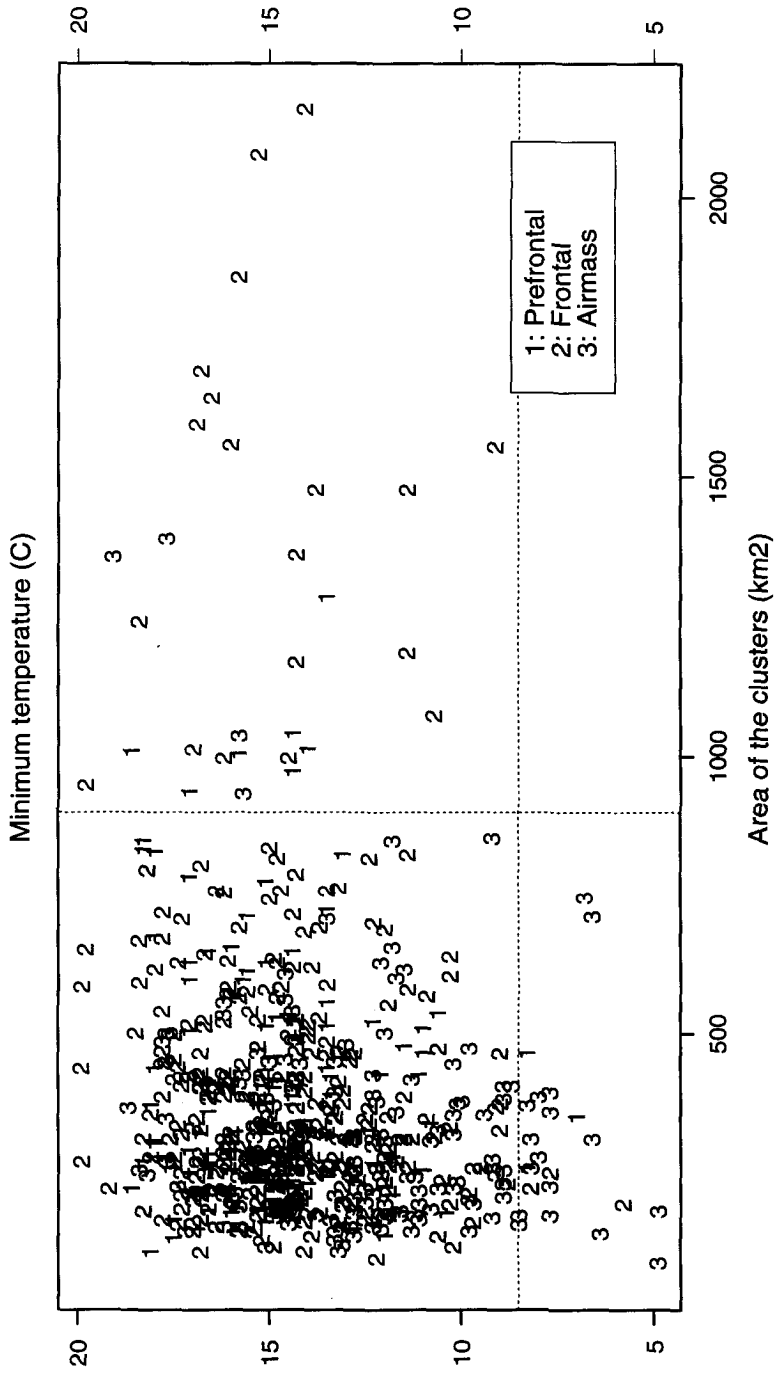

Figure 5.3.6 Relation between the area of the single clusters and the minimum temperature measured on the corresponding day.

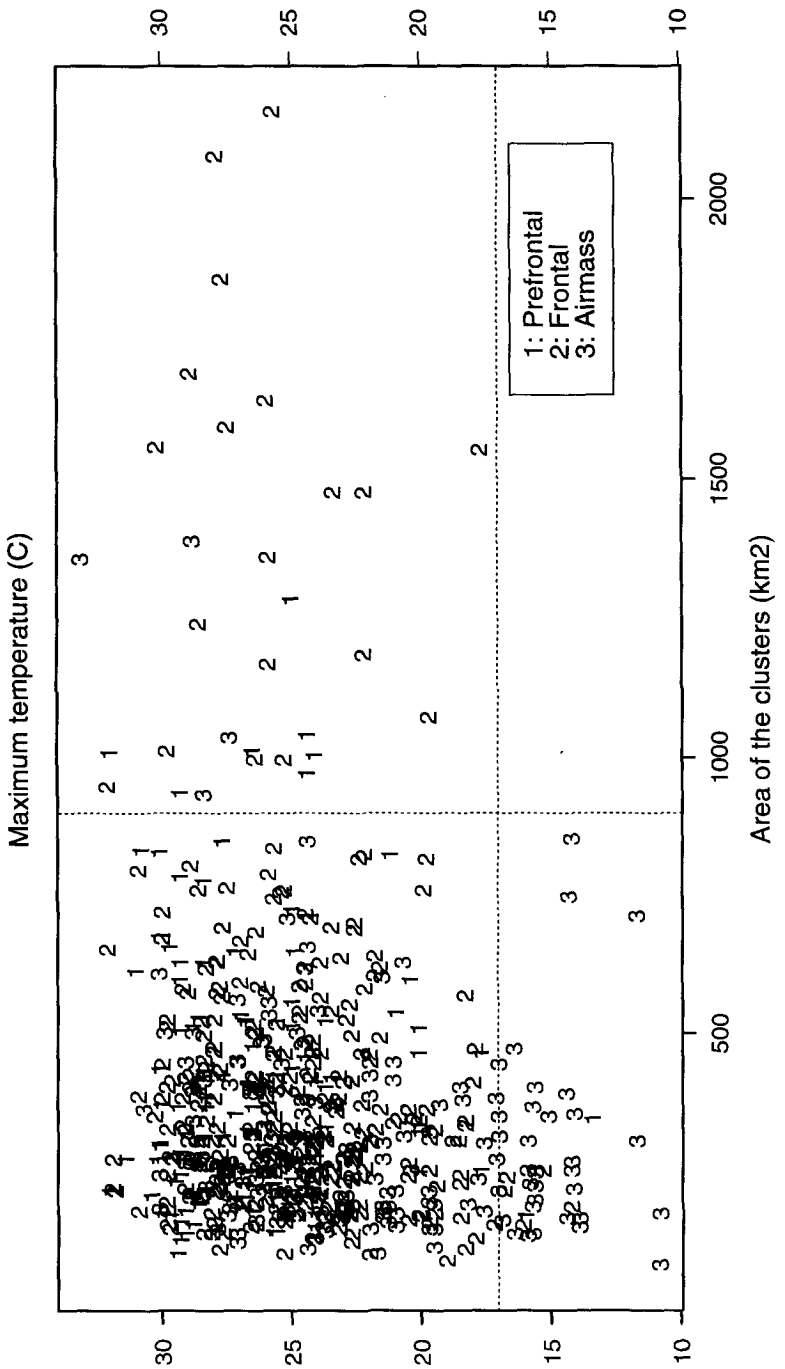

Figure 5.3.7 Relation between the area of the single clusters and the maximum temperature measured on the corresponding day.

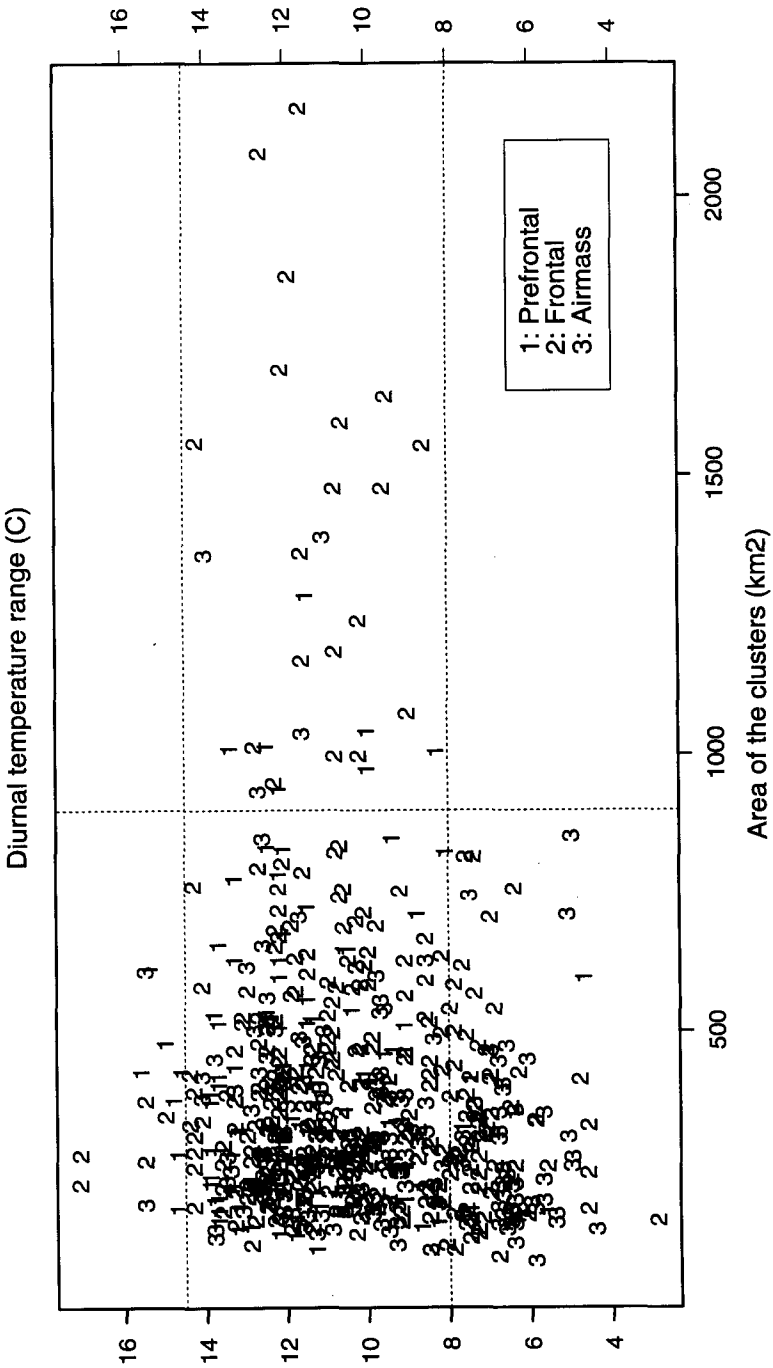

Figure 5.3.8 Relation between the area of the single clusters and the diurnal temperature range measured on the corresponding day.

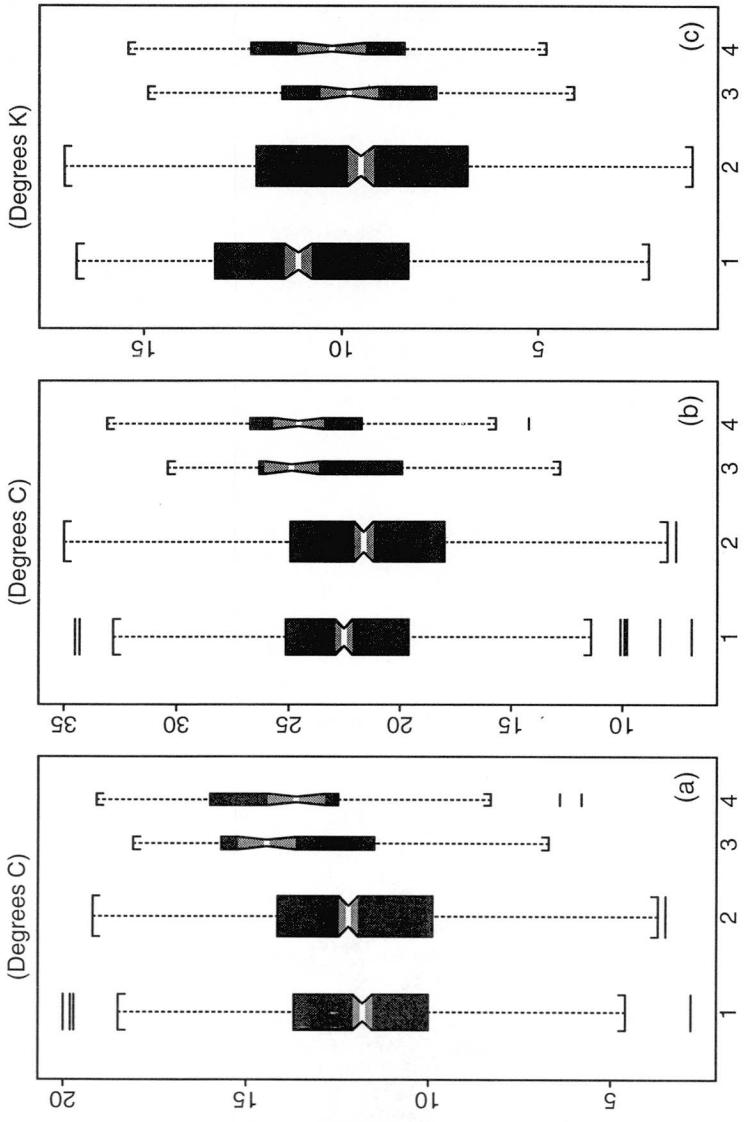

Figure 5.3.9 a) Distribution of the minimum temperature for the four categories described in Section 5.2 (1: no damage claims; 2: 0 < claims < 30; 3: > 29 claims but no clusters; 4: days with clusters). **b)** The same as a) but for the maximum temperature. **c)** The same as a) but for the daily temperature range.

5.4 Weather classifications

Unlike instrumental records data like temperature or pressure, which are quantitative, spatially limited meteorological parameters whose precision is mainly dependent on the quality of the instruments, a weather type is a parameter describing qualitatively a whole set of meteorological measurements in a spatially extended area. The time resolution of the weather type data set is quite broad (1 day) and its precision is more dependent on human errors (assignment of the weather types to every day of the year) than on the measurements of the parameters on which the weather maps are based.

Before looking at the weather types on cluster days, it might be useful to take a look at the frequency of every type during the whole test season. The bar plots in Figure 5.4.1 a) and b) illustrate this frequency computed with the data of the years 1949 to 1991 (included) for both classifications (SC and HBC, see Section 5.1).

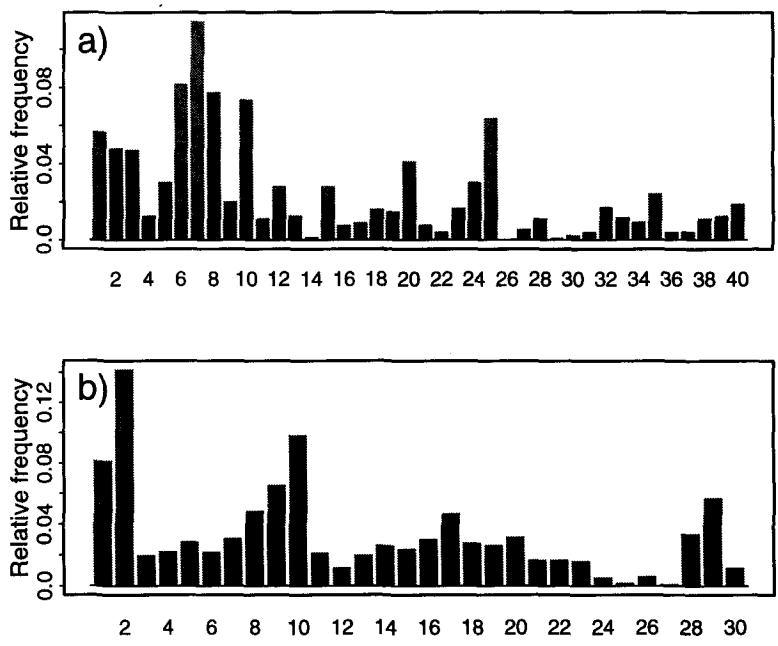

Figure 5.4.1 Relative frequency of all weather types during the test period computed with data of the years 1949 to 1991. a) Schüepp classification (explanation of the numbers in Table 5.1.1). b) Hess-Brezowsky classification (Table 5.1.2).

The height of the bars is expressed as portion of the total number of days considered for the analysis.

As one might expect for the summer months, the SC shows a high frequency of occurrence of the convective weather types (situations with small pressure gradients in particular), and a low frequency of the weather types with easterly flow. The most frequent weather type is No. 7: flat pressure distribution with westerly upper level flow (more than 10 % of the days). Type No. 26 (easterly flow with jetstream) was never recorded. The HBC assigns a large number of the analysed days to situations of cyclonic and anticyclonic westerly flow and to situations of high pressure over central Europe. Types with south-easterly and southerly flow happen rather rarely (for further explanations on the classifications see Tables 5.1.1 and 5.1.2).

Now we want to see on how many days with a certain weather type hailstorms were recorded. This is illustrated in Figures 5.4.2 (SC) and 5.4.3 (HBC) for categories 3 and 4 of the grouping described in Section 5.1 E), in the form of relative frequency of hail-, respectively cluster-days, per weather type.

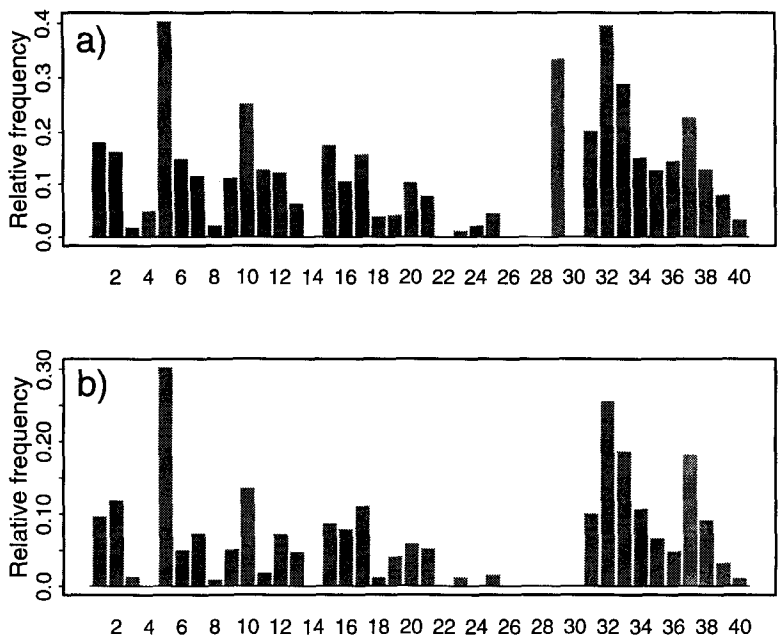

Figure 5.4.2 Relative frequency of hail- (a), respespectively cluster-days (b), per weather type of the Schüepp classification.

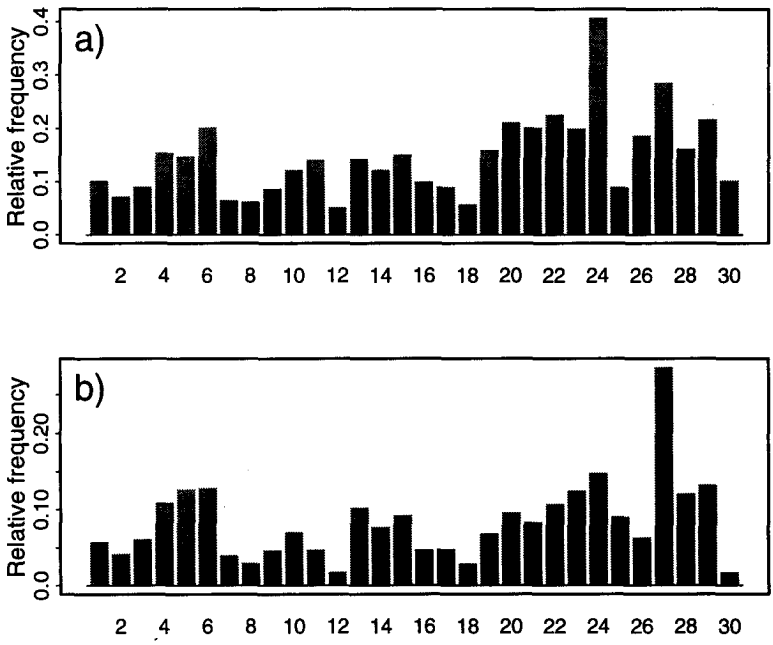

Figure 5.4.3 Relative frequency of hail- (a), resp. cluster-days (b), per weather type of the Hess-Brezowsky classification.

For the SC we observe a shift toward the advective types except for the case of type No. 5 (Hs) (high pressure with southerly upper level flow), which in 40 % of the cases is connected with strong hailstorms and in 30 % of the cases with damage clusters. Roughly 40 % of type No. 32 (+Sp) days produce strong hailstorms and 25 % produce also clusters, but this type appears only on 2 % of the total number of analysed days. These findings confirm the previously found results that frontal passages favour the development of strong hailstorms. In fact, as soon as the high pressure centre of the type No. 5 - day moves to the east, it can be followed by one of the advective types which steer moist warm air from the south sector toward the Alps (this is particularly the case with types No. 31 to 35). Type No. 29 (+Ex) causes strong hailstorms in 30 % of the cases but disappears completely on cluster days; however, this weather type is generally very rare, so that this result is not as important as it seems. All types with easterly flow (He, Fe, Le and Ej to -Ex) are almost never connected with damage clusters.

A fairly even distribution of the frequencies over all HBC weather types is shown in Figure 5.4.3 (the absolute number of days with types No. 24, 25, 26 and 27 is very small, so that only a few

thunderstorm days are enough to cause high relative values). This might point to the fact that the HBC has a bad separating effect on Swiss hailstorm days. A look at a similar representation but relative to the total number of days with at least 30 damage claims, respectively of cluster days (Figure 5.4.4), reveals a slightly stronger differentiation, with clearly higher frequencies of type No. 1, 2, 10 and 29 - days. Types No. 1, 2 and 29 (anticyclonic and cylonic westerly flow, trough over western Europe) are comparable to the SC types No. 2, 5 and 31 to 35, while HBC type No. 10 (high pressure bridge over central Europe), which is defined for an area north of Switzerland, allows many variations in the remaining parts of Europe and is not comparable with one or two SC types. However, also with this representation the HBC does not show sufficient separating properties on hailstorm days in the Swiss Mittelland, mainly because of the too broad and, with respect to our TA, badly centered area for which this classification is defined. For this reason we decided to concentrate the analyses on the SC.

The same representation with the frequency relative to the total number of storm days for the SC (Figure 5.4.5) shows that the largest number of strong haildays and cluster days are classified in the

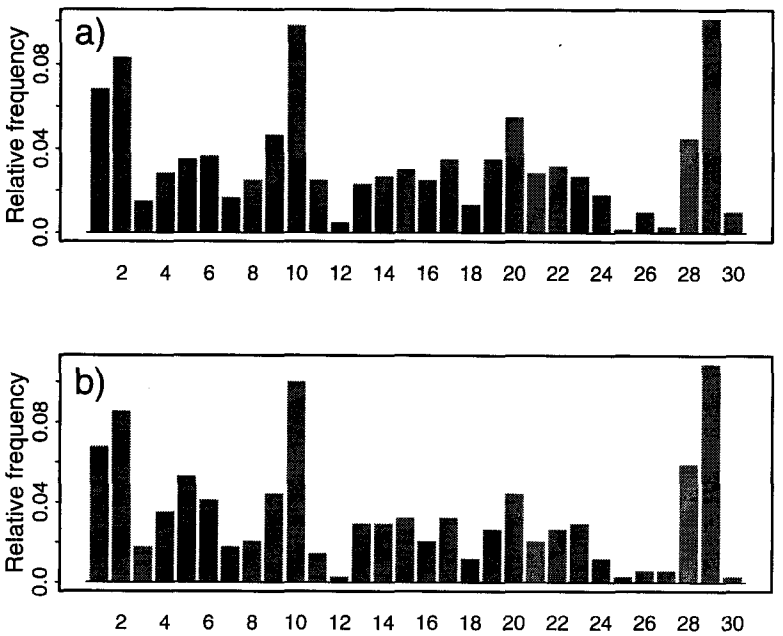

Figure 5.4.4 Frequency of hail- (a), resp. cluster-days (b) per weather type, relative to the total number of such days for the Hess-Brezowsky classification.

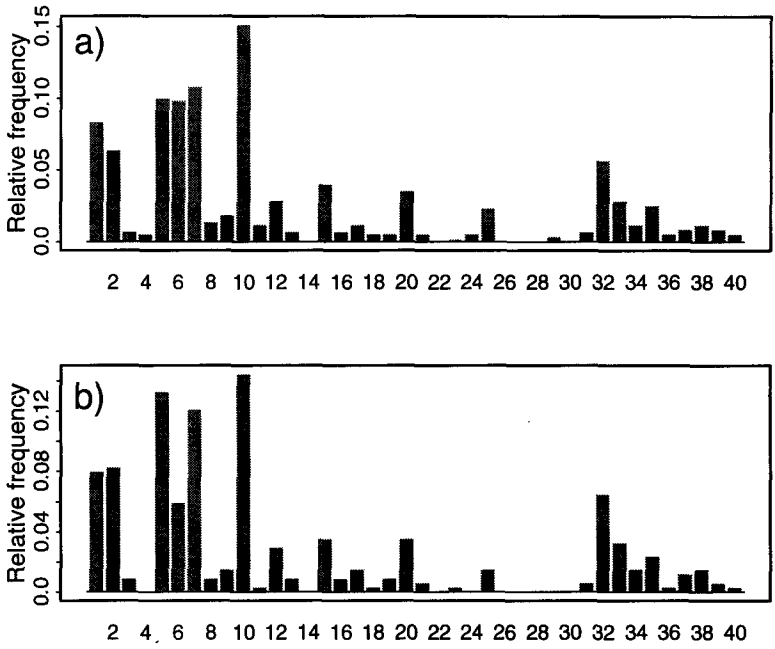

Figure 5.4.5 Frequency of hail- (a), resp. cluster-days (b) per weather type, relative to the total number of such days for the Schüepp classification.

convective types: No. 1, 2, 5, 7 and 10. The only advective type that is quite often connected with hailstorms is No. 32.

An analysis of the absolute frequency of the SC types per decade (see Figure 5.4.6) reveals some variability from decade to decade. The relative distribution is fairly the same for all decades, the total number of days with advective and cyclonic situations between No. 26 and 40 denote a slight decreasing tendency in the last two decades with respect to the first two. We will take a closer look at some of the types further on, while for a more detailed discussion of the whole classification the reader is referred to the work by Wanner (1994).

A more detailed overview on the temporal evolution of SC-weather types is given in Figure 5.4.7 for the most hailstorm-favouring types. The most important variations are to be seen in type No. 2 and 5 (H_W and H_S), that are among the most often recorded types associated with hailstorms, with an above normal high frequency during the 80's. Types No. 7 and 10 (F_W and F_S) do not show remarkable long term variations, while No. 32 (+Sp) had relative maxima around 1970 and in the mid-80's. However, these curves

have to be interpreted with some caution because the frequency of appearance (y-axis) is not the same for every type.

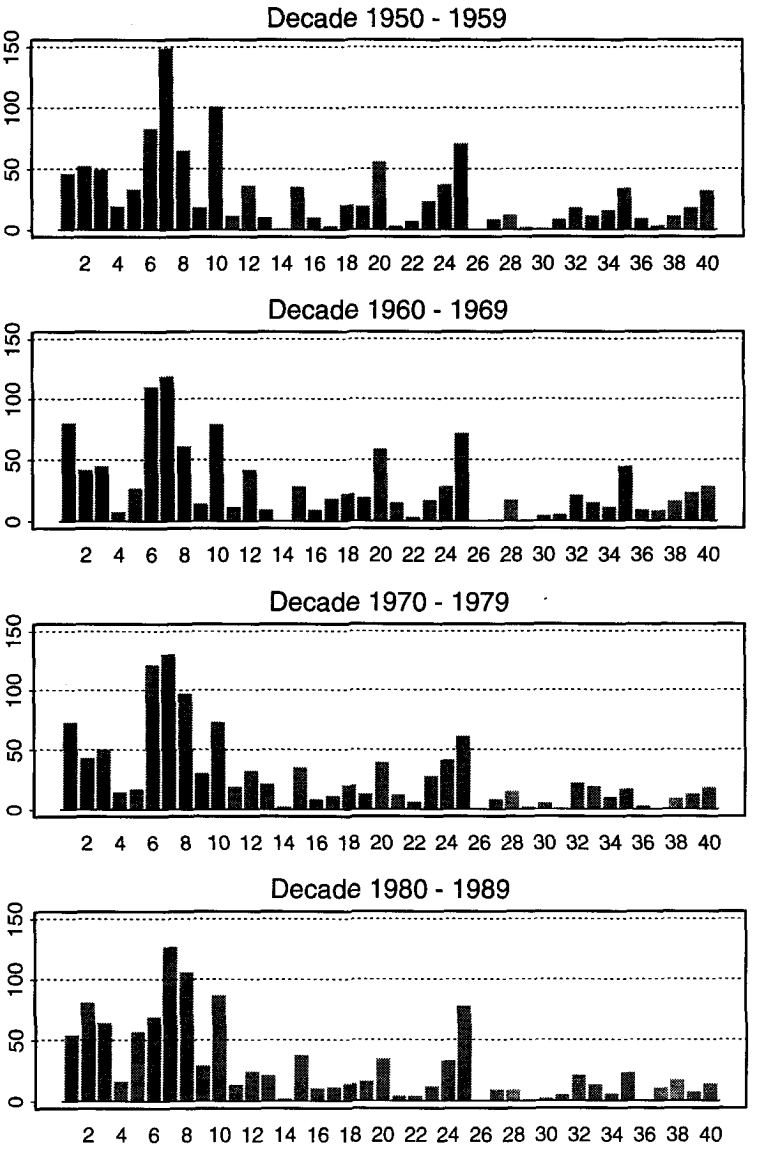

Figure 5.4.6 Frequency of the SC-weather types per decade

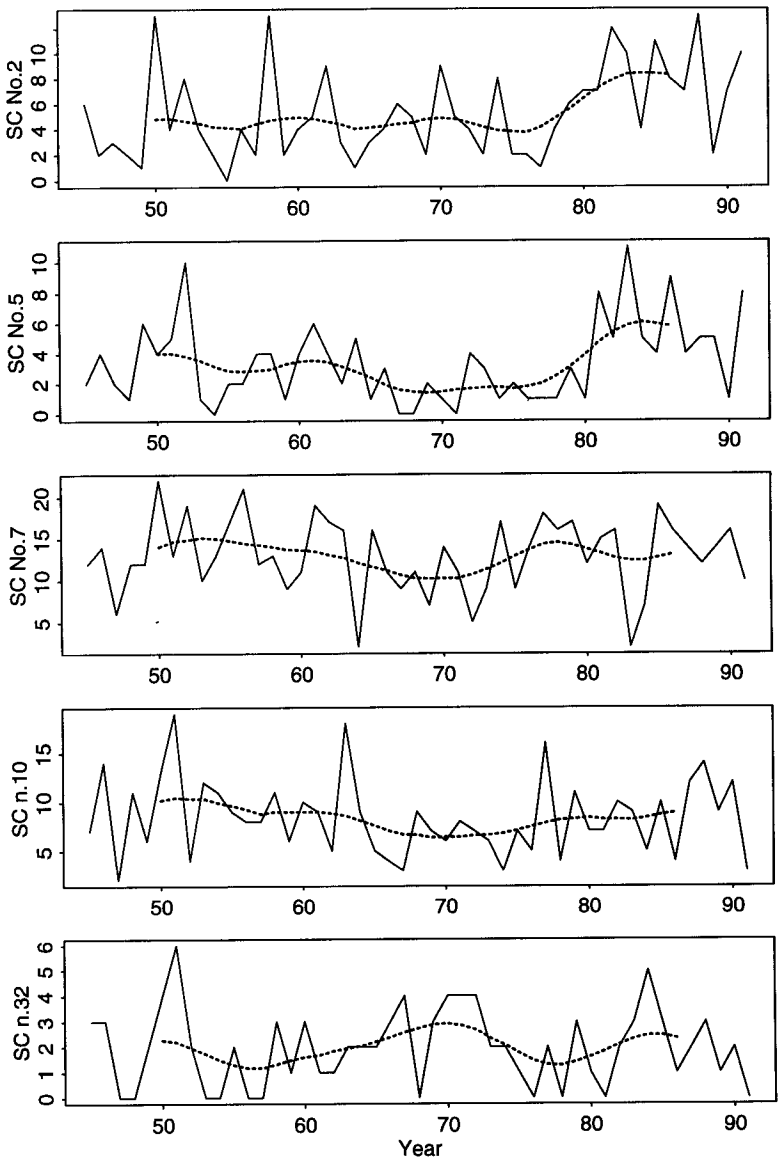

Figure 5.4.7 Temporal evolution of SC weather types between 1945 and 1991. Smoothed curve: 11 point Gaussian low pass filter. Caution: the vertical axes are not the same for every plot.

Furthermore, a comparison with cluster lengths (see Figure 5.4.8) shows that more than 50 % of the SC types are found to be associated with at least one larger cluster (50 km or more), but types 2, 5, 7, 10 and 32 (Hw, Hs, Fw, Fs and +Sp) are linked to the highest number of these clusters.

In Section 4.2 (Figure 4.2.11) it has been shown that most of the cluster-producing hailstorms were triggered in the afternoon hours. As can be seen in Figure 5.4.9, some weather types seem to enable the triggering of large hailstorms only in the afternoon hours, others favour hailstorms also in the morning hours. The most frequently recorded types of the first kind are 5, 6, 12, 32, and 33, while 7, 10, 15 and 37 are the types which showed hailstorm activity also in the morning hours. Actually, one would rather expect all flat pressure distribution-types (n. 6 to n. 10) to be of the first kind and the advective types as *morning types*. However, the significance of the results obtained with the morning clusters is rather low due to the small number of cases recorded.

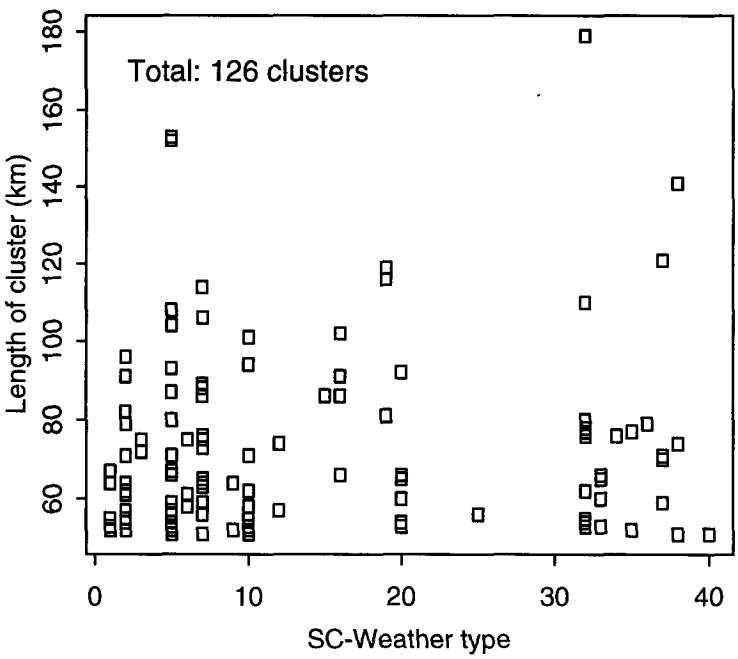

Figure 5.4.8 SC weather types recorded on days with large clusters (50 km or more).

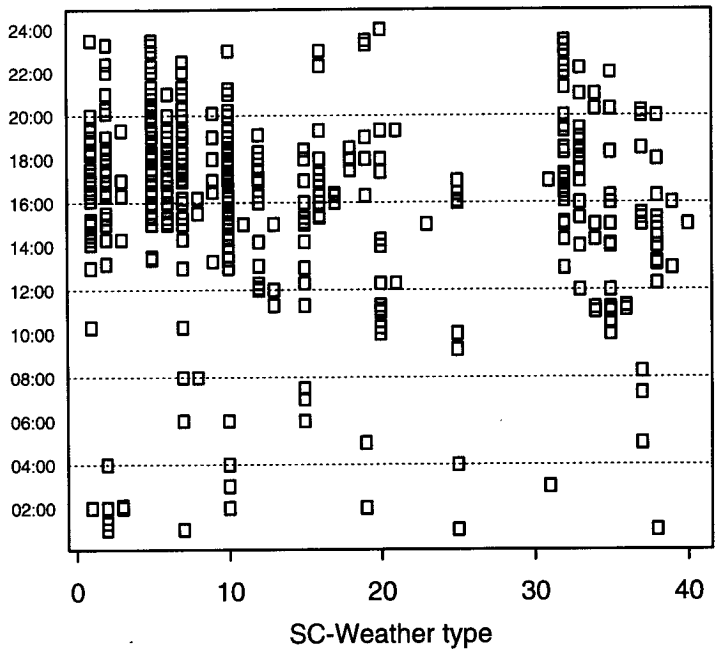

Figure 5.4.9 Time of appearance depending on the SC weather type.

5.5 Radiosoundings

In the first part of these evaluations the daily number of damage claims, on days with at least one damage claim, is plotted against meteorological parameters (0 °C-level, CAPE, wind shear and CCL) obtained from the corresponding radio sounding.

The 0 °C level derived from the 12 UTC-sounding ranges from heights around 1'000 to nearly 5'000 m above sea level (Figure 5.5.1). However, on days with a number of damage claims larger than 100 the 0 °C level tends to be concentrated within the layer between 3'000 and 4'500 m (except for a small group of days around the 2'000 m level), and on all days with more than 210 damage claims the 0 °C level is concentrated between 3'400 and 4'400 m MSL. The same plot produced with the data of the midnight sounding looks very similar. (For this comparison it was possible to use a more extensive data set now available on the data base (1954 - '93), which in this case delivered 2'642 data points).

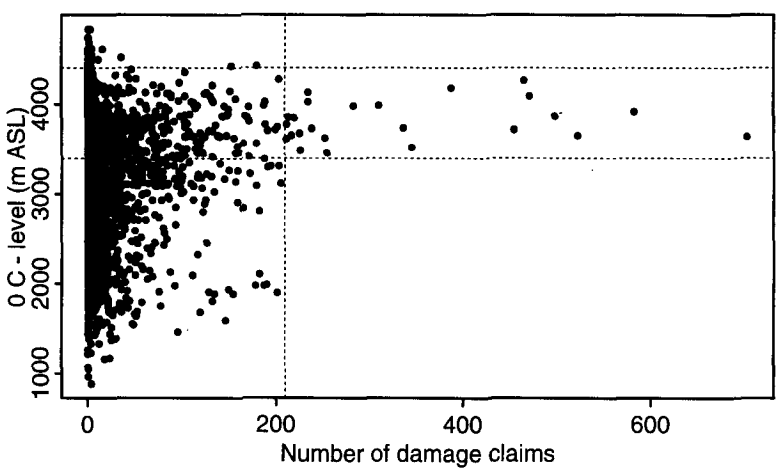

Figure 5.5.1 0 °C level of the 12 UTC sounding plotted against the number of damage claims on days with at least one damage claim (1954 - '93).

The convective available potential energy (CAPE) does not show such a clear delimitation of the days with a very large number of damage claims. On days with more than 260 claims the CAPE generally reaches at least 1'000 J/kg, but this result is not very representative because the number of days with such a large amount of claims for which the CAPE was available is very small (5 days). There is a general tendency of the data points having a very high CAPE in the

midnight sounding to descend to lower CAPE values in the noon sounding.

Although the number of damage claims does not say much about the size of the thunderstorm cells that produced the damage, the fact that larger thunderstorm cells need at least some wind shear to survive seems to be valid also for days with a large amount of claims. The wind shear at midnight on days with more than 160 damage claims is mostly limited to values between 3 and 7 m/s (for a definition of wind shear see Chapter 1, Section 6). At noon the situation is less clear and the distribution has shifted toward larger shears, but the stronger hailstorm days are still connected with a limited range of shear values similar to the one found at midnight.

In order to produce widely distributed damage claims (more than 200 claims) a convective condensation level (CCL) between 2'000 and 4'000 m above sea level seems to be necessary. CCL's above 4'000 m enable only very small hailstorms. This is valid for both soundings.

A similar analysis with the cluster data did not change the picture shown above. On days with large clusters the midnight sounding indicates a wind shear of approximately 5 m/s, which tends to shift to higher values in the 12 UTC-sounding. The CAPE shows a rather low correlation with the area of the clusters (0.30 with the CAPE of the 00 UTC-sounding and 0.25 with the 12 UTC-sounding, (computed with the square root of the CAPE and the logarithm of the cluster area to obtain normal distributions).

The second part of this analysis consists of a comparison between days without damage claims and hail days to look for some parameter that separates them. For this purpose the same classification as described in Section 5.1 E) was used. The main features of the box plots have been described in Section 5.3 in connection with Figure 5.3.9.

The first series of boxplots in Figure 5.5.2 illustrates the temperature distribution at three levels. The only significant difference between the categories is to be seen at 850 hPa, where the temperature on strong hailstorm days (cat. 3 + 4) is a few degrees higher. The temperature on the 700 hPa level does not show any significant difference between the four categories, whereas the difference between the temperature changes (00 UTC - 12 UTC) of the four categories (not shown here) is only just significant for category 1 compared to categories 2, 3 and 4, showing a slight cooling between midnight and noon on thunderstorm days. During the summer months the 700 hPa level is almost identical to the 0 °C level, therefore box plots of this parameter are assumed to be very similar

to those in Figure 5.5.2 b). At 500 hPa it is cooler on thunderstorm days, but the difference is not significant.

A better separating effect is given by the vertical temperature gradient. In Figure 5.5.3 the boxplots show three temperature

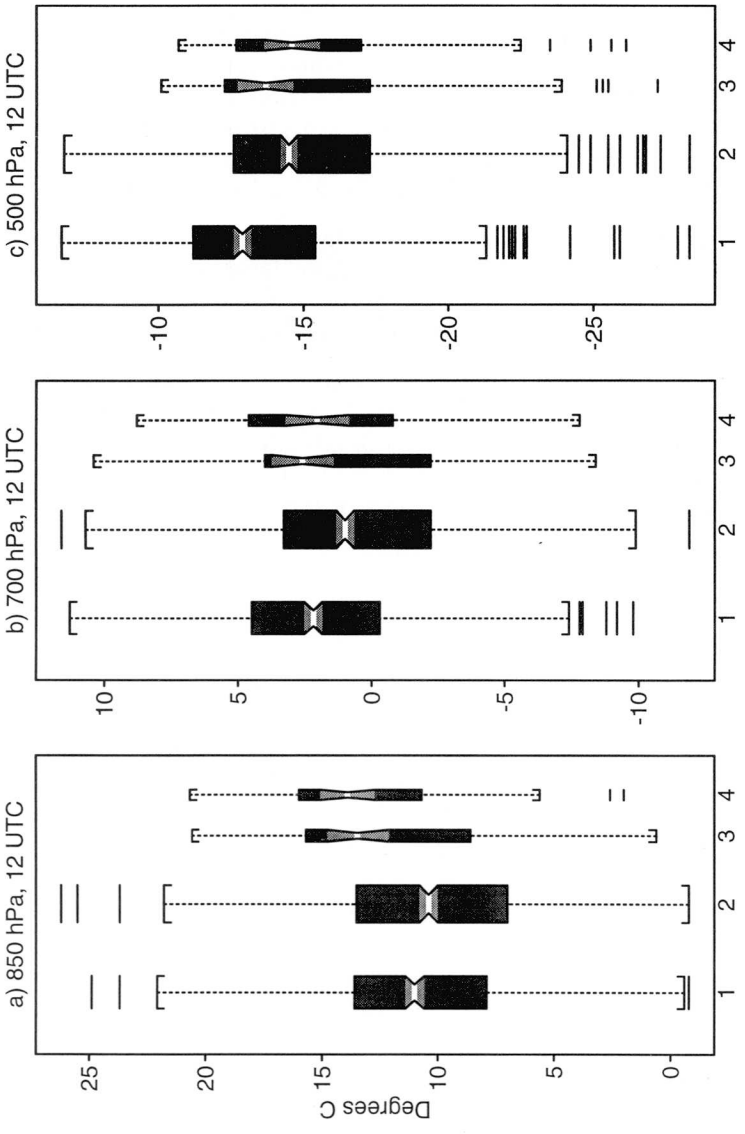

Figure 5.5.2 Temperature at a) 850 hPa, b) 700 hPa, c) 850 hPa of the 12 UTC soundings.

differences: between the 850 and the 500 hPa, between the 850 and the 700 hPa, and between the 700 and the 500 hPa layers. The temperature gradients are stronger on strong hailstorm days in all three cases, but the clearest differences between the gradients are found in the layer between 850 and 700 hPa.

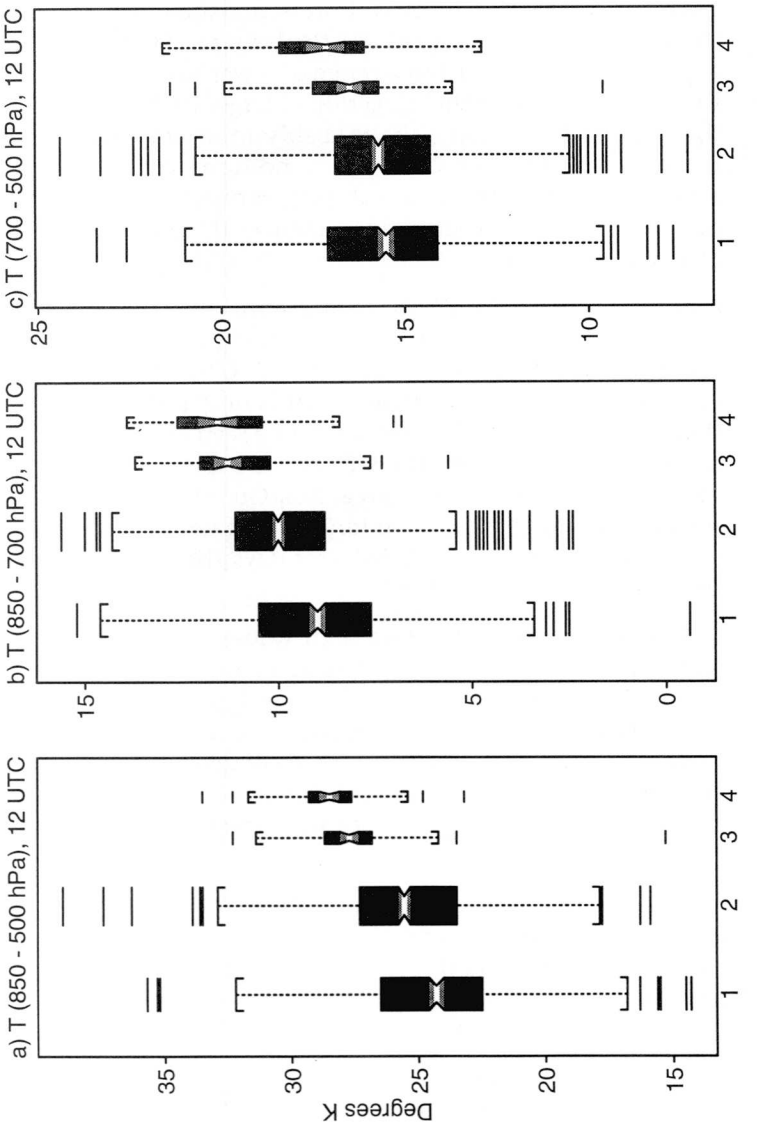

Figure 5.5.3 Temperature difference between a) 850 and 500 hPa, b) 850 and 700 hPa, c) 700 and 500 hPa

Another important parameter is the water vapour content of the air. In Figure 5.5.4 it is expressed in terms of dew point depression, which is inversely proportional to the relative humidity. Although the ranges within the whiskers of the four categories overlap completely, at mid levels the dew point depression is significantly higher on days without damage claims than on days where hail was recorded. Therefore, the advection of moist air at mid levels favours thunderstorm development. Particularly at 700 hPa the dew point depression must lie within a range of lower values (between 0 and 12 K) in order to enable the triggering of larger hailstorms, which means that the moisture supply is probably more important around this level. At 850 hPa the humidity conditions don't show important differences from category to category, probably because at this height the surface humidity strongly influences the measurements and acts as a damping factor.

Among the two kinds of condensation levels (CCL and LCL) described in Section 5.1, the CCL gives slightly better results as it has a feeble separating effect using the 12 UTC-sounding. In fact, the CCL on days without damage claims is only just significantly higher than on days with hailstorms, as can be seen in Figure 5.5.5. The LCL for both soundings and the CCL for the midnight sounding are on the same level for all four categories. On all observed days, the LCL rises about 500 m between midnight and noon, while the CCL rises the same distance only on *hail-free* days (these statements were all made looking at the median).

Although the CAPE can have high values also on fair weather days (category 1), among the parameters considered up to now it is the one with the best separating effect on larger hailstorms (see Figure 5.5.6). The range within the whiskers is smaller for categories 1 and 2 than for categories 3 and 4 and the medians of the last two categories are remarkably higher (between 500 and 700 J/kg). The CAPE-values of the 00 UTC soundings are not significantly different from those of the 12 UTC soundings.

The wind velocity at 700 hPa, which is the level where moisture advection has shown to be of greatest importance, shows a constant median value of roughly 8 m/s for the first three categories in both soundings, while in category 4, initially at the same level as the others, it increases to 11 m/s in the 12 UTC sounding.

The wind shear (S) does not show any remarkable difference between the four categories (median values between 3 and 5 m/s), except for a small increase of approximately 1 m/s between midnight and noon on thunderstorm days (categories 2, 3 and 4). Furthermore, no

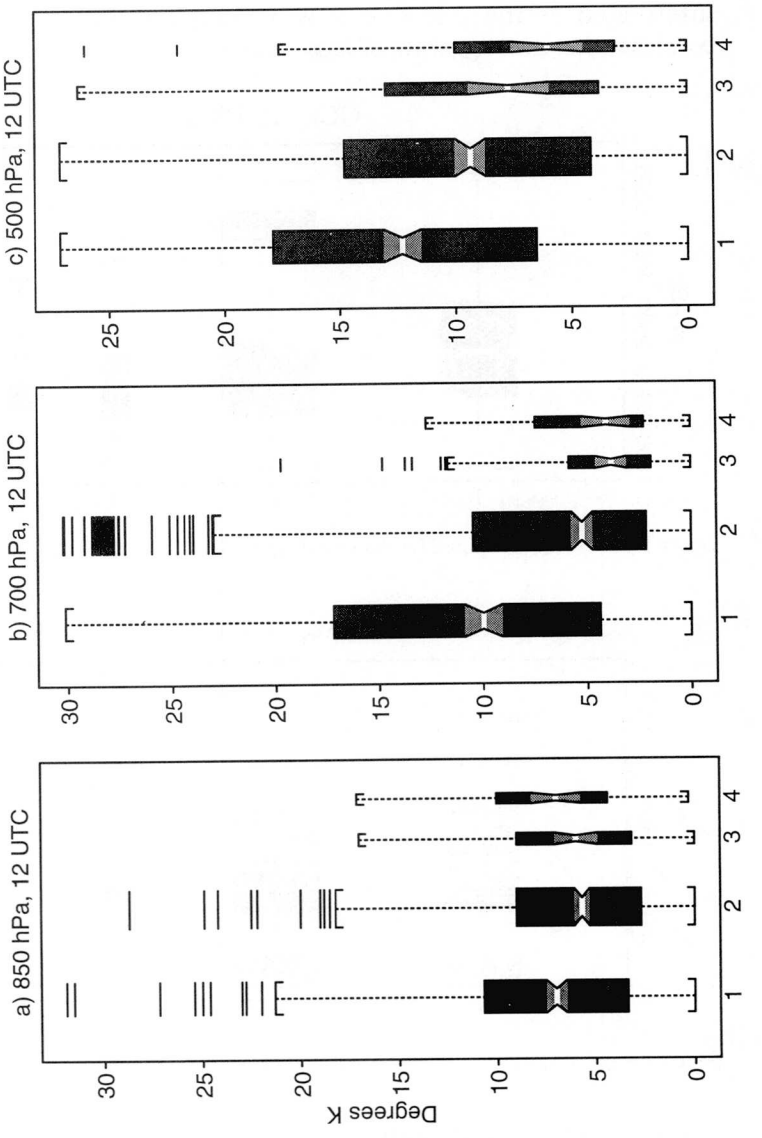

Figure 5.5.4 Dew point depression at 850 (a), 700 (b) and 500 hPa (c) of the 12 UTC soundings

clusters were found on days with S < 1 m/s. This lack of separating effect of the S parameter might contradict the commonly known thunderstorm theory which states that large hailstorm cells need a wind shear which is stronger than usual, but it should rather be

interpreted as the fact that it is a necessary but not sufficient condition for the triggering of large cells.

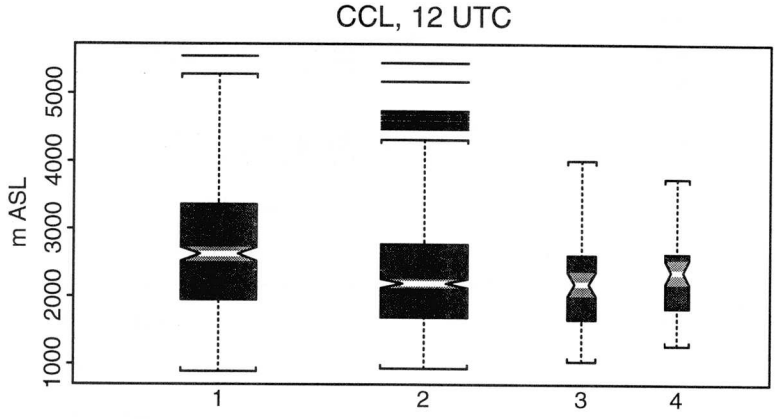

Figure 5.5.5 CCL computed for the sounding of 12 UTC.

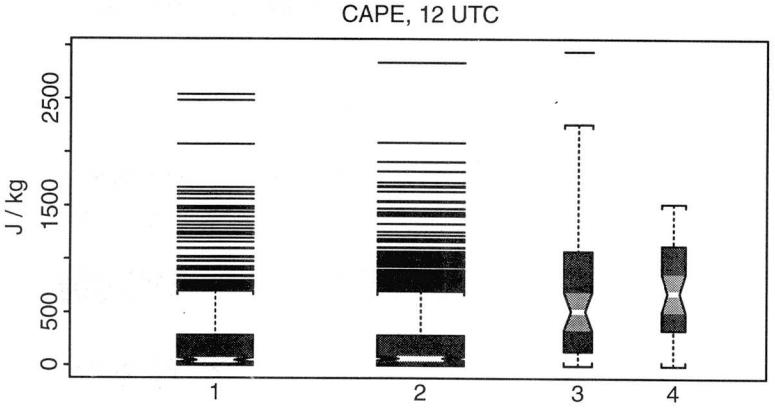

Figure 5.5.6 CAPE computed for the sounding of 12 UTC

Another contradictory feature is shown by the wind direction, where the rotation with height decreases with the strength of the hailstorm activity (Figure 5.5.7), unlike the findings of most case studies known from literature (Chisholm and Renick 1972; Browning 1986), which report a rotation (mostly clockwise) of the wind direction with height on thunderstorm days.

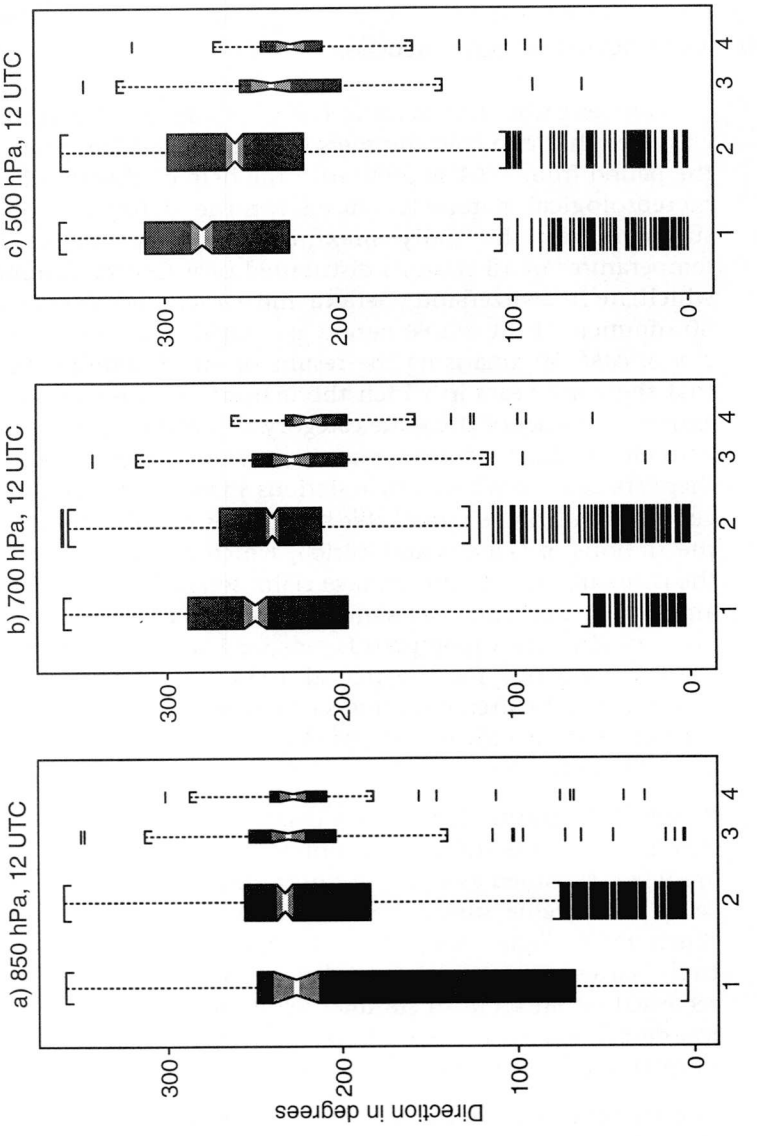

Figure 5.5.7 Wind direction at three levels (a: 850, b: 700 and c: 500 hPa) measured with the 12 UTC sounding.

5.6 Time series of other studies

Gerstengarbe and Werner (1992) made an attempt to define extremely hot and cold summers for the Central European region in the period from 1901 to 1980 with the help of cluster analysis . The meteorological parameters used for the definition of extreme summers are the daily maximum and the daily mean air temperatures of 18 stations distributed over Central Europe, two of which are in Switzerland (Geneva and Zürich). For every station the 80 summers of the whole period are classified as *hot, warm, normal, cool* or *cold*. Summarising the results of all 18 stations, they found that there are years in which the majority of the stations show an extreme summer of the same category and that in some time periods extreme summers of the same category are accumulated. However, there are cases in which single stations show a contrary course to the general trend. Some remarkable differences can also be seen between the stations of Geneva and Zürich, which are the stations used for the comparison with the damage claim series. Geneva shows a larger amount of cold and cool summers, particularly during the first 20 years of the series (compare Figure 5.6.1 a + b). Compared to the general tendency for the period 1954 - 1980 of a nearly equal distribution of extreme summers observed for the complete set of 18 stations, the two Swiss stations show a larger amount of cool and cold summers.

A plot of the seasonal number of haildays against the classification of extreme summers shows that summers with more than 65 haildays are never classified as warm or hot. A direct comparison of the time series of extreme summers with the seasonal hailday anomaly is illustrated in Figure 5.6.1. No striking correlation is found between these series. The small anomalies between 1925 and 1970 were recorded on all kinds of summer, while the larger anomalies of the last decade are, with a few exceptions in Geneva, all connected with normal or cool summers.

The moisture variability can be described by means of the Palmer Drought Severity Index (PDSI), as was done by Briffa et al. (1994) for the summers between 1892 and 1991 in Europe The PDSI is an instrument for drought studies which is better known in the USA. Despite its title, the PDSI represents the full range of moisture conditions, from extremely dry to extremely wet. It does not represent drought in absolute terms, it rather expresses varying moisture conditions on a common scale, generally within a range of

– 6 to 6, with greater negative values indicating increasingly severe moisture deficit and positive values indicating moisture excess.

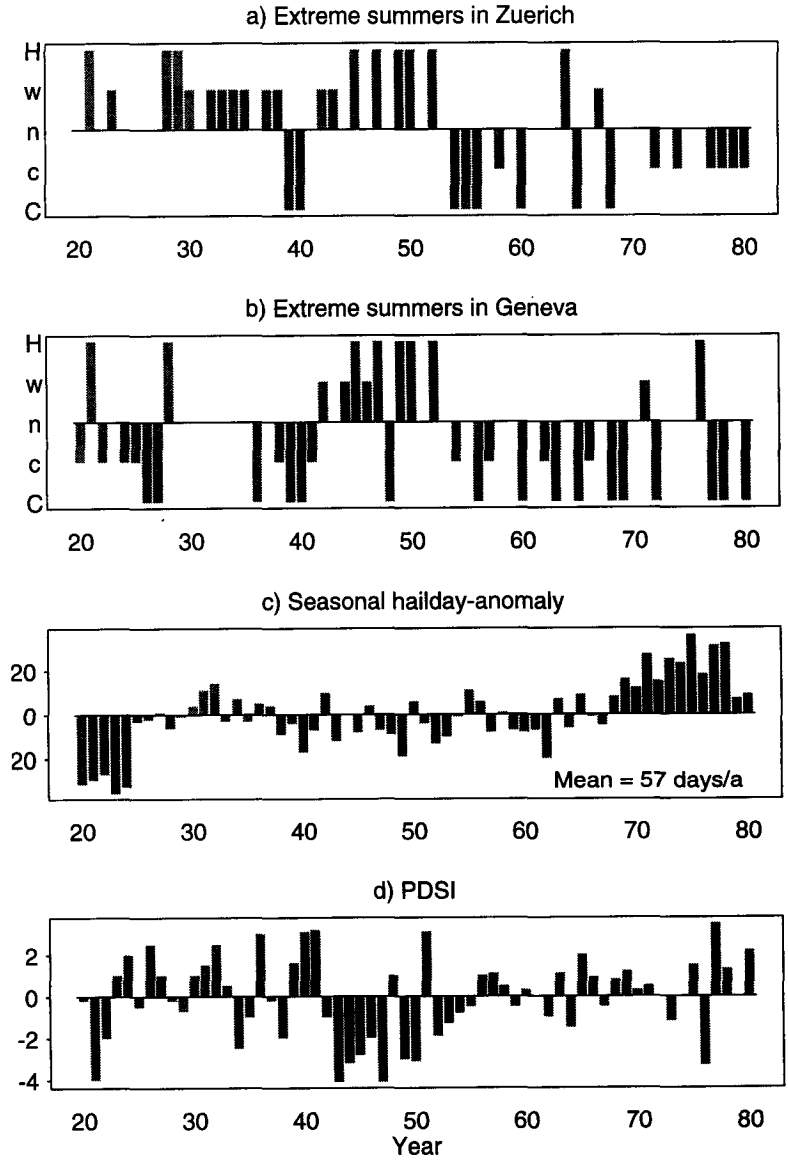

Figure 5.6.1 Time series of: a) and b) classification of extreme summers for Zürich, resp. Geneva, c) the seasonal hailday anomaly, and d) PDSI for Switzerland (Bern).

The values used for the present evaluation were taken out of the maps of summer mean (June - August) PDSI roughly at the coordinates of Bern. These were calculated for each 5° latitude by 5° longitude grid box and covering the area between 35 ° N and 70 ° N and between 10 ° W and 60 ° E. The computation is based on equivalent grids of monthly mean precipitation and temperature. The obtained time series for the PDSI is illustrated, together with the previously described classification, in Figure 5.6.1 d. The seasonal hailday anomaly (Figure 5.6.1 c) does not show any particular relationship with the PDSI. A comparison with the classification of extreme summers evidences that, as one might expect, cold (and cool) summers are usually accompanied by wet conditions, while hot (and warm) summers are accompanied by dry conditions (particularly between 1940 and 1950).

5.7 Summary

Most of the meteorological quantities analysed in the previous sections are limited to a restricted range of values on days with large hailstorms. On the other hand, these values are not restricted to thunderstorm days, and are almost always included in a larger range of values that can be recorded on thunderstorm-free days. This means that on days where meteorological quantities like temperature, wind direction and velocity, moisture advection etc. are not included in the small range mentioned at the beginning, most probably no large hailstorm will be observed. However, even on days where these parameters are included in the range, there is still a large probability that no big hailstorm will appear.

Summarising the results we can say that large hailstorms are favoured by:

- airflow from the south-west (mostly maritime tropical air)
- the passage of a front. Usually connected with SC weather type Hs (high pressure with southerly upper level flow) or Hw (high pressure with westerly upper level flow) followed by one of the advective types with south-west or westerly flow), preferably in the afternoon
- minimum temperature > 9 °C, maximum temperature > 17 °C and daily range between 8 and 15 K. Among these three measures the minimum temperature seems to have the strongest influence the triggering of hailstorms. On the other hand, very high values of maximum temperature (above ~ 33 °C) are fairly never measured on hailstorm days. This is probably due to the fact that such values can only be reached, in our regions, in very dry conditions.
- temperature difference between 850 and 700 hPa around 12 K
- 0 °C-level between 3'000 and 4'500 m MSL. With lower 0 °C levels convection usually does not reach very high and only smaller hailstorms can develop. On days with higher 0 °C levels the fact that hail is fairly never observed at ground level can have two explanations. One possibility is that the air has to be very dry in order to reach such high 0 °C levels, and consequently thunderstorm triggering is inhibited. On the other hand, if thunderstorms can be triggered on such days, hail melts before it reaches the ground.
- CAPE > 500 J/kg

- 3 < wind shear < 7 m/s
- CCL between 2'000 and 4'000 m
- moisture advection around the 700 hPa level

6 Hail damage and RADAR data

The remote sensing of hail with RADAR is a promising alternative to ground measurements. The unique resolution in space and time makes RADAR an indispensable instrument in cloud physics research in general and in the study of thunderstorm dynamics in particular.

A thunderstorm climatology based on RADAR measurements would be independent from all social, political and seasonal factors influencing hail insurance data, but regular RADAR measurements are available only in recent times. In fact, although RADAR instruments have been used for meteorological measurements for 40 years, regular, uninterrupted measurements are available only in the last one or two decades.

For the Swiss Mittelland regular RADAR measurements are available since 1983. Since that year the SMA has been recording one picture every 10 minutes with two RADARs located at a distance of 210 km from each other (one on the mount La Dôle, near Geneva, and one on the mount Albis, near Zürich). Although this data set is too short from the climatological point of view, it is nevertheless useful for the calibration of the hail damage-data.

In this chapter the available RADAR measurements for the years 1983 to 1993 are compared to the corresponding damage data. A short description of the basic RADAR principles, a few words on the SMA-RADAR data and a quick review of the main findings on hail measurements with RADAR are presented in Sections 6.1 and 6.2. Sections 6.3 and 6.4 are dedicated to two kinds of comparison: two case studies comparing RADAR areas with damage areas, and a longer term comparison of the seasonal number of RADAR cells with the number of damage clusters.

6.1 RADAR measurements

RADAR is an acronym for *radio detection and ranging*. It is an electronic device which is capable of transmitting an electromagnetic signal, receiving back an echo from a target, and determining various things about the target from the characteristics of the received signal.

The use of RADAR in meteorology began in the first years after World War II. Since these years RADAR technique has undergone a continuous evolution and several different kinds of RADARs were

developed. One of the greatest advances was the development of Doppler techniques, which also enable the measurement of the speed of the target toward or away from the RADAR, i.e. the radial velocity of the target. Another advance is the polarisation information, which makes it possible to determine the kind, the shape and the size of the detected hydrometeors.

As a complete description of RADAR theory would go beyond the aim of this work, we will only mention the main features of the RADAR equation and refer to literature for further information (Atlas 1990; Rinehart 1992).

Given a transmitted power p_t, which depends on the technical characteristics of the RADAR instrument itself, the received power p_r is described by the RADAR equation for distributed targets:

$$p_r = \frac{C_1 \, |K|^2 z}{r^2} \qquad (6.1)$$

C_1 contains all parameters which are constant when associated with a specific RADAR, like the transmitted power, the antenna gain, the wavelength and some geometrical characteristics of the beam. $|K|^2$ depends mainly on the material of the target and secondarily on the temperature and on the wavelength of the signal. If one assumes that the targets in the scanned area are entirely made up of one material (water or ice), $|K|^2$ can be included in the constant C. z is called the RADAR reflectivity factor. Given a drop-size distribution from a sample of rain, z can be calculated as follows:

$$z = \sum N_i \, D_i^6 \qquad (6.2)$$

where N_i is the number of drops of diameter D_i to $D_i+\delta D$ per unit of volume and δD is the diameter interval. Consequently, the most simplified version of the RADAR equation looks as follows:

$$p_t = \frac{C \, z}{r^2} \qquad (6.3)$$

The reflectivity z is usually converted to logarithmic units (dBZ) to reduce its enormous range of magnitudes:

$$Z = 10 \, \log_{10}\left(\frac{z}{1 \, \mathrm{mm}^6 / \mathrm{m}^3} \right) \qquad (6.4)$$

where dBZ for *decibels relative to a reflectivity of 1* mm^6/m^3.

When Z is obtained from measured reflectivity values rather than from observed drop diameters, it is called equivalent Z and denoted Z_e.

In equation (6.3) we have seen that, assumed that C and r are constants, the received power p_r is dependent on the raindrop size distribution. But such a size distribution depends on many factors (kind of cloud, height within the cloud, geographical location, etc.), is different from case to case and changes with time.

There are different ways to display RADAR data. Perhaps the most universal display for weather information is the plan position indicator (PPI), which displays the data in map-like format with the RADAR at the centre. Another kind of useful display is the range height indicator (RHI). In this display the horizontal axis indicates the distance from the RADAR and the vertical axis is the height above the RADAR.

RADARs used by weather forecasters usually display their measurements in the form of rain rate R (in mm/h). As it is impossible to know the drop size distribution for every measured cloud, a constant size distribution is assumed, and the most commonly used empirical relationship between reflectivity and rain rate is

$$z = a R^b \qquad (6.5)$$

where z is in mm^6/m^3 and A and b are empirical constants.

The SMA RADARs display their measurements as rain rate, calculated with the relationship (6.5) and the constants A = 300 and b = 1.5. Both RADARs have a wavelength of 5.6 cm and scan a volume with a radius of 230 km and a height of 12 km every 10 min, 24 hours a day. From the volume scan, local data processing assembles a 3D display (ground, front and side view), depicting the maximum of the precipitation rates. Since 1983 the two pictures are post-processed to obtain a composite picture of the individual frames (Galli 1984). No information on the polarisation is available. An example of such a picture is given in Figure 6.1.1.

In a mountainous country like Switzerland RADAR measurements cannot cover evenly the whole territory. The main obstacle is given by the Alps, which hide the southern part of Switzerland and make measurements possible only above approximately 4'000 m. Furthermore, the Albis RADAR is positioned in such a way that its range covers the whole Swiss territory north of the Alps, but the La Dôle RADAR cannot reach the eastern part of Switzerland (y-coordinates larger than 700). Therefore, the quality of the measurements is somewhat reduced on this side of the country.

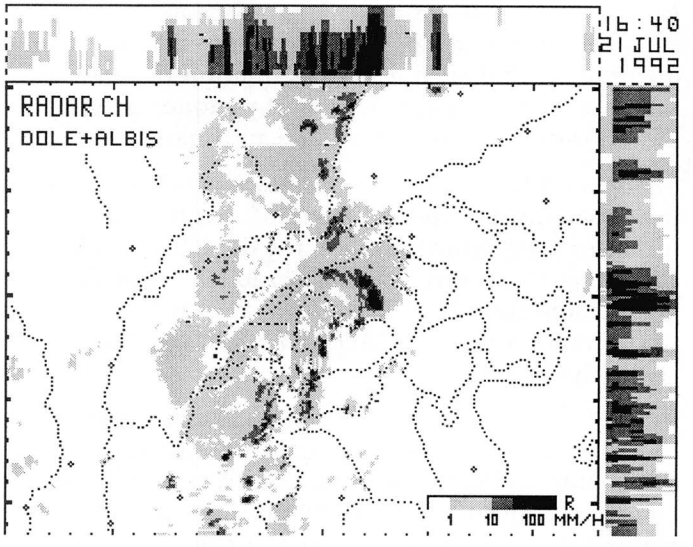

Figure 6.1.1 Example of a composite RADAR picture of the SMA RADAR system.

A comparison made by Vanolli (1993) between pictures of the LAPETH RADAR and pictures of the SMA composite showed that, in spite of the broader resolution, the latter ones cover better the whole thunderstorm area. This is mainly due to the fact that measuring a thunderstorm cell with a second RADAR from another location compensates the attenuation caused by the strong precipitation with respect to the first RADAR .

For the comparison with the hail damage-data only the ground view was used, which is the central part of the picture, with 281 pixel on the x-axis by 217 pixel on the y-axis. Each pixel represents the maximum intensity found in a vertical column with a base of 2×2 km^2 and a height of 12 km. Thereby the resolution is 2×2 km^2, which is roughly comparable to the resolution of the hail damage-data.

The displayed precipitation intensity is divided in 6 levels on a logarithmic scale. The lowest level indicates intensities between 0.3 and 1 mm/h, while the two highest levels, which are the ones considered in this study, indicate intensities between 30 and 100 mm/h and, respectively, above 100 mm/h. These rain intensity limits correspond to reflectivities of 47 and 55 dBZ.

Although these pictures are being measured since 1983, they are available in a digital form only since 1991. Before that time they were recorded on 16 mm films directly from the screen.

Hail measurements with RADAR

The measurement of thunderstorm cells containing hail causes some particular problems. In equation (6.1) we have seen that the part of the RADAR beam scattered back to the antenna depends, among others, on the material of the target. This is expressed by the term $|K|^2$, which has a value of 0.93 for water and 0.197 for ice. If the whole cloud would contain only ice particles, one would just have to change the value of the constant C in equation (6.3). But thunderstorm cells never contain only ice, they always contain also a certain amount of liquid water, which varies in time and space. Therefore, in reality $|K|^2$ is a variable that cannot be defined more precisely. Furthermore, the reflectivity of hail depends on its size but also on whether the outside surface is wet or dry or if there is any water enclosed in the hail (i.e., spongy hail). Dry hail has a lower reflectivity than wet hail of the same size.

A further complication for hail is that it is often large enough that Rayleigh scattering conditions do not apply. That is, hailstones larger than approximately 2 cm are in the Mie region. This is valid particularly for RADARs with wavelengths of 5 cm.

Nevertheless, in spite of all these problems, many studies on the relationship between RADAR reflectivity and the hail content of a cloud have been made, and useful results have been attained.

6.2 Hail in the clouds and at the ground

The detection of hail by RADAR measurements has captured the attention of many meteorologists for different reasons. The ability of forecasting hailfall at least half hour in advance can help prevent damage to objects that can be put under shelter before the hail hits the ground. In cloud seeding experiments aimed to the reduction of hailstone size, criteria of minimum reflectivity at which hail can be expected have to be defined. An exact knowledge of the area hit by hail can help insurance companies in checking claimed hail damage.

One problem in the definition of the relationship between RADAR reflectivities and hailstone content is that in situ measurements are

fairly impossible. Only an armoured aircraft (Smith al. 1984) can penetrate a thunderstorm cloud and none of them has been able to enter the strongest updraft or downdraft areas up to now. For this reason all direct hail measurements are made at the ground.

The most commonly used instruments for the detection of hail are hailpads. The first ones consisted of a foam rubber plate covered with an aluminium foil, the newer ones consist of a 2 cm thick plate of Styrofoam. The hailstones leave imprints proportional to their size, which can be measured and counted after the hailfall.

A long work of comparison between RADAR derived kinetic energies of hailfalls and kinetic energies calculated from the hailstone imprints on hailpads has been carried out in Switzerland north of the Alps in connection with a large international field experiment called Grossversuch IV (Federer et al. 1986). Waldvogel et al. (1978 a, 1978 b) derived theoretical and semi empirical relationships between hail kinetic energy and RADAR reflectivity, based on time resolved hailstone size distributions. Waldvogel et al. found a good agreement between global hail kinetic energy measured with hailpads and a 10 cm RADAR. The term global refers to the area-time integral of kinetic energy over the whole hailfall. Point comparisons between hailpads and RADAR showed less favourable results. Some of the error sources were treated in (Waldvogel and Schmid 1982). Considering the horizontal transport of hail from the RADAR measured level to the ground improves substantially the point to point agreement between hailpad and RADAR derived kinetic energy of hail (Schmid et al. 1992).

The main reason of concern about hailfall is the damage it causes at the ground. Therefore, the definition of a direct relationship between RADAR reflectivity and damage would have practical applications. Wojtiw (1983) defined two reflectivity-damage relationship with a direct and an indirect approach on the base of measurements with a 10 cm RADAR, hailpad measurements and crop damage-data from 9 hailstorms in Alberta, Canada . Both relationships are of the form

$$S = a\, E(Z)^b$$

where S is the area weighted crop loss, E(Z) is the area weighted impact energy and a and b are constants ($b < 1$). The correlation coefficients obtained with the two approaches is in both cases slightly higher than 0.5. These results are obtained for cereal crops and probably cannot be applied directly to the Swiss conditions.

Schiesser (1990). made a similar attempt with hailstorm data measured during the same field experiment mentioned above (Grossversuch IV). For one strong hailstorm he tested a damage function connecting the RADAR derived hail kinetic energy with hail damage of crops, developed by Katz and Garcia (1981). This function has the following form

$$d = \frac{e^{(P_1 + P_2 E_r)}}{1 + e^{(P_1 + P_2 E_r)}}$$

where d is the proportion of hail damage, E_r is the corresponding RADAR derived hail kinetic energy and P_1 and P_2 are parameters which have to be estimated by the data. The investigation was carried out for nine different crops and showed that E_r relates very well to d. Furthermore, the correlation between E_r and d improves considerably if the drift of the hailstones between the RADAR measuring level and the ground, and the kind of crop and the stage of maturity are taken into account.

The definition of a threshold value for the RADAR reflectivity above which the presence of hail is certain is necessary for weather modification experiments aimed to the reduction of hailstone size and is also useful for comparisons between RADAR measurements and hail records at the ground. One of the first extensive studies correlating RADAR reflectivity measurements with surface observations of hailfall was by Geotis (1963). He found that if hailstorms in New England exceed 55 dBZ the occurrence of hail at the ground is very likely, and if the reflectivity criterion is exceeded continuously for several minutes hail at the ground is virtually certain. During the experiment Grossversuch IV Waldvogel et al. (1979) tested one of the Soviet seeding criteria that uses six RADAR parameters and found that it can be replaced by a simpler criterion which uses only one parameter. The new criterion is defined as follows

$$H_{45} \geq H_0 + 1.4\ km$$

where H_{45} is the height of the 45 dBZ contour and H_0 is the height of the 0°C level measured with a radiosonde. This criterion needs a vertical RADAR measurement (RHI) and considers a fairly low threshold value in order to detect the hail cell before it has developed to its maximum size. Another RADAR reflectivity-threshold was found by Wojtiw (1986), who calculated a correlation of 0.74 between the time-integrated RADAR reflectivity (measured

as PPI) equal to or greater than 50 dBZ and the damage to cereal crops which were more or less at the same stage of maturity.

6.3 Clusters of RADAR reflectivity and hail clusters

The cluster pictures produced by HAAN (Section 3.5) enable a first rough comparison between RADAR reflectivity and damage at the ground.

The SMA RADAR pictures are available in a digital form since 1991, therefore this kind of comparison could not yet be used for climatological purposes. For this reason, in this section we will present two case studies to show the agreement between RADAR derived hail information and the damage information. The first case was observed on the 20th of May 1993 and is a rather simple case since the single hail tracks can be distinguished quite easily. The second case was recorded on the strongest hailday for 1993, i.e. the 5th of July, where 466 communities claimed hail damage. In this case it is much more difficult to distinguish the single hailtracks. On both days maritime tropical air flowed between a trough over northern Spain and a high pressure ridge over the Mediterranean and reached the country from a south-westerly direction.

In the following comparisons the drift of the hailstones between the RADAR measured level and the ground, and the height of the maximum reflectivity will not be considered, because the resolution of the RADAR pictures and of the damage claims do not enable a detailed work like the one by Schiesser (1988, 1990). In our case the uncertainty given by the broad resolution of the measurements is roughly of the same order of magnitude of the drift of the hailstones. In fact, with a height of the maximum reflectivity of 3 km and a fall angle of 45° (worst case), the drift would be of 3 km, which lies approximately between the resolution of the RADAR pictures and the resolution of the damage claims. On the other hand, the fact that the data are processed digitally has the advantage that it enables the analysis of a large amount of data covering a relatively big area.

The evaluation is carried out in two steps. First we consider the RADAR echo-envelope of the 47 and 55 dBZ reflectivity contours of thunderstorm cells satisfying a certain criterion. In connection with a monitoring program currently operated at LAPETH, this criterion was defined as follows: a thunderstorm cell is recorded only if it reaches the maximum reflectivity ($\geq$ 55 dBZ) for at least half an hour (which corresponds to three consecutive RADAR

pictures). Furthermore, the second highest reflectivity of the considered cell must at least touch once (one picture) the RADAR test area indicated by a dashed line in all pictures of Figures 6.3.1 and 6.3.2. For a correct interpretation of the results, it is important to remark that the indicated reflectivities are actually reflectivity ranges (between 47 and 54 dBZ for the second highest level, ≥ 55 dBZ for the highest level). With an interactive computer program the echoes of the cells satisfying the criterion can be selected and extracted from the RADAR picture. The echo envelopes are then compared to the damage clusters to see if the maximum reflectivity is always connected with hail at the ground or if hail damage is recorded also when the RADAR echo does not reach the maximum reflectivity.

In the second step all echoes (i.e not only larger cells) exceeding 47, respectively 55 dBZ, measured on the considered day are gathered in one single picture. With such a representation it can be determined how much of the echo with a given reflectivity is connected with hail damage at the ground.

Both comparisons are made for the TA defined in chapter 4 and not for the RADAR test area, since no damage data are available for the areas beyond the Swiss border.

A) 20th of May 1993

On the 20th of May 1993 three RADAR cells satisfied the monitoring criterion. Two of them are located in central Switzerland and can be compared to the damage clusters, while the third one is outside of the TA. The extent and the orientation of the envelopes of the two chosen RADAR cells coincide fairly well with the corresponding damage clusters. On the other hand, the first larger cluster from the left is not reproduced by the RADAR echoes. In general, the features of the damage clusters are reproduced better by the 47 dBZ echoes than by the 55 dBZ echoes.

A comparison of the damage clusters with the complete set of 47 and 55 dBZ reflectivities (Figures 6.3.1 d) and e) shows that the damage cluster on the left side which is not found among the RADAR cells satisfying the monitoring criterion coincides with a 47 dBZ RADAR cell that reached 55 dBZ only once.

Therefore, this first case leads to the conclusion that the hail damage distribution at the ground is best represented by the 47 to 54 dBZ echo range of the SMA-RADAR pictures.

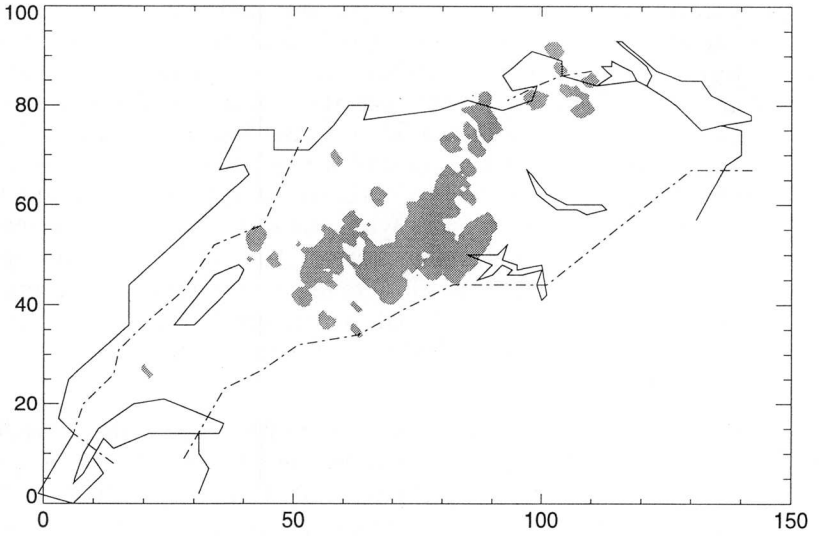

Figure 6.3.1 a) damage clusters of the 20.5.93

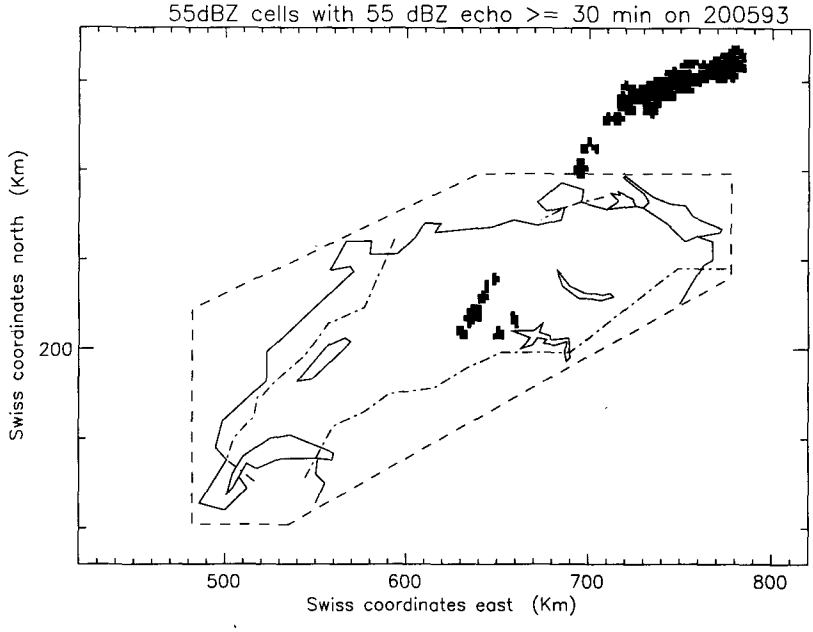

Figure 6.3.1 b) envelope of the ≥ 55 dBz echoes for the cells satisfying the criterion

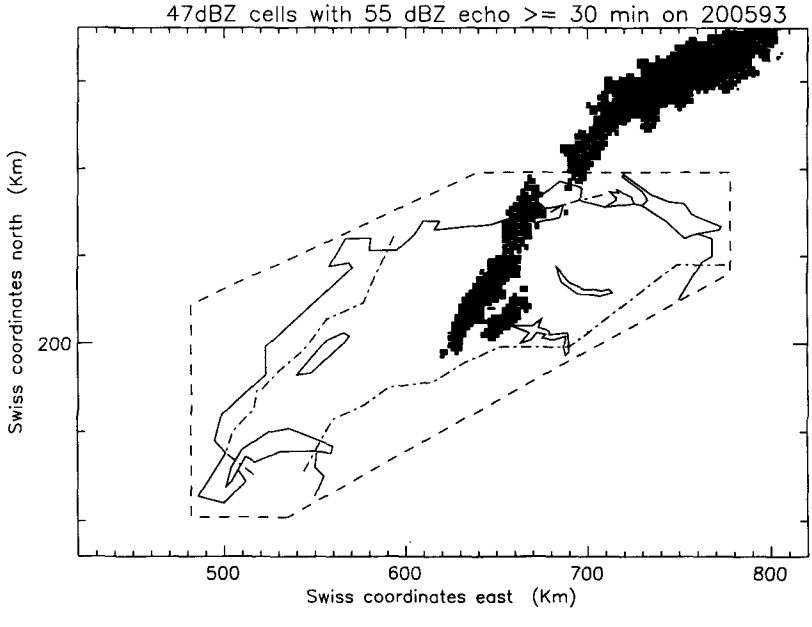

Figure 6.3.1 c) the same as b) but for ≥ 47 dBZ

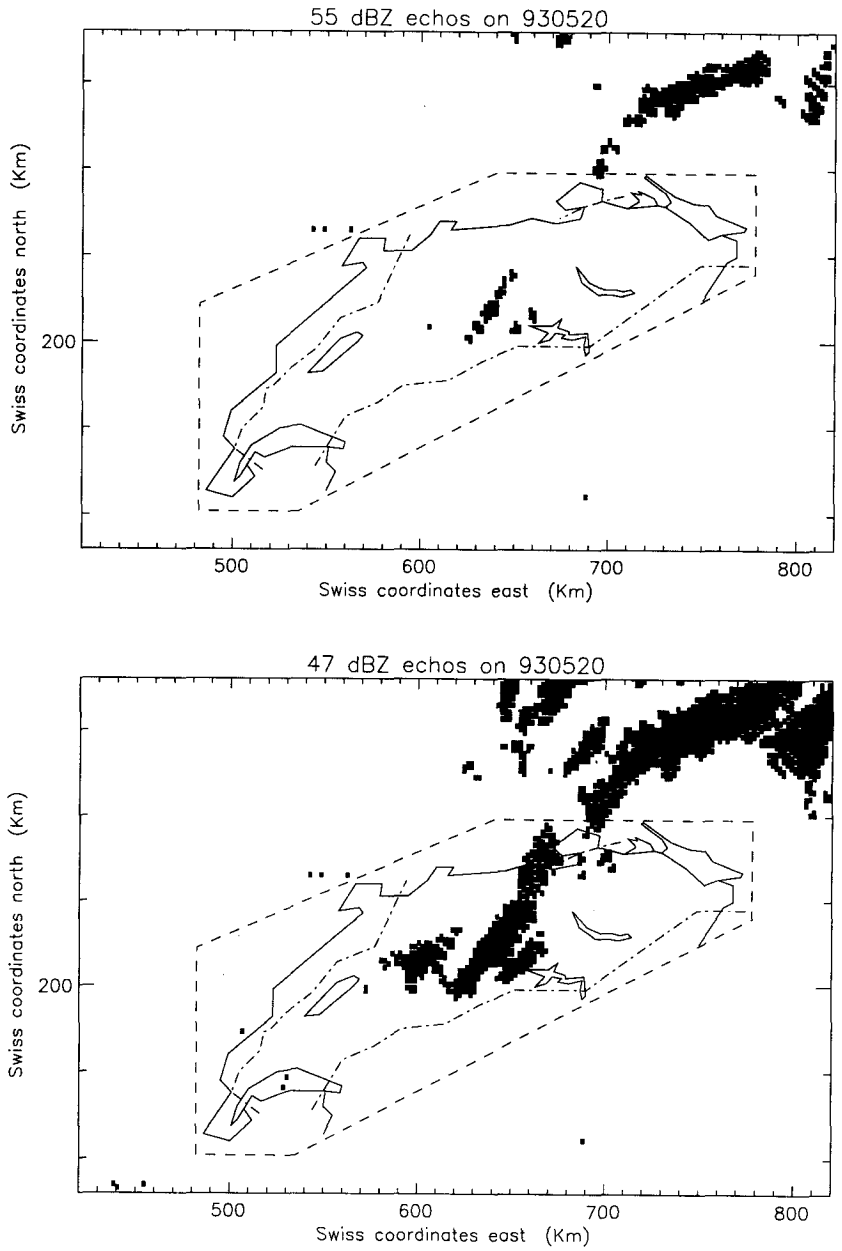

Figure 6.3.1 d) all echoes ≥ 55 dBZ recorded on the 20.5.93
e) the same as d) but for ≥ 47 dBZ

B) 5th of July 1993

The 5th of July 1993 hail fell almost in the whole TA, producing a complicated pattern of hailswaths. Eight cells satisfied the criterion, six of which occurred in the TA. The analysis of the damage clusters (without the consideration of the RADAR pictures) yielded six cell tracks. Two of them coincide well with the RADAR cells, while the other four coincide only partly. This time the comparison with the complete set of RADAR echoes is more difficult. Particularly in the western part of the TA some 47 dBZ echoes do not have a corresponding damage area on the ground. Again, the 47 dBZ echoes coincide with the potential damage areas much better than the 55 dBZ echoes.

This comparison leads to the conclusion that with the damage claims almost all larger hail cells can be detected. The 47 dBZ echo of the cells reaching a maximum reflectivity of 55 dBZ represents the best approximation of the hail damage at the ground. Thunderstorm cells reaching only a maximum reflectivity of 47 dBZ can also produce hail damage at the ground. Smaller, scattered 47 dBZ echoes are usually not connected with hail damage. Thereby it must be emphasized that with *47 dBZ echo* we mean the whole range covered by this measuring level. In fact, a cell that reached only the level indicated with 47 dBZ might, in reality, have reached 54 dBZ and, therefore, caused hail at the ground. On the other hand it should also not be forgotten that the area covered by the damage clusters is often larger than the real area touched by hail damage (because of the rather broad resolution of the damage data).

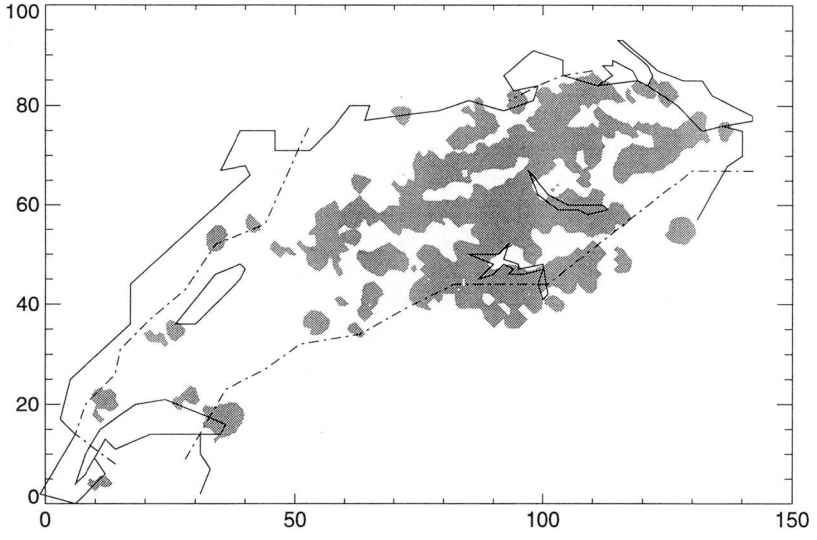

Figure 6.3.2 a) damage clusters of the 5.7.93

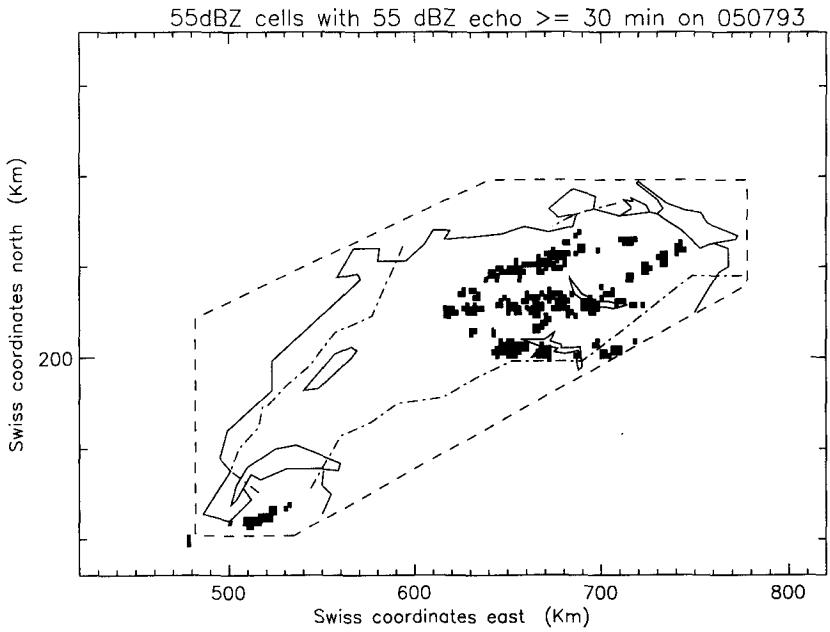

Figure 6.3.2 b) envelope of the ≥ 55 dBz echoes for the cells satisfying the criterion

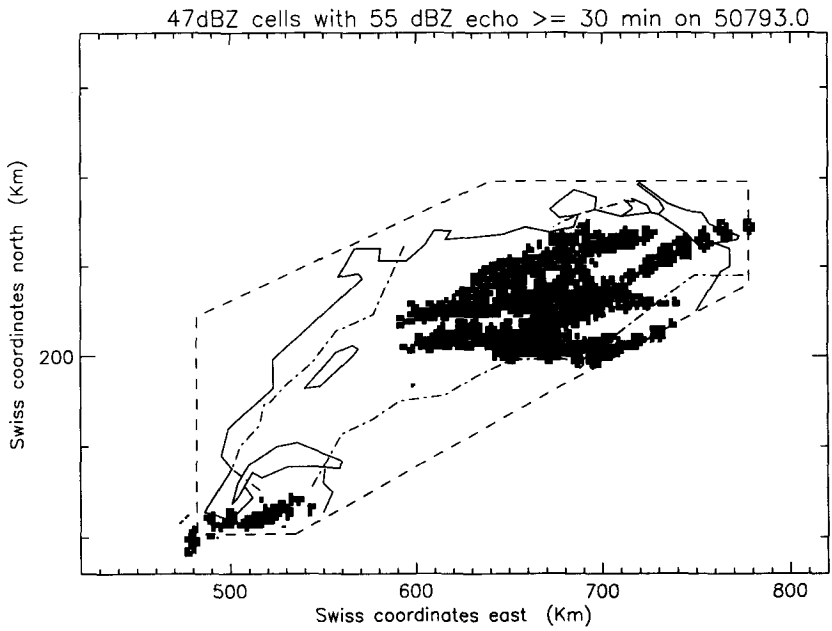

Figure 6.3.2 c) the same as b) but for ≥ 47 dBZ

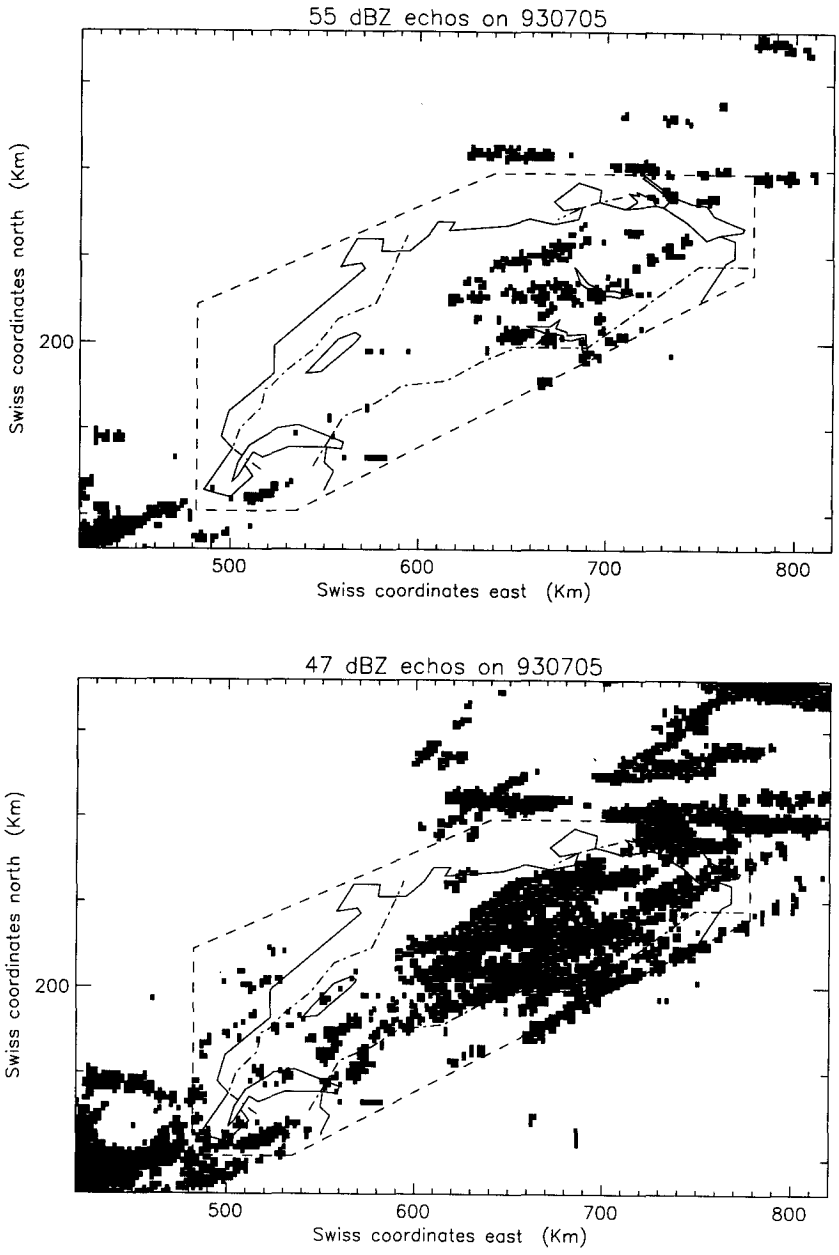

Figure 6.3.2 d) all echoes ≥ 55 dBZ recorded on the 5.7.93
e) the same as d) but for ≥ 47 dBZ

6.4 Eleven years of hailstorm tracks

The damage data and the damage clusters analysed in Chapter 4 reveal an increasing tendency in the last 15 years (Figures 4.1.1 to 4.1.3). In order to be sure that this increase is due to a real increase of hailstorm frequency and not to an increase of the claim potential, it is advisable to make a check with another data set which is independent from the damage data. The best data available for this purpose, although only for the last 11 years, are the SMA-RADAR data. Since the pictures of the first nine years are available only on films the analysis has to be done manually and is restricted to the detection of the position of the cell tracks.

The check is based on the comparison between the annual number of RADAR cells and the annual number of damage clusters. The RADAR cells are chosen with the same monitoring criterion mentioned in Section 6.3, and only those cells are selected which reach a length of at least 25 km. During this selection the distribution of the damage clusters is not considered.

A direct comparison of the detected RADAR cells with the damage clusters shows that sometimes one RADAR cell corresponds clearly to two or more clusters or vice versa. In such cases the number of cells or clusters is corrected to obtain the same number on both sides.

The result of this comparison is illustrated in Figure 6.4.1. The annual number of RADAR cells is often larger than the number of damage clusters (on average 1.33 times larger), but qualitatively both curves follow a similar course for this eleven year period. Therefore we conclude that the increase observed plotting the cluster-time series are mainly due to the natural course of the hailstorm frequency.

The fact that both curves do not correspond exactly can be attributed to different factors:

- In this comparison the vertical structure of the hailstorms and of the environment was not considered. However, it has been observed that the height of 0 °C level is one of the factors determining whether the hail reaches the ground or not (Section 6.2). Therefore, it is possible that in the months of May and June, where the 0 °C level is generally lower than in July and August, a larger part of the hail measured by the RADARs reaches the ground, causing more detectable damage.

- On days with extended hailstorms, the RADAR measurements of the farthest storm cells can be attenuated by the hydrometeors of the nearer ones. In such cases, hail damage at the ground is connected with RADAR echoes which are too weak to satisfy the criterion.
- The reflectivity levels of the SMA RADAR pictures are fixed and cover relatively large ranges. This makes it very difficult to define a selection criterion for hailstorm cells that separates hailstorms from smaller thunderstorms. The limit between the highest and the second highest reflectivity levels is too high as to take only the echos of the highest level as hail cells. But the 47 dBZ level is measured also in the case of precipitating systems which do not develop hail that reaches the ground.
- Another influencing factor is the harvest of some important cultures, like wheat, in a period of strong hailstorm activity. This happens particularly in August, causing a possible decrease of the CP (Section 3.5) and, consequently, the missed detection of clusters in the case of small or medium hailstorms.
- In years where larger hailstorms cause extended damage at the beginning of the hail season, the claim potential is reduced during a longer time span, depending on how fast the cultures recover, if they recover at all.

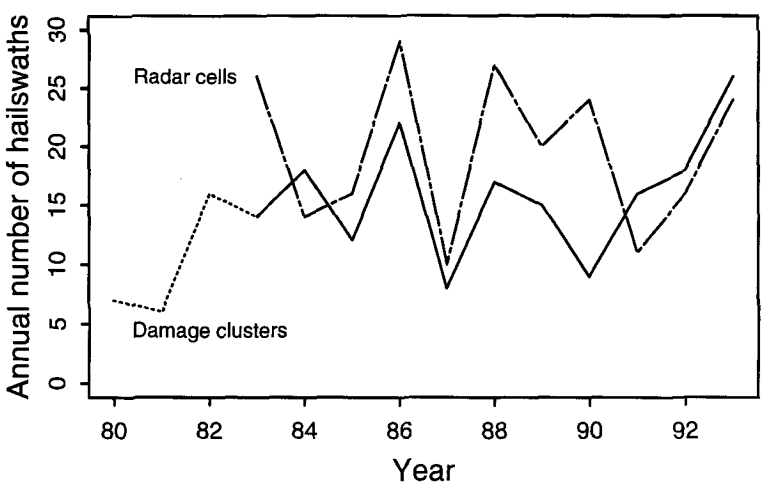

Figure 6.4.1 Annual number of RADAR cell-tracks and of cluster tracks longer than 25 km within the TA.

The increasing tendency observed on a longer time span for the damage clusters is not detectable with the RADAR measurements because the RADAR cell data begin only in 1983 and the variability in this short time span is high.

Plots of the RADAR cell-tracks (Figure 6.4.2) and of the cluster tracks (Figure 6.4.3) show the same areas of major hailswath concentration. This indicates that areas with smaller hailswath density are rather due to natural phenomena than to attenuation effects of the RADAR measurements or to a reduced claim potential. The number of hailswaths detected with the RADAR pictures is much larger than the one detected with the damage data because the observation area of the RADAR pictures is larger and independent from political borders. Many RADAR swaths which do not reach a length of 25 km within the TA are also represented in the plot.

Figure 6.4.2 Distribution of the RADAR cell-tracks for the period 1983-'93.

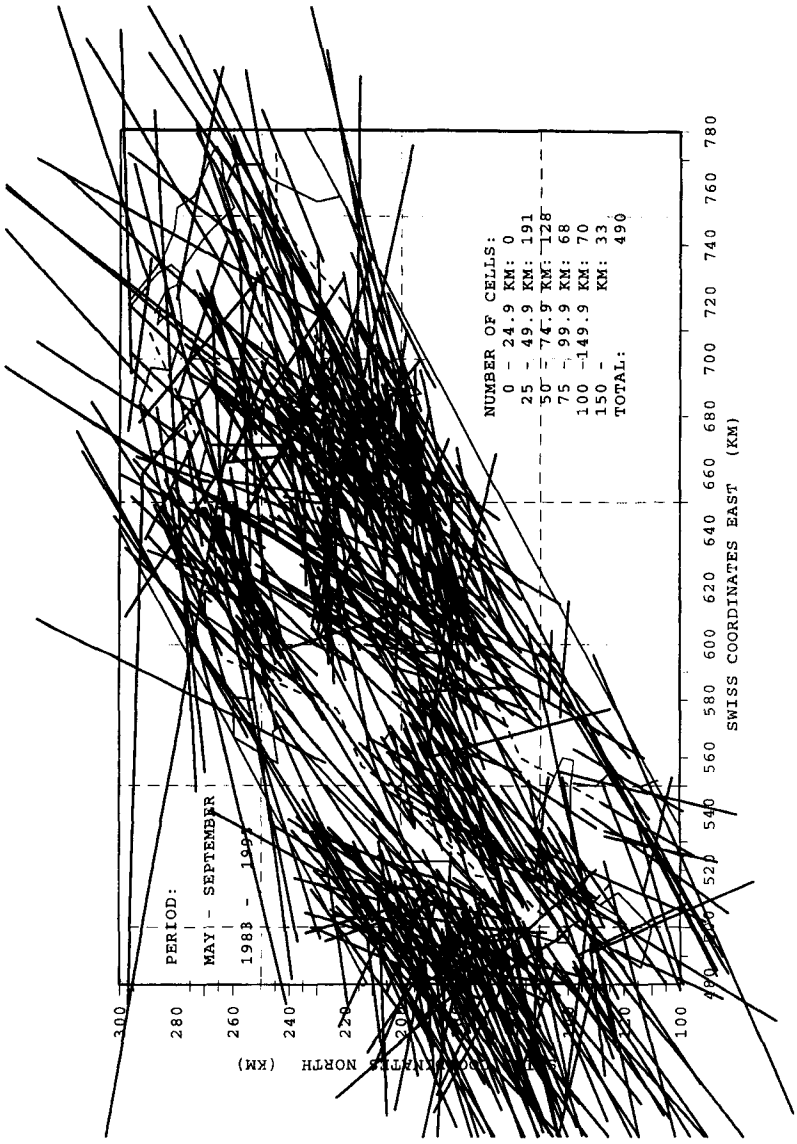

Figure 6.4.3 The same as in 6.4.2 but for the damage cluster-tracks.

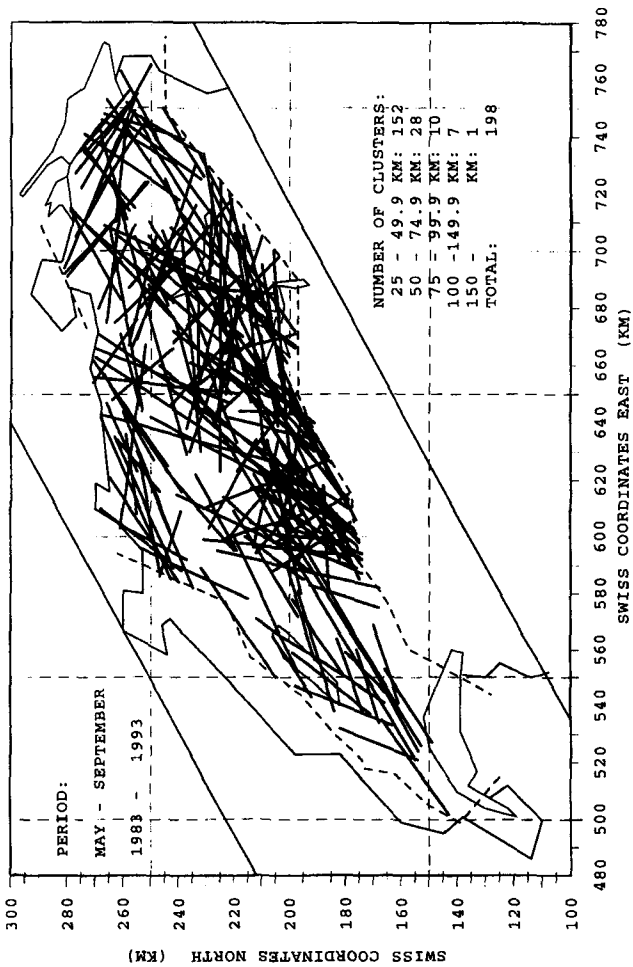

7 Discussion and conclusions

The main results of the investigations described in Chapters 4 and 5 can be summarised as follows:

The variability of hailstorm frequency is very large. Although there appears to be a slight tendency toward an increasing number of annual hailstorms, the considered time series is too short as to allow a clear statement on the past and the future evolution of such storms. An increase of mean temperature of a few tenths of degree (see IPCC statements, Chapter 1) does not lead to a clear increase of hailstorms. A prediction of the future thunderstorm activity is only possible in the form of scenarios.

The development of large hailstorms is dependent on the stratification of the whole troposphere and, at mid-latitudes, on larger scale phenomena like synoptic scale disturbances and frontal activity. Consequently, a climatological change of the tropospheric stratification and of mid-latitude larger scale phenomena cannot be ignored in the definition of future thunderstorm scenarios.

The triggering of a thunderstorm requires many meteorological parameters to contemporaneously reach a given critical range. Mean values of the single parameters averaged over a whole season are poorly correlated to the seasonal frequency of thunderstorm events. Therefore, the IPCC-scenarios described in Chapter 1 cannot be directly used for thunderstorm prediction.

The contemporary occurrence of the right value of these meteorological parameters can be expressed by a classification of weather situations. Among the already existing classifications which were employed for our evaluation, the classification created by Schüepp for the Alpine region (SC) yielded the best separating effect. However, it should be possible to obtain better results with a classification specially created for thunderstorm days, containing more details about the vertical stratification.

7.1 The past of the troposphere

The main meteorological parameters of the troposphere (temperature, humidity and wind direction and velocity) are usually measured with radiosondes. Such kind of measurements are carried out systematically only since a rather short time (40 to 50 years), so that our knowledge of the climatological evolution of the troposphere is rather limited.

Nevertheless, in the last decade, several studies based on the last half century of radiosounding data have been published. The results of these studies will be useful for the definition of future scenarios.

A general feature recognisable in all the studies is a decrease of the mean tropospheric temperature in the first half of the sixties, a period of negative anomalies in the following decade and an increase afterwards.

Boer and Higuchi (1980) made an analysis of variance of the 1'000 - 500 hPa thickness field in the years 1949 - '75 with the help of twice daily latitude-longitude grid point values for the Northern Hemisphere (poleward of 25 °N). They concluded that the climate has not become significantly more variable during the observed period nor is there a significant connection between variability and either mean temperature or north-south variation of temperature.

Angell and Korshover (1983) and Angell (1988) analysed radiosonde data of 63 radiosonde stations distributed all over the world. Over the 30 year interval 1958 - '87, their data indicate a global temperature increase at the earth's surface and in the tropospheric 850 - 300 hPa layer of 0.08 K $(10\ yr)^{-1}$ and 0.09 K $(10\ yr)^{-1}$, respectively, just significant at the 5 % level. However, for the same levels in the north temperate zone they found a non-significant decrease of 0.01 K $(10\ yr)^{-1}$ and 0.09 K $(10\ yr)^{-1}$, respectively. During the same period the global 300 - 100 hPa temperature shows a decrease of 0.18 K $(10\ yr)^{-1}$, significant at the 1 % level. Furthermore, they found an increase in the meridional temperature gradient between the equatorial zone and the north polar zone both at the surface and in the 850 - 300 hPa layer.

Oort and Liu (1993) carried out a very similar investigation with 700 to 800 stations and compared it to Angell's results. In spite of the big difference in the number of stations, the results are astonishingly similar, as can be seen in Figure 7.1.1. While the temperature around the tropopause (300 - 100 hPa) did not experience important changes, the temperature anomalies in the lower stratosphere (100 - 50 hPa) have become increasingly negative. Van den Dool (1993) obtained a very similar curve for the contiguous United States except for a stronger positive anomaly in the late 80's.

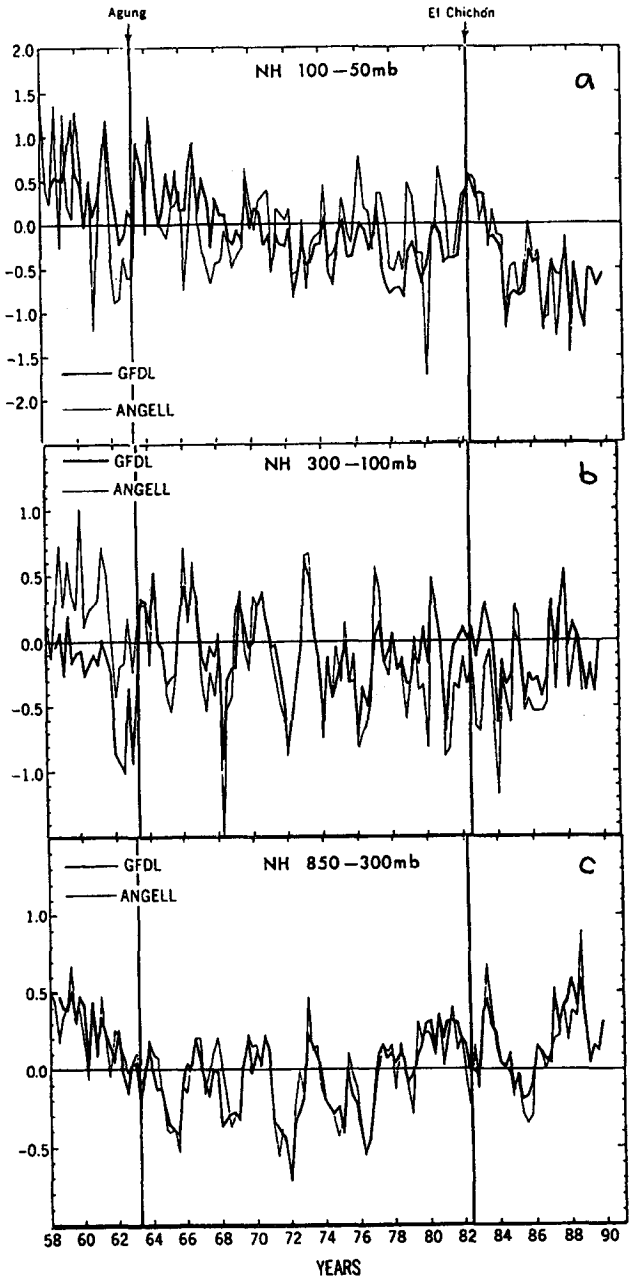

Figure 7.1.1 Time series of the seasonal mean temperature anomalies in the northern hemisphere during the period December 1958 - November 1990 for three layers: a)100 - 50 hPa, b) 300 - 100 hPa and c) 850 - 300 hPa. The thick line was computed by Oort (1983) at the Geophysical Fluid Dynamics Laboratory (GFDL) with 700 to 800 stations, the thin line is the one by Angell (1988), with 63 stations.

Sahsamanoglou and Makrogiannis (1992) and Makrogiannis and Sahsamanoglou (1992) analysed mean temperature values of the 1'000 - 500 hPa layer over Europe calculated on the basis of 72 grid point data for the years 1945 - 1988. Their results show that the mean temperature of the considered layer over the Mediterranean area follows a positive trend, which is partly due to horizontal thermal advection and mainly to diabatic heating. During the 1970 - '88 sub-period, the range of the trends computed for the different grid points is different from that of the 1945 - '88 period. They attribute the reason for this difference to a circulation change occurred in the last twenty years.

An analysis of the Payerne radiosounding data yielded results which are very similar to the ones described above. This analysis was carriedout with the complete data set of Payerne radiosoundings (1954 - 1993). Although great efforts were made by J. Bader at LAPETH to filter out the inhomogeneities, it was not possible to eliminate completely all uncertainties due to the continuous evolution of the sounding procedure (mainly given by changes of the instruments and of the data processing algorithms). The largest uncertainties were found in the moisture measurements.

Figure 7.1.2 b) represents the mean temperature anomaly of the 850 - 500 hPa layer at 12 UTC (the yearly values are obtained by averaging the daily values of the test season). A very similar curve is obtained for the 700 - 500 hPa layer, showing that the changes observed at the surface extend to the whole lower troposphere. The upper troposphere, represented here by the 500 - 300 hPa layer, shows a slightly different behaviour, with a slightly less marked increase in the last twenty years (Figure 7.1.2 a)).

The mean dew point departure at 700 hPa reveals an increasing tendency, particularly after the end of the 70's, as can be seen from Figure 7.1.3. Assumed that this is really a natural effect (i.e. not given by some inhomogeneity of the soundings) it means that the atmosphere has become dryer in the summer season at that height. We have not found similar observations in the work of other researchers yet.

The mean vertical temperature difference does not show important changes in the lower troposphere, while a more remarkable increase is observed in the higher levels, particularly between the beginning of the time series and the end of the 70's (Figure 7.1.4).

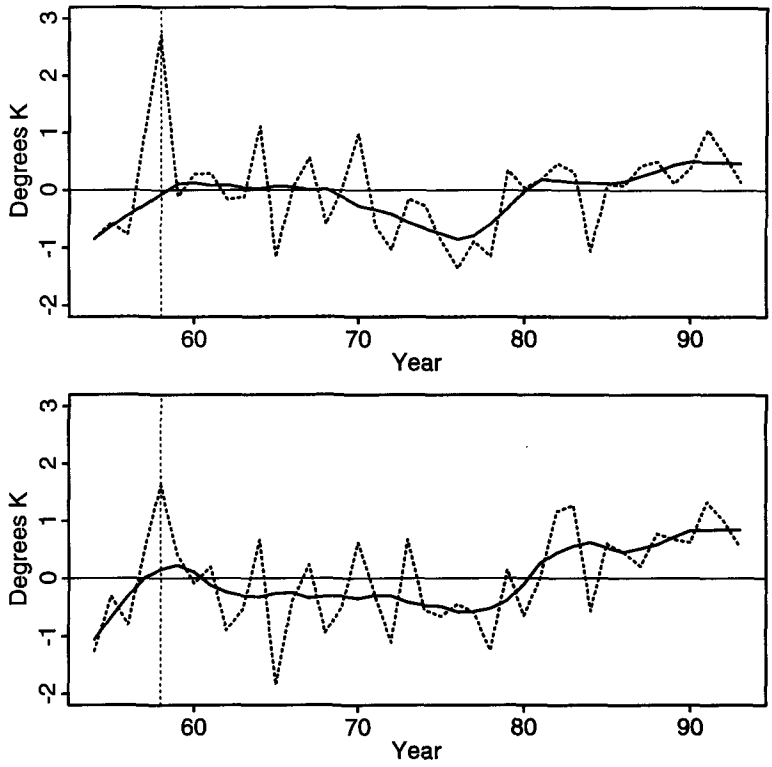

Figure 7.1.2 Payerne - radiosounding at 12 UTC: **a)** Mean temperature anomaly of the 500 - 300 hPa layer (yearly means computed averaging the daily values of the test season) **b)** the same for the 850 - 500 hPa layer.

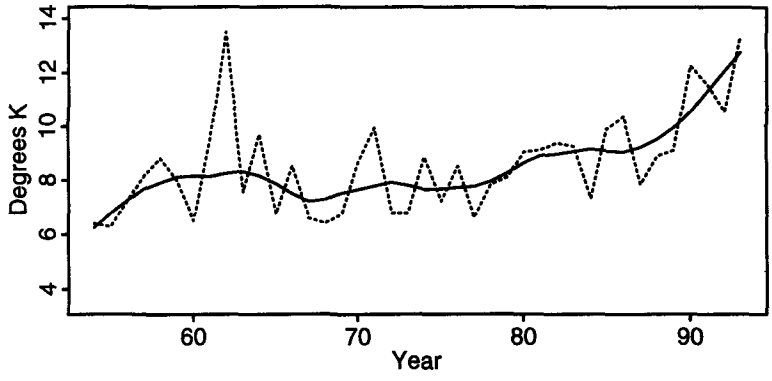

Figure 7.1.3 Payerne radiosounding of 12 UTC: mean dew point departure at 700 hPa (yearly means computed averaging the daily values of the test season)

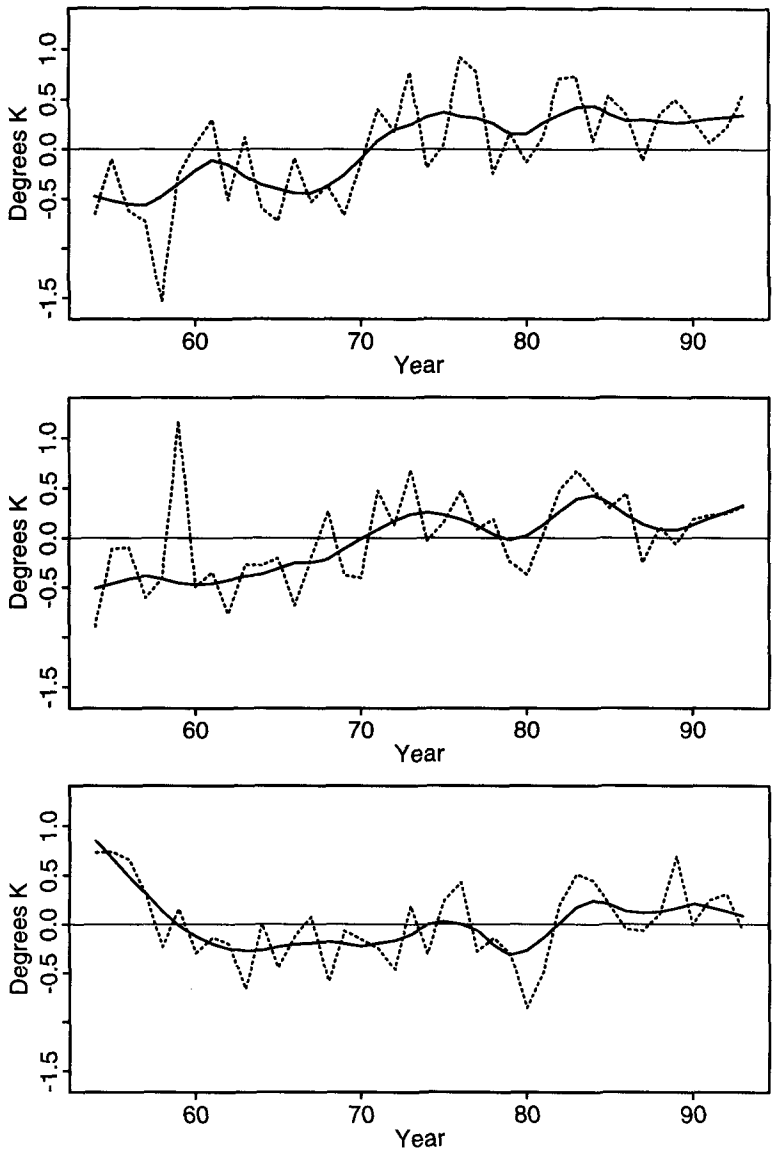

Figure 7.1.4 Payerne-radiosounding of 12 UTC: mean temperature difference anomalies in three layers, namely a) 500 - 300, b) 700 - 500 and c) 850 - 500 hPa)

Summarising we can say that the strongest heating has taken place in the lower troposphere, causing an increase of the temperature difference between the middle and the higher troposphere.

The vertical structure of the troposphere can be changed by convective and by advective motion of the air. The advective motion

is strongly influenced by synoptic scale disturbances which also cause frontal passages. As already mentioned in Section 1.2, the IPCC expects the equator-to-pole temperature contrast to decrease in a warmer world, causing a weakening of mid-latitude storms. No study is mentioned on which this statement is based. Therefore, the knowledge of the past evolution of synoptic scale disturbances is very useful for the definition of future thunderstorm scenarios. However, it is difficult to define cyclonic activity quantitatively. Every analysis is carried out following different criteria, which makes it quite difficult to compare the different studies with each other.

Most of the studies found in literature were made for the North American area and are all based on the same monthly cyclone and anticyclone track maps published by the NOAA Environmental Data Service (Reitan 1974; Reitan 1979; Zishka and Smith 1980; Whittaker and Horn 1981). The analysed time spans of these studies are included in the period 1950 - 1977 and they all find a decrease of the cyclonic (and anticyclonic) frequency (see Figure 7.1.5). Whittaker and Horn (1981) analysed also data from the entire extratropics of the Northern Hemisphere. They found that these data did not reveal a significant secular variation, implying that the decrease in North American activity has been compensated for by increases elsewhere. This hypothesis is confirmed by a study by Chen and Kuo (1994), who analysed the cyclonic frequency in the Pacific and Asian regions with the help of surface maps. For the time span between 1958 and 1987, they found an increase in the frequency of cyclogenesis in the NW Pacific and a decrease over the East Asian continent during the period of North Hemispheric warming. Parker et al. (1989) analysed 500 hPa cyclones and anticyclones over the western half of the Northern Hemisphere for the period 1950 - 1985. Comparisons with surface cyclogenesis statistics suggested that surface and 500 hPa cyclogenesis regions do not generally coincide. Linear regression revealed that 500 hPa cyclone frequency declined by two events per year from 1950 to 1970, and increased by five events per year from 1971 to 1985. Agee (1991) examined the studies by Hosler and Gamage (1956), Zishka and Smith (1980) and Parker et al. (1989) searching for statistical trends in the cyclone and anticyclone frequency during periods of warming and cooling. He concludes that warming and cooling trends are accompanied, respectively, by increases and decreases in both cyclone and anticyclone frequencies. The increase of frequency, however, is connected with a flatter pattern of shorter waves that carries more numerous but weaker disturbances.

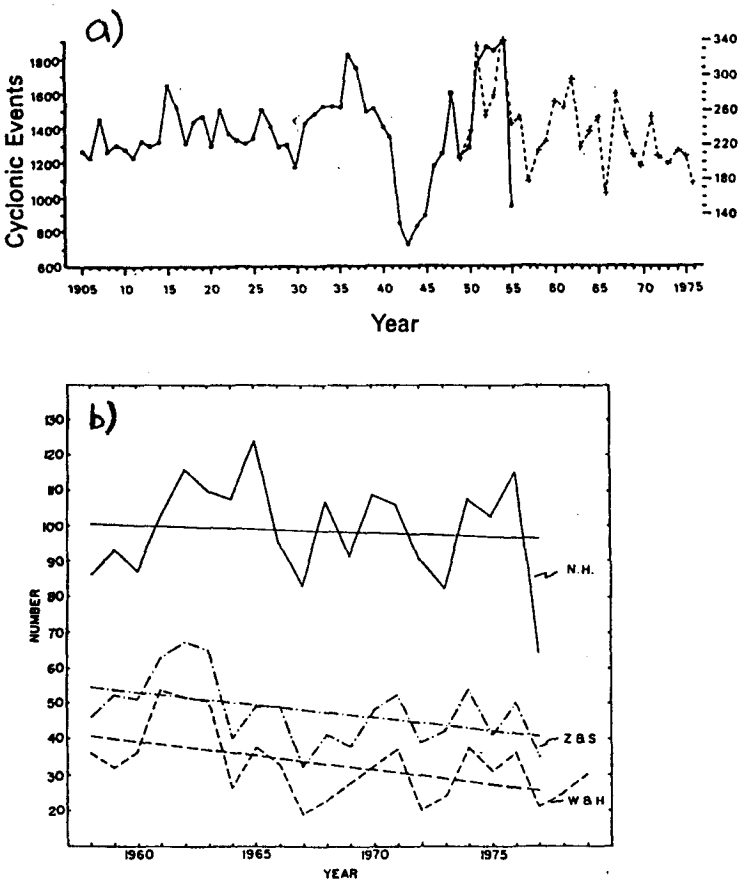

Figure 7.1.5 a) Time series of cyclonic events for North America determined by Hosler and Gamage (1956) (continuous line) and by Reitan (1979) (dashed line) (from Reitan (1979)) (the two ordinate scales were chosen such that their orientation and approximate linear variation correspond to the means and ratio of the means in the seven overlapping years); b) Frequency of cyclogenesis and regression line for the Northern Hemisphere (continuous line), North America (dashed line) computed by Whittaker and Horn and from the study by Zishka and Smith (1980) (dashed-dotted line). (From Whittaker and Horn (1981)).

Balling et al. (1991) analyse the cyclonic flow data obtained from the Lamb Catalogue of Daily Weather Types for the British Isles for the period 1861 - 1986 in connection with the annual surface temperature anomalies of the British Isles and of the source region of the cyclones. As against to the previous studies, they find a decrease of cyclonic events in case of higher mean annual local and source region temperatures and no particular change in case of lower than normal temperatures. However, the comparison is restricted to the single annual values, i.e. no time series analysis is presented. Another

Study covering the European area and large parts of the North Atlantic Ocean for the years between 1930 and 1991 found an increasing trend of deep cyclones (central pressures ≤ 990 hPa) (Schinke 1993). Figure 7.1.6 shows the annual number of cyclones which was found for cyclones with central pressures ≤ 970 hPa and ≤ 950 hPa. The very low values of the 30's are supposed to be due to missing synoptic observations. Furthermore, a general decrease of the mean central pressure was observed.

Although the studies for the North American area are more numerous and yield more or less corresponding results, the fact that similar studies carried out for other parts of the world lead to almost opposite results cannot be overlooked. It evidences that a clear statement on the connection between cyclonic frequency and temperature distribution can still not be made.

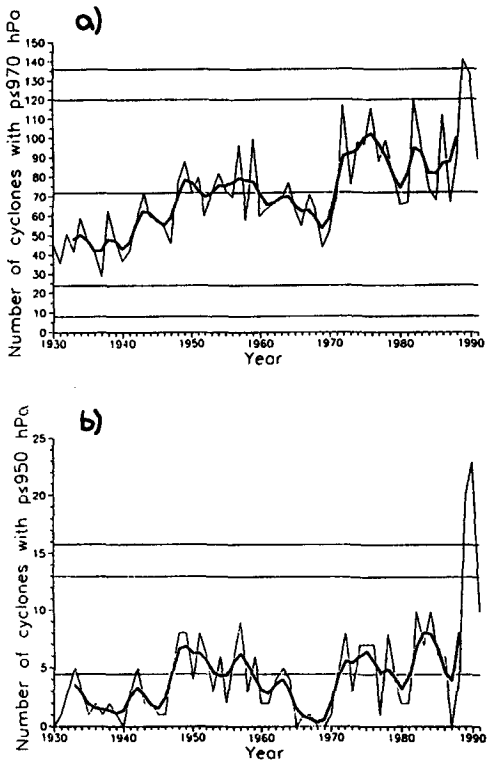

Figure 7.1.6 Absolute annual number of deep cyclones 1930 - 1991 with central pressures ≤ 970 (a) and ≤ 950 hPa (b). The thick line was obtained with a 6 point Gaussian low pass filter, the other lines represent the mean of the entire period as well as the 95 % and 99 % significance levels (from Schinke (1993)).

7.2 Scenarios

The NFP31 has defined a scenario for different Swiss regions which should enable the comparison of the different studies participating within this program (see Chapter 1). This scenario merely describes the mean temperature and precipitation evolution. Precise values (probably too precise compared to the error which can be made) are given for the Mittelland area, but no indication on their variability. As we have seen in Chapter 6, the correlation between mean annual or seasonal values of meteorological parameters and thunderstorm frequencies is very weak or even non-existent. Therefore, the scenario indications of the NFP31 can be considered only marginally for the definition of future thunderstorm scenarios.

In Chapter 6 different meteorological parameters have been tested on their separating effect on days with and without hailstorms. Some showed some separating skill, but none of them reached values on hailstorm days not attained on days without hailstorms. This is surely due to the choice of the four categories, but also to the fact that one parameter alone cannot determine the triggering of a thunder- or hailstorm. If, for example, the CAPE reaches 2'000 J/kg but no triggering mechanism is available to start the convection, this huge amount of energy will not be used to build up a thunderstorm.

The number of parameters influencing the thunderstorm development is very large and the parameters themselves concern phenomena which happen on different scales. Furthermore, these parameters are not completely independent, e.g. a frontal passage is usually preceded by south-westerly winds at lower levels and cold air advection at higher levels (which increases the temperature gradient and can cause an increase of the CAPE). Therefore, the definition of the weight of every parameter in the thunderstorm-process is fairly impossible. This means that the scenario *Hailstorm,* which will be discussed in the following, will not lead to clear statements on the future thunderstorm evolution.

Scenario *Hailstorm*

- According to the NFP31, the mean **temperature** will increase by roughly 2.5 K by the year 2030. As has been shown in Chapter 6, the temperature increase recorded in the last decades in the Swiss Mittelland is mainly due to an increase of the minimum (or night-time) temperature. We assume that this will be the case also in the next decades, due to an increase in moisture in the boundary layer. In Chapter 6.3 it was found that the largest

clusters, and the strongest haildays in general, are connected with relatively high minimum temperatures.

- The **total precipitation** measured during a longer time span is given, particularly in summer, by a combination of heavy and light rain events. Light rain is mostly connected with stratiform cloud systems and can last quite a long time (up to one day or more), while heavy rain is usually connected with convective systems, whose duration is of the order of magnitude of hours. The NFP31 predicts a decrease of the total summer precipitation by about 10 % by 2030. Assuming that precipitation falling from thunderstorm cells makes out at the most 30 % of total precipitation in summer (after a personal communication with Dr. Ch. Frei, LAPETH), we decide to neglect this precipitation decrease for this scenario.

- In Section 7.1 we have seen that, because of a general warming of the lower troposphere, the **vertical temperature difference** in this layer has not changed. On the other hand, the vertical difference of the upper half of the troposphere shows a slight increase due to the fact that no important warming was observed at these heights. We assume that this tendency will continue also in the future. Mainly two kinds of evolution can lead to a larger mean value of the temperature difference at higher levels:

  a) the number of cases with higher lability does not change, but the degree of lability of the single cases increases.

  b) the number of cases with higher lability increases, but the degree of lability of the single cases stays constant.

  In case of evolution a) the main consequence would be an intensification of thunderstorms, but no particular increase of the frequency. Evolution b) would cause an increase in frequency but no particular intensification.

- The mean summer values of the **moisture content** at 700 hPa measured by the Payerne-radiosounding show a gradual decrease, particularly in the last two decades. Although a physical explanation of this phenomenon could still not be found, as a possible evolution of our scenario we assume that a further slight decrease of moisture content will take place also in the future and that it will have an inhibiting effect on thunderstorm activity in general.

- According to the North American studies mentioned in Section 7.1, the **cyclonic activity** denotes an increase of frequency and a decrease of intensity in case of a temperature rise. This would probably cause an increase of the number of frontal

passages, and, as a consequence from it, an increase of the number of long-living thunderstorms. Furthermore, we assume that the decrease of cyclonic intensity causes also a reduction of thunderstorm intensity, which probably is accompanied by weaker hail development. None of the studies on the evolution of cyclonic activity mentions an explicit shift of cyclone tracks toward the North or the South, therefore we assume that in our scenario no particular shift will take place.

These are only some of the parameters which could be taken in consideration for a thunderstorm scenario. However, a further definition of the assumptions would complicate the scenario but not necessarily lead to better results. Complex parameters, like weather classifications or CAPE, are defined by a large number of simple parameters, each of which can in turn follow a thunderstorm-favouring or a thunderstorm-inhibiting evolution. This makes it difficult to make a meaningful assumption. Figure 7.2.1 summarises the choices made for scenario *Hailstorm* and evidences how difficult it is to make a forecast of the future thunderstorm activity with the knowledge available nowadays.

Obviously, scenario *Hailstorm* is only one of many possible scenarios. This can be seen from Figure 7.2.1, where every possible evolution of the single parameters is indicated. More precise statements with the other scenarios will not be made and therefore they will not be described in detail. It is probably more meaningful to make a few comments on other possible evolutions of the considered parameters.

It is important to note that the assumption of a change in mean value of a given parameter does not say anything about its variability and vice versa. E.g., an increase in mean (surface) temperature does not exclude the occurrence of very low minima, and even an increase of the mean minimum temperature can still be connected with some very low minima.

The increase of mean surface temperature forecast by the IPCC might also be given, other than by a rise of the mean minimum temperature, by a higher mean maximum temperature. Higher maximum temperatures are usually connected with dry air, otherwise convection would cause condensation and inhibition of solar heating, which prevents a further temperature rise. A higher mean surface temperature can also be given by an increase of both maximum and minimum. But if the increase of the mean minimum is really due to a higher moisture content, the contemporary increase of the maximum would be a contradiction.

In scenario *Hailstorm* we assume that the decrease of total precipitation is merely due to a reduction of stratiform precipitation.

However, in summer, stratiform precipitation is often preceded by convective precipitation. Particularly in the case of squall lines, mature convective cells build up anvils that join together to form a stratiform cloud layer, which shields solar heating and inhibits further convection. The convective system goes over into a stratiform system, and, if the conditions are favourable, several hours of stratiform precipitation can follow the thunderstorms. Therefore, a reduction of total precipitation could also be caused by a slight decrease of larger thunderstorms. The contribution of local, thermally triggered thunderstorms to the total precipitation amount is fairly negligible in today's situation. This contribution will become more important only in case of a large reduction of synoptic disturbances.

The heating of the troposphere, instead of being limited mainly to the lower half of the layer, could gradually extend to the higher levels. This would stop the increase of the vertical temperature gradient considered in scenario *Hailstorm*. On the other hand, the detected cooling of the stratosphere could continue also in the next decades, which would further complicate the situation.

The negative trend of the moisture advection at mid levels in the past ten to fifteen years (see Figure 7.1.4) could also be part of a short term oscillation that has already reached its maximum instead of being the beginning of a long term positive trend. In fact, the time series of radiosounding data is too short to estimate the natural variability of moisture advection.

The studies mentioned in Section 7.1 show that the evolution of future cyclonic activity is still very uncertain and that many different assumptions are still justified. In general, a drop (rise) of intensity probably leads to weaker (stronger) frontal thunderstorms, while a reduction (increase) of cyclone frequency results in a smaller (larger) number of such thunderstorms. A not too large southward shift of the cyclonic tracks is expected to cause a stronger advection of warm moist (mostly maritime tropical) air at low levels ahead of the cold front connected with the cyclone (Huntrieser et al. 1994), favouring the development of strong thunderstorms. In case of a northward shift, the most active part of the cold fronts would not reach our test area and the air reaching it ahead of the fronts would have a stronger westerly component (i.e. colder air with a lower moisture content).

In conclusion, the future thunderstorm activity cannot be predicted, even qualitatively, before more precise information on the future evolution of other climatological parameters will be available.

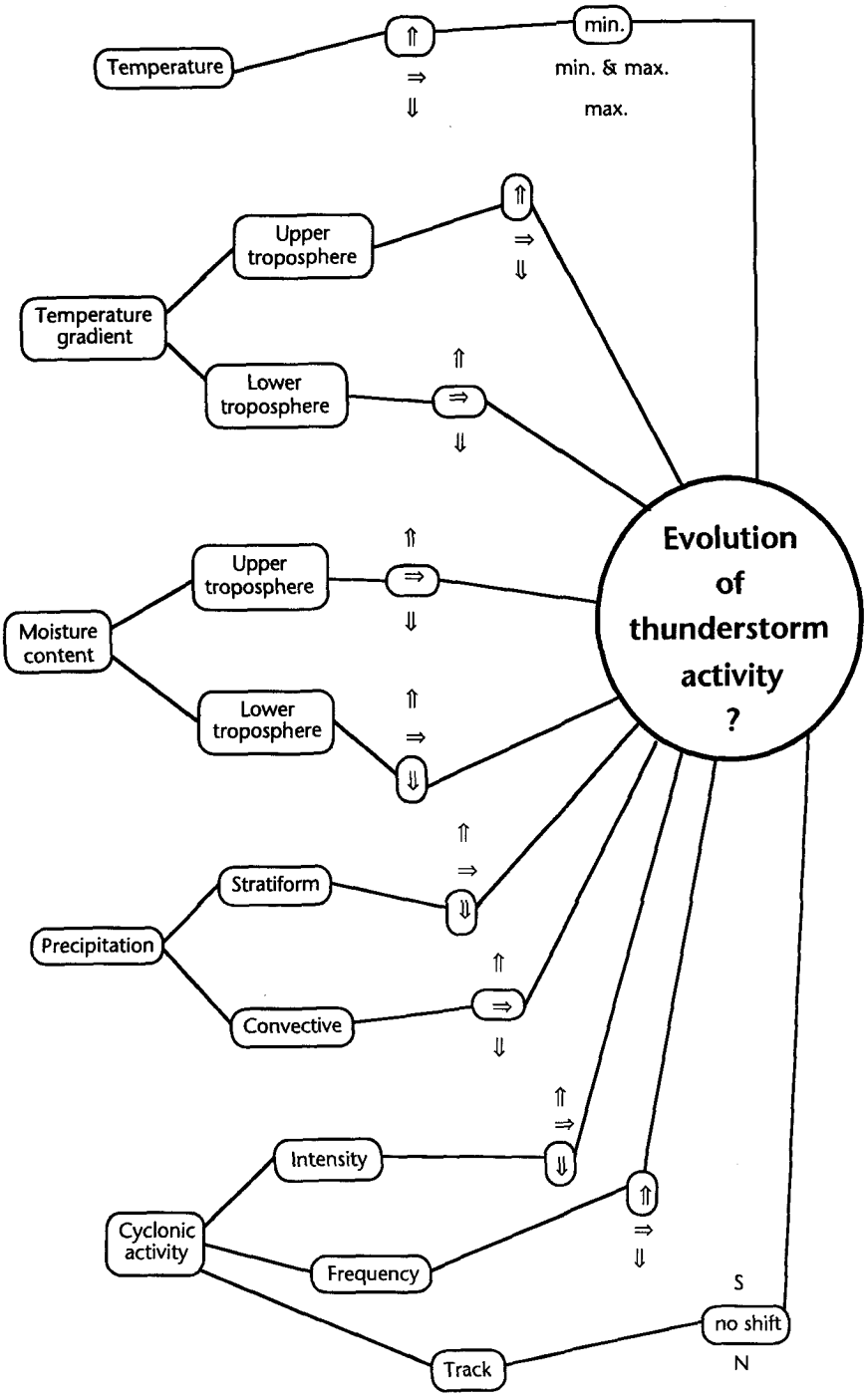

Figure 7.2.1 Scenario *Hailstorm*.

8 Outlook

The present study constitutes the first step of what could be completed by many other studies. The information contained in the damage claims has probably been reasonably exhausted, but the complete data set presented in Chapter 6 could and should enable further evaluations.

In the analyses described previously, the connection between the meteorological factors and the intensity of the hailstorms is studied individually for every single parameter. In reality, however, the triggering of hailstorms depends on the combined interaction between all the factors. The simplest way of describing this interaction is to assume that the hailstorm-intensity is described by a linear combination of all parameters that have shown to influence the life cycle of hailstorms. (Theory on multiple regression can be found in books on multiple statistics , e.g. Linder and Berchtold, 1982; Hartung and Elpert, 1992). A first attempt to obtain a multiple linear regression with these parameters did not lead to satisfactory results, as the separating power of the obtained model on the four-category classification was not larger than the separating power of the single parameters. There are several reasons for this failure, some are given by the characteristics of the data and cannot be avoided, others are caused by the simplified method adopted and can be at least partially eliminated with the application of more refined methods. The non-linear dependence of certain parameters on the intensity of the thunderstorm days, for example, was not considered in the model. It might be worthwhile to make use of transformed parameters.

In the present work the radiosonde data have been analysed only for 12 years (1978 - 1989), because at the time that the evaluations were carried out the whole data set was not yet available. At present the whole set (1954 - 1994) is available on the data base, so that the analysis could be completed. Nevertheless, some caution is necessary, as the resolution of the soundings was repeatedly increased in the course of the years, which might cause inhomogeneities in the data set.

Furthermore, additional parameters could be derived from the radiosoundings (e.g. stability indices, some measure of potential lability or the equivalent potential temperature) and tested for their separating effect on hailstorm days. The large scale temperature advection could also be derived from the sounding with the help of the thermal wind equation. This would enable the distinction of

unstable stratifications from stable stratifications. However, a study carried out by Huntrieser (1995) examining several commonly known stability indices shows that the CAPE has the best separating effect between days with isolated and days with widespread thunderstorms. The other stability indices prove to be useful only for the distinction of fair weather and thunderstorm days, and this is less useful for our purposes since the present work considers mainly stronger hailstorms.

Another possible extension of this study is to define a weather classification that separates thunderstorm days from fair weather days better than the existing classifications. The results obtained in Chapter 5 and 6 give the necessary information on which to base this classification. However, the application of a new classification implies a significant amount of work, since every day of the observation period has to be classified once again.

Clearly, it is desirable to continue the monitoring efforts, with the damage data and particularly with the RADAR data, in order to extend the hail- and thunderstorm-time series begun in this study. Some difficulties might arise concerning the data collection. Since 1994 the Swiss Hail Insurance Company is not the only one insuring crops in Switzerland, which implies a greater effort to obtain a uniform and complete data set (assuming that the other insurance companies are willing to deliver information on the damage claims). Concerning the RADAR data, since fall 1994 the composit RADAR pictures of the SMA have changed: the Albis RADAR has been substituted by a new one and a third RADAR located on the Monte Lema, in southern Switzerland, has been added to the network. Additionally, the measurements of foreign (particularly German) RADARs are being added to the composit picture, too. Later on, after the substitution of the La Dôle RADAR, the resolution of the obtained pictures will probably be doubled. All these changes lead to discontinuities in the data which can influence the quality of the monitoring time series.

Last but not least, further climatological works can provide an important input to the continuation of this study. A climatological study of the cyclonic (and anticyclonic) activity in the Alpine area in the past and modelling experiments of the future activity would be very useful.

References

Chapter 1

1991: *Meteorological Glossary.* HMSO, London, pp. 335.

Banta, R. M., 1990: The role of mountain flows in making clouds. In: W. Blumen (ed.), Atmospheric processes over complex terrain, American Meteorological Society, Boston, 229 - 283.

Bider, M., 1954: Statistische Untersuchungen über die Hagelhäufigkeit in der Schweiz und ihre Beziehungen zur Grosswetterlage. *Arch. Meteor. Geophys. Bioklimat.*, **Bd. 6**, 66 - 90.

Böhme, W., 1993: Untersuchungen zur Reaktion des Klimasystems auf grosse vulkanische Eruptionen mittels Phasenebenen-Darstellung. *Meteor. Zeitschrift*, 2, 76-80.

Browning, K. A., 1986: Morphology and classification of mid-latitude thunderstorms. In: E. Kessler (ed.), *Thunderstorm morphology and dynamics*, University of Oklahoma Press, Norman, 133 - 152.

Byers, H. R. and R. R. Braham Jr., 1949: *The thunderstorm.* U. S. Govt. Printing Off., Washington D.C., pp. 287.

Changnon, S. A. and J. M. Changnon, 1992: Storm Catastrophes in the United States. *Nat. Hazards* , 6, 93 - 107.

Changnon, S. A., Jr. and G. E. Stout, 1967: Crop-hail intensities in central and northwest United States. *J. Appl. Meteor.* , 6, 542 - 548.

Chisholm, A. J. and J. H. Renick, 1972. The kinematics of multicell and supercell Alberta hailstorms. Research Council of Alberta Hail Studies.

Dessens, J., 1994: The hail problem in the context of a nighttime global warming. *Sixth WMO Scientific Conference on Weather Modification*, Peastum, Italy, WMO, 75 - 78.

Dutton, E. G. and J. R. Christy, 1992: Solar radiative forcing at selected locations and evidence for global lower tropospheric cooling following the eruptions of El Chichón and Pinatubo. *Geoph. Res. Lett.*, **19**, 2313-2316.

Emanuel, K. A., 1987: The dependence of hurricane intensity on climate. *Nature*, **326**, 483-485.

Flohn, H., 1989: Singuläre Vorgänge und Katastrophen in der Klima-Entwicklung. *Nova acta Leopoldina NF 62*, **270**, 99 - 113.

Foote, G. B. and C. A. Knight (ed.), 1977: *Hail: a review of hail science and hail supression.* Meteorological Monographs. Boston, Amer. Meteor. Soc., pp. 277.

Frey - Buness, A., 1993. Ein statistisch-dynamisches Verfahren zur Regionalisierung globaler Klimasimulationen. DLR, Inst. für Physik der Atmosphäre, pp. 149.

Hansen, J. and S. Lebedeff, 1988: Global surface air temperatures: update through 1987. *Geoph. Res. Lett.*, **15**, 323 - 326.

Houghton, J. T. (ed.), 1984: *The global climate.* Cambridge, Cambridge University Press, pp. 233.

Houghton, J. T., B. A. Callander and S. K. Varney (ed.), 1992: *Climate change 1992. The supplementary report to the IPCC scientific assessment.* Cambridge, University Press, pp. 200.

Houghton, J. T., G. J. Jenkins and J. J. Ephraums (ed.), 1990: *Climate change. The IPCC scientific assessment.* Cambridge, University Press, pp. 365.

Houze, R. A., Jr., 1993: *Cloud dynamics.* Academic Press, San Diego, pp. 573.

Hutter, K., H. Blatter and A. Ohmura, 1990. Climatic changes, Ice sheet dynamics and sea level variations. ETH Zürich (Geographisches Institut).

Idso, S. B., R. C. Balling Jr. and R. S. Cerveny, 1990: Carbon dioxide and hurricanes: implications of northern hemispheric warming for atlantic/caribbean storms. *Meteorol. Atmos. Phys.*, **42**, 259-263.

Johns, R. H. and C. A. Doswell III, 1992: Severe local storms forecasting. *Weather and forecasting*, **7**, 588 - 612.

Jones, P. D., 1988: Hemispheric surface air temperature variations: recent trends and an update to 1987. *J. Climate*, **1**, 654 - 660.

Kessler, E. (ed.), 1986: *Thunderstorm morphology and dynamics.* Norman, University of Oklahoma Press, pp. 411.

List, R., 1986: Properties and growth of hailstones. In: E. Kessler (ed.), *Thunderstorm morphology and dynamics*, University of Oklahoma Press, Norman, 259 - 276.

Lorenz, E. N., 1968: Climatic determinism. In: J. M. M. Mitchell Jr. (ed.), *Causes of climatic change*, Amer. Meteor. Soc., Boston.

Lorenz, E. N., 1976: Nondeterministic theories of climatic change. *Quatern. Res.*, **6**, 495 - 506.

Macklin, W. C., 1977: The characteristics of natural hailstones and their interpretation. In: G. B. Foote and C. A. Knight (ed.), *Hail: a review of hail science and hail suppression*, Amer. Meteor. Soc., Boston, 65 - 88.

Mitchell, J. M., Jr., 1976: An overview of climatic variability and its causal mechanisms. *Quatern. Res.*, **6**, 481 - 493.

Morgan, G. M. and P. W. Summers, 1986: Hailfall and hailstorm characteristics. In: E. Kessler (ed.), *Thunderstorm morphology and dynamics*, University of Oklahoma Press, Norman, 237 - 257.

Paul, A., 1991: Studies of long-lived hailstorms in Saskatchewan, Canada from Crop Insurance Data. *Nat. Hazards*, **4**, 345 - 352.

Press, F. and R. Siever, 1986: *Earth.* W. H. Freeman and Company, New York, pp. 656.

Rasmusson, E. M. and J. M. Wallace, 1983: Meteorological aspects of the El Nino / Southern Oscillation. *Science*, **222**, 1195 - 1202.

Ruddiman, W. F. and J. E. Kutzbach, 1991: Plateau uplift and climatic change. *Sci. Amer.*, **264**, 66 - 75.

Schönwiese, C.-D., 1994: *Klimatologie.* Verlag Eugen Ulmer, Stuttgart, pp. 436.

Schönwiese, C.-D., J. Rapp, T. Fuchs and M. Denhard, 1993. Klimatrend-Atlas Europa 1891 - 1990. Zentrum für Umweltforschung, J. W. Goethe - Universität.

Schönwiese, C. D., 1979: *Klimaschwankungen.* Springer - Verlag, Berlin, pp. 181.

Shapiro, L. J., 1982: Hurricane climatic fluctuations. Part I: patterns and cycles. *Mo. Wea. Rev.*, **110**, 1007 - 1013.

Shapiro, L. J., 1982: Hurricane climatic fluctuations. Part II: relation to large-scale circulation. *Mo. Wea. Rev.*, **110**, 1014 - 1023.

Vinnikov, K. Y., P. Y. Groisman and K. M. Lugina, 1990: Empirical data on contemporary global climate changes (temperature and precipitation). *J. Climate*, **3**, 662 - 677.

Wallace, J. M. and P. V. Hobbs, 1977: *Atmospheric Science, An Introductory Survey.* Academic Press, New York, pp. 467.

Weisman, M. L. and J. B. Klemp, 1982: The dependence of numerically simulated convective storms on vertical wind shear and buoyancy. *Mo. Wea. Rev.*, **110**, 504-505.

Chapter 2

Bundesamt für Statistik, 1970: *Statistisches Jahrbuch der Schweiz.* Bern.

Bundesamt für Statistik, 1987. Eidg. Betriebszählung 1985: Die Nutzung des Kulturlandes.

Bundesamt für Statistik, 1990: *Statistisches Jahrbuch der Schweiz.* Verlag Neue Zürcher Zeitung, Bern.

Eidg. Statistisches Amt, 1959. Bodenbenützung in der Schweiz, 1955.

Kipfer, W., 1988. Die schweizerische Landwirtschaft; Bilder, Zahlen, Kommentare. Bundesamt für Statistik, Bern.

Schiesser, H.-H., 1988. Fernerkundung von Hagelschäden mittels Wetterradar untersucht an Ackerkulturen. Zürich.

Chapter 3

LAPETH, Gruppe für Radarmeteorologie, 1995. Monitoring von starken Hagelstürmen in der Schweiz 1994. Report n. 33. Zürich, Juni 1995.

Schiesser, H.-H., 1988. Fernerkundung von Hagelschäden mittels Wetterradar untersucht an Ackerkulturen. Zürich.

SHV, 1972. Raps. Schweizerische Hagel-Versicherungs-Gesellschaft Zürich.

SHV, 1975. Wein. Schweizerische Hagel-Versicherungs-Gesellschaft Zürich.

SHV, 1979. Hackfrüchte. Schweizerische Hagel-Versicherungs-Gesellschaft Zürich.

SHV, 1981. Tabak. Schweizerische Hagel-Versicherungs-Gesellschaft Zürich.

SHV, 1982. Getreide. Schweizerische Hagel-Versicherungs-Gesellschaft Zürich.

SHV, 1982. Mais. Schweizerische Hagel-Versicherungs-Gesellschaft Zürich.

SHV, 1984. Obst. Schweizerische Hagel-Versicherungs-Gesellschaft Zürich.

SMA, 1991. Annalen der Schweizerischen Meteorologischen Anstalt. Schweizerische Meteorologische Anstalt.

Chapter 4

Bider, M., 1954: Statistische Untersuchungen über die Hagelhäufigkeit in der Schweiz und ihre Beziehungen zur Grosswetterlage. *Arch. Meteor. Geophys. Bioklimat.*, **Bd. 6**, 66 - 90.

Schönwiese, C.-D., 1992: *Praktische Statistik für Meteorologen und Geowissenschafter.* Gebrüder Borntraeger, Berlin-Stuttgart, pp. 231.

Schönwiese, C.-D., J. Rapp, T. Fuchs and M. Denhard, 1993. Klimatrend-Atlas Europa 1891 - 1990. Zentrum für Umweltforschung, J. W. Goethe - Universität.

Chapter 5

Banta, R. M., 1990: The role of mountain flows in making clouds. In: W. Blumen (ed.), *Atmospheric processes over complex terrain*, American Meteorological Society, Boston, 229 - 283.

Beniston, M., M. Rebetez, F. Giorgi and M. R. Marinucci, 1994: An analysis of regional climate change in Switzerland. *Theor. Appl. Climatol.*, **49**, 135 - 159.

Briffa, K. R., P. D. Jones and M. Hulme, 1994: Summer moisture variability across Europe, 1892 - 1991: an analysis based on the Palmer Drought Severity Index. *Int. J. Climatol.*, **14**, 475 - 506.

Browning, K. A., 1986: Morphology and classification of mid-latitude thunderstorms. In: E. Kessler (ed.), *Thunderstorm morphology and dynamics*, University of Oklahoma Press, Norman, 133 - 152.

Chisholm, A. J. and J. H. Renick, 1972. The kinematics of multicell and supercell Alberta hailstorms. Research Council of Alberta Hail Studies.

Dessens, J., 1994: The hail problem in the context of a nighttime global warming. *Sixth WMO Scientific Conference on Weather Modification*, Peastum, Italy, WMO, 75 - 78.

Fankhauser, J. C., A. C. Modahl, C. G. Mohr and M. E. Solak, 1976. Final Report-National Hail Research Experiment Randomized Seeding Experiment 1972-1974. National Center for Atmospheric Research.

Federer, B., U. Görner, D. Högl and A. Waldvogel, 1973. Bericht über das Feldexperiment im Bassin Lémanique vom 23. Mai-15. August 1972. LAPETH.

Gerstengarbe, F.-W. and P. C. Werner, 1992: The time structure of extreme summers in central Europe between 1901 and 1980. *Meteor. Zeitschrift*, **1**, 285 - 289.

Gerstengarbe, F.-W. and P. C. Werner, 1993. Katalog der Grosswetterlagen Europas nach Paul Hess und Helmuth Brezowski 1881-1992. Deutscher Wetterdienst.

Hess, P. and H. Brezowsky, 1952. Katalog der Grosswetterlagen Europas. Deutscher Wetterdienst in der US-Zone.

Houze, R. A., Jr., W. Schmid, R. G. Fovell and H. H. Schiesser, 1993: Hailstorms in Switzerland: left movers, right movers, and false hooks. *Mo. Wea. Rev.*, **121**, 3345-3370.

Karl, T. R., G. Kukla, V. N. Razuvayev, M. J. Changery, R. G. Quayle, R. R. Heim et al., 1991: Global warming: evidence for asymmetric diurnal temperature change. *Geoph. Res. Letters*, **18**, 2253-2256.

Mahrt, L., 1976: Mixed layer moisture structure. *Mon. Wea. Rev.*, **104**, 1403-1407.

Marwitz, J. D., 1972: The structure and motion of severe hailstorms. Part I: Supercell Storms. *J. Appl. Meteor.*, **11**, 166 - 201.

Rind, D., R. Goldberg and R. Ruedy, 1989: Change in climate variability in the 21st century. *Climatic Change*, **14**, 5-37.

Schiesser, H. H., 1985: Grossversuch IV: "extended area" effects on rainfall. *J. Climate Appl. Meteor.*, **24**, 236 - 252.

Schüepp, M., 1979. Witterungsklimatologie. Schweizerische Meteorologische Anstalt.

Wanner, H., 1994. The atlantic european circulation patterns and their significance for climate change in the Alps. National Science Foundation.

Weber, R. O., P. Talkner and G. Stefanicki, 1994: Asymmetric diurnal temperature change in the Alpine region. *Geoph. Res. Lett.*, **21**, 673 - 676.

Chapter 6

Atlas, D., 1990: *Radar in Meteorology.* Am. Meteor. Soc., Boston, pp. 806.

Federer, B., A. Waldvogel, W. Schmid, H. H. Schiesser, F. Hampel, M. Schweingruber et al., 1986: Main results of Grossversuch IV. *J. Climate Appl. Meteor.*, **25**, 917 - 957.

Galli, G., 1984: Generation of the Swiss radar composite. *22nd Conf. on radar meteorology, Zürich*, 208 - 213.

Geotis, S., 1963: Some radar measurements of hailstorms. *J. Appl. Meteor.*, **2**, 270 - 275.

Katz, R. W. and R. R. Garcia, 1981: Statistical relationships between hailfall and damage to wheat. *Agric. Meteorol.*, **24**, 29 - 43.

Rinehart, R. E., 1992: *Radar for Meteorologists.* Dep. of Atmosph. Sciences, University of North Dakota, Grand Forks, North Dakota, pp. 334.

Schiesser, H.-H., 1988. Fernerkundung von Hagelschäden mittels Wetterradar untersucht an Ackerkulturen. Zürich.

Schiesser, H. H., 1990: Hailfall: the relationship between radar measurements and crop damage. *Atmosph. Res*, **25**, 559 - 582.

Schmid, W., H. H. Schiesser and A. Waldvogel, 1992: The Kinetic energy of hailfalls. Part IV: patterns of hailpad and radar data. *J. Appl. Meteor.*, **31**, 1165-1178.

Smith, P. L., D. J. Musil and A. Waldvogel, 1984: Aircraft observations inside Swiss hailstorms. *9th Int. Conf. Cloud Physics Conf.*, Tallinn, 109 - 112.

Vanolli, F., 1993. Comparaison de deux dispositifs de radars météorologiques, en utilisant des mesures de reflectivité faites au sein d'orages violents et de mesures de précipitations et de grêle faites au sol. ETH.

Waldvogel, A., B. Federer and P. Grimm, 1979: Criteria for the detection of hail cells. *J. Appl. Meteor.*, **18**, 1521-1525.

Waldvogel, A., B. Federer, W. Schmid and J. F. Mezeix, 1978: The kinetic energy of hailfalls. Part II: Radar and hailpads. *J. Appl. Meteor.*, **17**, 1680 - 1693.

Waldvogel, A. and W. Schmid, 1982: The kinetic energy of hailfalls. Part III: Sampling errors inferred from radar data. *J. Appl. Meteor.*, **21**, 1228 - 1238.

Waldvogel, A., W. Schmid and B. Federer, 1978: The kinetic energy of hailfalls. Part I: Hailstone spectra. *J. Appl. Meteor.*, **17**, 515 - 520.

Wojtiw, L., and Ewing, C.G., 1983: The use of radar to estimate crop damage for hailstorms in Alberta, Canada. *21st Conf. on radar meteorology, Edmonton.*

Wojtiw, L., and Ewing, C., 1986: The relationship of time-integrated radar reflectivity with hail crop damage. *23rd Conf. on radar meteorology, Snowmass.*

Chapter 7

Agee, E. M., 1991: Trends in cyclone and anticyclone frequency and comparison with periods of warming and cooling over the northern hemisphere. *J. Climate*, **4**, 263 - 267.

Angell, J. K., 1988: Variations and trends in tropospheric and stratospheric global temperatures, 1958-87. *J. Climate*, **1**, 1296 -1313.

Angell, J. K. and J. Korshover, 1983: Global temperature variations in the troposphere and stratosphere, 1958 - 1982. *Mo. Wea. Rev.*, **111**, 901 - 921.

Balling, R. C., Jr., R. S. Cerveny, T. A. Miller and S. B. Idso, 1991: Greenhouse warming may moderate British storminess. *Meteorol. Atmos. Phys.*, **46**, 181 - 184.

Boer, G. J. and K. Higuchi, 1980: A study of climatic variability. *Mo. Wea. Rev.*, **108**, 1326-1332.

Chen, S.-J. and Y.-H. Kuo, 1994: Cyclones and northern hemisphere temperature. *Theor. Appl. Climatol.*, **49**, 85 - 89.

Hosler, C. L. and L. A. Gamage, 1956: Cyclone frequencies in the United States for the period 1905 to 1954. *Mo. Wea. Rev.*, **84**, 388 - 390.

Huntrieser, H., H. H. Schiesser and A. Waldvogel, 1994: The synoptic and mesoscale environment of severe convective activity in Switzerland. *The life cycles of extratropical cyclones*, Bergen, Norway, 101 - 106.

Makrogiannis, T. J. and H. S. Sahsamanoglou, 1992: Analysis of mean temperature variations at the 1000/500 hPa layer over Europe, 1945-88. *Theor. Appl. Climatol.*, **45**, 193 - 200.

Oort, A. H. and H. Liu, 1993: Upper-air temperature trends over the globe, 1958-1989. *J. Climate*, **6**, 292 - 307.

Parker, S. S., J. T. Hawes, S. J. Colucci and B. P. Hayden, 1989: Climatology of 500 mb cyclones and anticyclones, 1950 - 85. *Mo. Wea. Rev.*, **117**, 558 - 570.

Reitan, C. H., 1974: Frequencies of cyclones and cyclogenesis for North America, 1951 - 1970. *Mo. Wea. Rev.*, **102**, 861 - 868.

Reitan, C. H., 1979: Trends in the frequencies of cyclone activity over North America. *Mo. Wea. Rev.*, **107**, 1684 - 1688.

Sahsamanoglou, H. S. and T. J. Makrogiannis, 1992: Temperature trends over the Mediterranean region, 1950-88. *Theor. Appl. Climatol.*, **45**, 183 - 192.

Schinke, H., 1993: On the occurrence of deep cyclones over Europe and the North Atlantic in the period 1930 - 1991. *Beitr. Phys. Atmosph.*, **66**, 223 - 237.

Van den Dool, H. M., O'Lenic, E.A., and Klein, W.H., 1993: Consistency ceck for trends in surface temperature and upper-level circulation: 1950-1992. *J. Climate*, **6**, 2288 - 2297.

Whittaker, L. M. and L. H. Horn, 1981: Geographical and seasonal distribution of North American cyclogenesis, 1958 - 1977. *Mo. Wea. Rev.*, **109**, 2312 - 2322.

Zishka, K. M. and P. J. Smith, 1980: The climatology of cyclones and anticyclones over North America and surrounding ocean environs for January and July, 1950 - 1977. *Mo. Wea. Rev.*, **108**, 387 - 401.

Chapter 8

Hartung, J. and B. Elpert, 1992: *Multivariate Statistik*. Oldenburg Verlag, München, pp. 815.

Huntrieser, H., 1995. Zur Bildung, Verteilung und Vorhersage von Gewittern in der Schweiz. ETH Zürich, Diss. Nr. 11020.

Linder, A. and W. Berchtold, 1982: *Statistische Methoden II. Varianzanalyse und Regressionsrechnung*. Birkhäuser Verlag, Basel, pp. 295.

Appendix B

Brugger, H., 1985: Die schweizerische Landwirtschaft 1914 - 1980. Huber Frauenfeld, pp. 320.

Schiesser, H.-H., 1988. Fernerkundung von Hagelschäden mittels Wetterradar untersucht an Ackerkulturen. Zürich.

Appendix D

Bundesamt für Statistik, 1970: *Statistisches Jahrbuch der Schweiz.* Bern.

Bundesamt für Statistik, 1987. Eidg. Betriebszählung 1985: Die Nutzung des Kulturlandes.

Bundesamt für Statistik, 1990: *Statistisches Jahrbuch der Schweiz.* Verlag Neue Zürcher Zeitung, Bern.

Kipfer, W., 1988. Die schweizerische Landwirtschaft; Bilder, Zahlen, Kommentare. Bundesamt für Statistik, Bern.

Appendix A:

Abbreviations

Cantons:	AA	Appenzell Ausserrhoden
	AG	Aargau
	AI	Appenzell Innerrhoden
	BE	Bern
	BL	Basel Land
	BS	Basel Stadt
	FR	Fribourg
	JU	Jura
	LU	Luzern
	NE	Neuchâtel
	NW	Nidwalden
	OW	Obwalden
	SG	St. Gallen
	SO	Solothurn
	SZ	Schwyz
	TG	Thurgau
	VD	Vaud
	ZG	Zug
	ZH	Zürich
CAPE:	convective available potential energy	
CCL:	convective condensation level	
CP:	claim potential	
GCM:	general circulation model	
HAAN:	computer program for hail damage-analysis	
HBC:	Hess - Brezowsky classification of weather types	
IPCC:	Intergovernmental Panel on Climate Change	

LAPETH:	Laboratorium für Atmosphärenphysik (Institute of Atmospheric Sciences at ETH)
LCL:	lifting condensation level
NFP31:	Nationales Forschungs Programm 31
OP:	days of the test season within the years 1949 - 1993
PDSI:	Palmer Drought Severity Index
RADAR:	radio detection and ranging
SC:	Schüepp classification of weather types
SHV:	Schweizerische Hagel Versicherung (Swiss Hail Insurance Company)
SMA:	Schweizerische Meteorologische Anstalt (Swiss Meteorological Institute
TA:	test area (see Figure 2.2.1)
TS:	Test season (20th of May until 10th of September)
UNEP:	United Nations Environmental Programme
UTC:	universal time coordinated
WMO:	World Meteorological Organisation

Definitions

Damage claim:	one community claiming damage
Damage cluster:	closed area of hail damage computed by the program HAAN

Appendix B: The *Schweizer Hagel Versicherung*

The following description of the SHV is a translated version of the one by (Schiesser 1988):

The SHV is a society founded in 1880 by farmers and its board of directors is composed by leading farmer agents. The aim of this form of insurance, defined as *agricultural* insurance, is to protect farmers against the economic consequences of unforeseen elemental damages to cultures. The company insures farming and gardening cultures against hail damages and other kinds of damages caused by windstorms, snow pressure, erosion, lightning, fire, earthquakes, landslides or floods and takes on all expenses for the restoration of the crop land.

In order to run the company in the most economic way and to keep the administrative expenses as low as possible most of the work is done by a part-time working staff. In spring 400 agents belonging to various professions and living in all parts of the country take out policies. Estimation of hail damage is done by 500 experts, whose main job is also in some way connected with agriculture.

The reimbursements in percent of the sum insured illustrated in Figure B1 (Brugger 1985) show the strong yearly variability of the damage accrual for the time period 1911 to 1980.

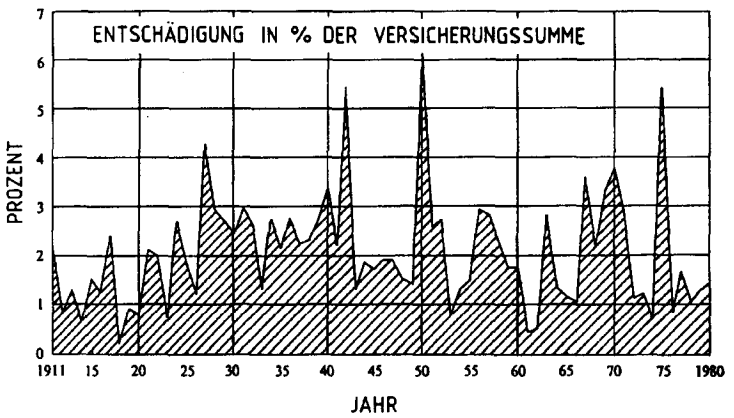

Figure B1 Reimbursement in percent of the sum insured (Brugger 1985).

Appendix C: Political and topographical maps of Switzerland

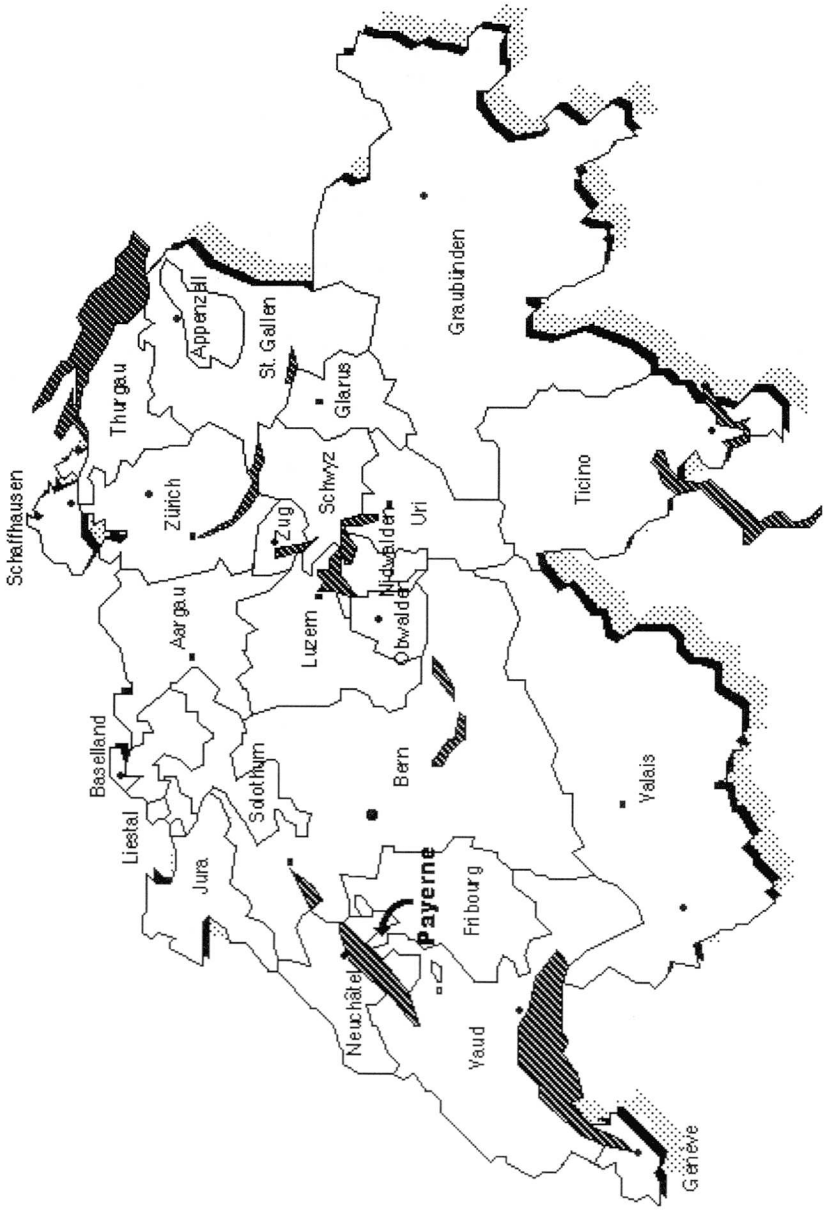

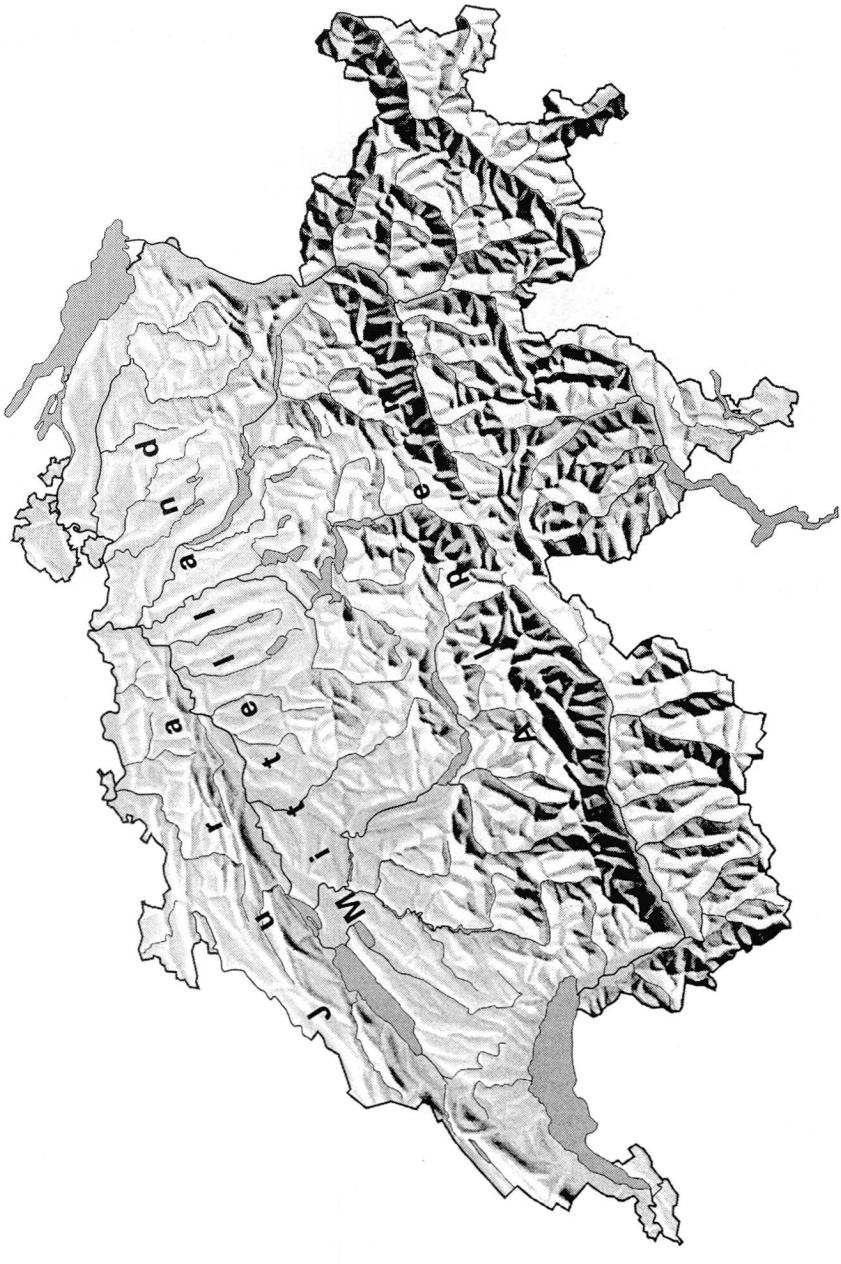

Appendix D: Distribution of the most widespread cultures

The following Figures were taken from Bundesamt für Statistik (1987) and Kipfer (1988):

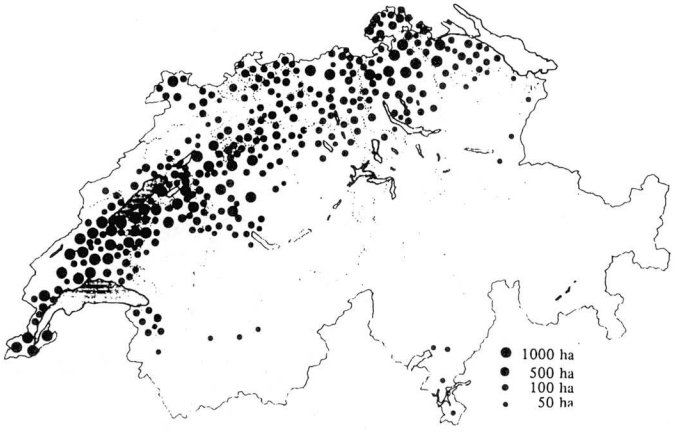

Figure D1 Wheat.

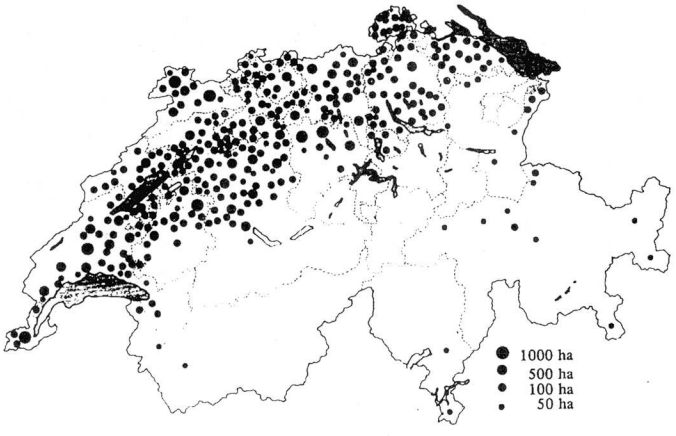

Figure D2 Barley.

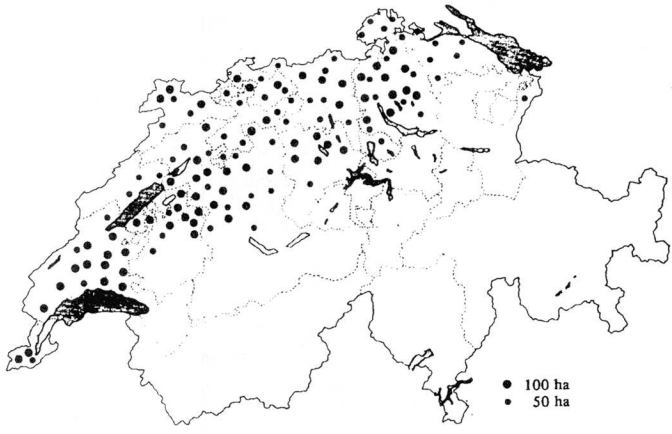

Figure D3 Oats.

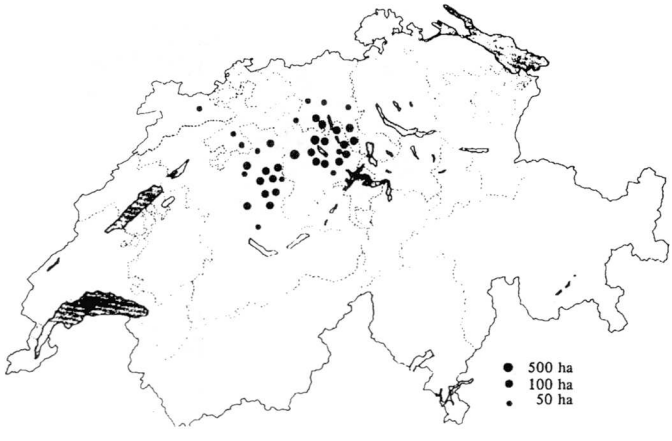

Figure D4 Dinkel: this is a special kind of summer cereal that is grown only in the region indicated by the dots, where it can be considered a substitute of wheat. In fact, if we fill in these dots in the wheat chart, the gap in the central Mittelland is eliminated.

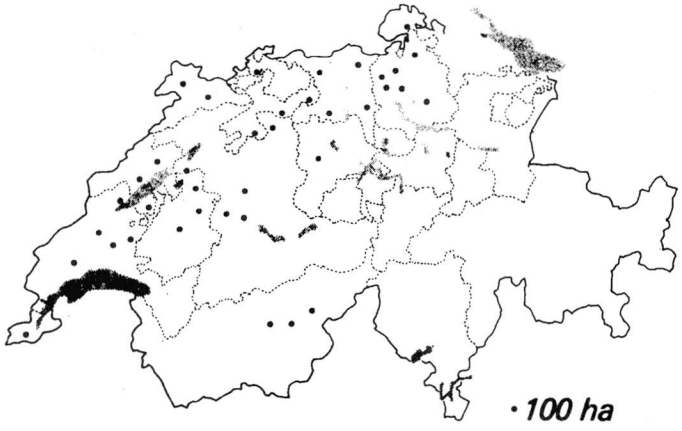

Figure D5 Rye.

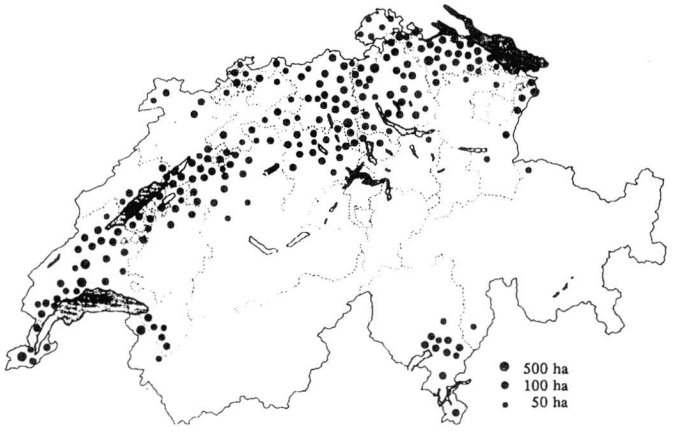

Figure D6 Grain maize.

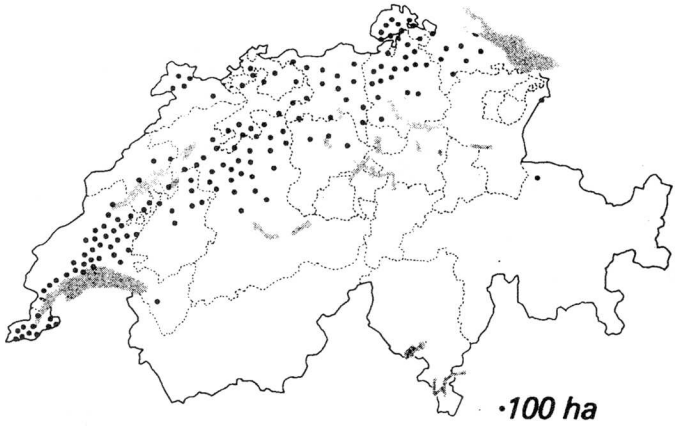

Figure D7 Rape.

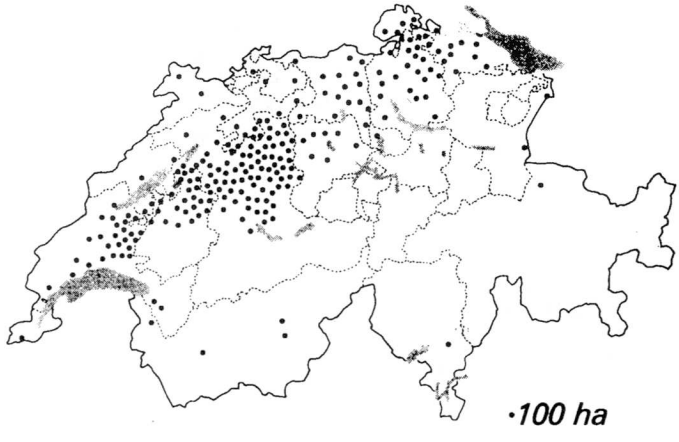

Figure D8 Potatoes.

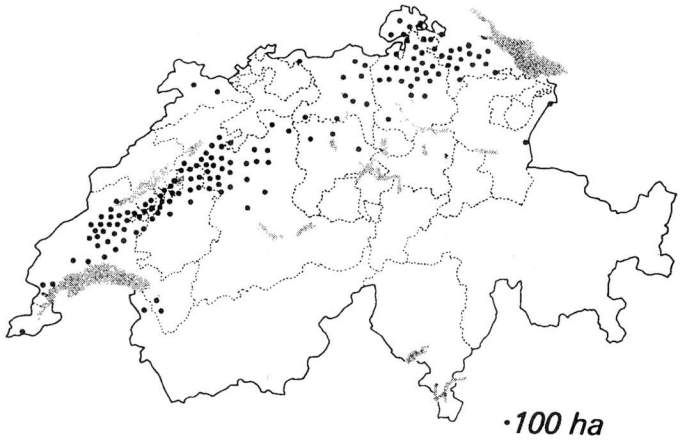

Figure D9 Sugar beet.

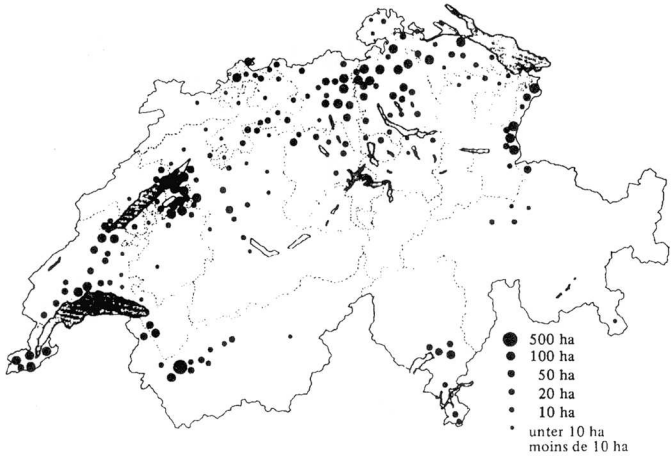

Figure D10 Vegetables (without thresh peas and machine beans).

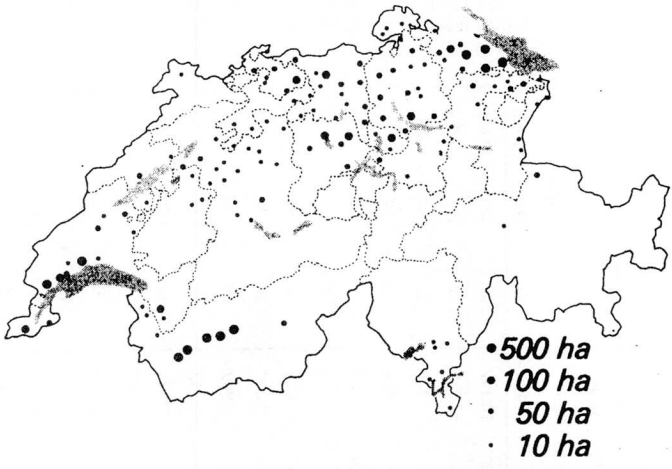

Figure D11 Fruit-growing cultures.

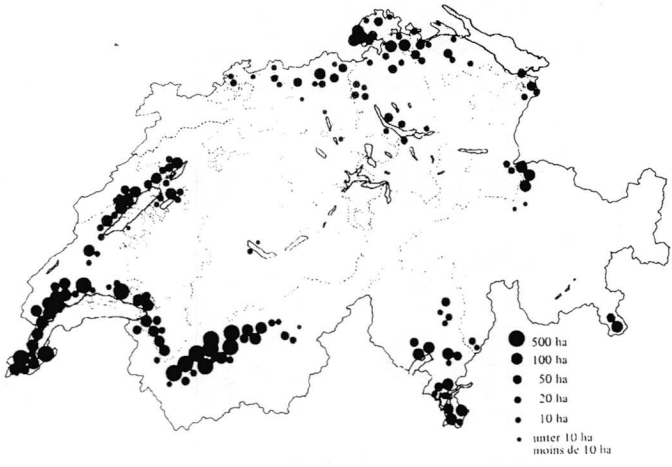

Figure D12 Grapevine.

Table D1 Agricultural productive land classified by kind of crops, in hectares (1955, 1969, 1990). The areas belonging to the Canton Jura in 1990 were still included in the Canton Bern in 1955 and 1969. (Bundesamt für Statistik 1970; Bundesamt für Statistik 1990).

Cantons	Cereals			Vegetables			Root crops and other arable land-cultures			Orchards		
	1955	1969	1990	1955	1969	1990	1955	1969	1990	1955	1969	1990
Zürich	15'126	16'163	21'711	1'774	886	1'062	7'733	7'698	10'392	207	324	431
Bern	44'385	44'087	38'405	1'606	1'416	1'020	21'363	19'115	19'930	112	169	294
Luzern	10'589	8'061	10'373	329	366	113	4'505	2'691	4'249	22	201	273
Schwyz	141	35	196	46	38	10	253	59	151	3	37	56
Obwalden	43	0	9	26	12	2	76	2	28	0	3	3
Nidwalden	11	0	1	13	5	0	25	2	15	0	2	2
Zug	772	416	1'095	41	27	23	446	295	676	7	82	116
Fribourg	15'754	15'092	17'862	680	463	364	6'190	5'325	8'000	30	27	37
Solothurn	7'883	7'869	8'926	205	135	109	3'601	2'979	3'909	18	48	75
Basel-Stadt	156	190	203	34	30	19	56	13	32	10	13	7
Basel-Landschaft	4'091	4'318	4'333	218	157	164	1'519	1'145	1'495	35	134	232
Appenzell A. Rh.	5	2	4	16	4	1	19	2	10	4	0	1
Appenzell I. Rh.	1	1	1	2	2	0	4	2	2	0	0	0
St. Gallen	2'024	1'363	2'711	565	253	286	1'674	952	2'244	47	224	273
Aargau	13'854	15'047	20'329	834	625	845	7'131	5'891	8'203	99	351	396
Thurgau	7'006	6'838	11'905	1'269	590	495	3'086	3'269	5'345	58	1'066	1'799
Vaud	32'217	36'992	41'390	1'058	432	704	12'096	11'460	17'211	445	894	1'055
Neuchâtel	3'359	3'548	4'849	110	63	36	793	743	1'307	33	70	64
Jura			9'907			17			3'329			11

Table D2 Insured areas per culture and per Canton, in percent of the total culture area (1951, 1976) (data supplied by the SHV)

Canton	Cereals		Maize	Rape		Root crops		Vegetables		Grapevine		Grasslands	
	1951	1976	1976	1951	1976	1951	1976	1951	1976	1951	1976	1951	1976
Zuerich	66	78	72	100	78	11	45	19	41	71	86	1.3	1.5
Bern	75	76	47	95	87	6	17	39	47	100	85	3	4
Luzern	68	68	60	53	79	4	15	45	50	100	43	8	4
Schwyz	30	55	36	0	0	15	28	22	71	30	14	4	5
Obwalden	0	0	92	0	0	7	3	15	30	0	0	5	2
Nidwalden	0	0	19	0	0	19	5	19	100	0	0	12	12
Zug	46	53	82	35	89	15	25	39	47	0	0	8	6
Fribourg	74	77	51	100	71	2	20	19	33	50	60	4	3
Solothurn	81	83	46	97	100	6	20	40	45	100	100	0.2	0.2
Basel-Stadt	100	69	100	0	0	83	20	100	75	100	100	3	0
Basel-Land	80	89	65	100	60	5	39	44	83	100	100	0.2	0.1
Appenzell A.	100	0	0	0	0	0	0	24	100	20	0	15	28
Appenzell I.	0	0	25	0	0	23	10	30	35	0	0	10	7
St. Gallen	35	27	27	46	40	15	16	26	40	58	58	8	9
Aargau	71	75	52	60	79	6	27	22	41	73	73	0.4	0.1
Thurgau	76	66	49	100	77	19	37	48	30	98	75	2	0.8
Vaud	97	77	39	65	66	1	23	2.8	40	100	94	0	0.2
Neuchatel	41	64	40	33	33	6	18	9	30	100	89	12	12

Acknowledgements

In the course of my dissertation at LAPETH I met many people who in some way contributed to the success of this work. It will be impossible to mention them all, but I will try at least to list the most important ones:

Professor Albert Waldvogel gave me the opportunity to carry out this dissertation at LAPETH. He insisted on the importance of the T structure of a scientist's knowledge (a broad superficial knowledge connected with a deep knowledge in a specific subject) and gave me a large freedom in my research work.

A special thank goes to Hans Heinrich Schiesser, who initiated the work on hail damage claims and followed my thesis with great interest. These three years of discussions and collaboration have been very instructive.

My co-examiners Professor Christian-Dietrich Schönwiese and Doctor Dietrich Heimann invested a lot of their precious time to review this dissertation. Thanks a lot for the interesting and pleasant collaboration!

I am indebted to Professor Huw Davies, who was so kind to correct the English language of this work.

I am also very grateful to Jürg Bader for his precious statistical advises and the interesting discussions on scientific, political and social subjects.

Another special thank goes to my colleague Heidi Huntrieser for her friendship and support during working hours and free time.

Ruedi Lüthi and Peter Isler were always ready to help in case of technical problems and to provide the best computer equipment: thank you!

Willi Schmid, with his cool *berner* humour, and Li Li, with his friendly Chinese manners, contributed to create a pleasant atmosphere in the office. The rather short time I shared the office with Eszter Barthazy was very pleasant and interesting.

Marco Volken helped me through difficult moments and shared some nicer times with me, confirming our long-lasting, special friendship.

I also thank Martin Widmann, Andrea Rossa, Heini Wernle, Michael Lehning, Martin Gassner, André Prevôt and all other colleagues at LAPETH for their help, the interesting and / or cheerful discussions and all other activities in and outside of the institute.

A very special thank goes to my parents Emmy and Dirk, who always sustained me, even in the most critical times. Without their support many things would have been much more difficult, or even impossible!

I am grateful to my brother Jochem and Irene, who were present when I most needed them. An additional thank goes to Jochem for the design of the cover of my dissertation.

I am also indebted to my dear friends Rahel and Thomas who shared with me nice moments and helped me out in less nice moments.

Furthermore, I want to thank Alex Primas for the encouraging discussions and the great interest in my work.

Maja Werfeli dedicated her precious time to interesting and helpful discussions: thank you!

Curriculum vitae

First name and family name	Saskia Willemse
Date and place of birth	2. Januar 1966 in Sorengo (TI)
Citizen of	Tesserete (TI), Switzerland

Education and professional training

1972 - 1977	Primary school in Roveredo (TI) and in Tesserete
1977 - 1982	Ginnasio in Canobbio (Lugano)
1982 - 1985	Liceo Lugano
July 1985	Graduation **(Matura Typus C)**
1985 - 1991	Study at ETH (Umweltphysik, XB4) April '88 - October '88 Scientific collaborator at the Institute of Atmospheric Sciences at the School of Mines and Technology in Rapid City (South Dakota)
Nov. '88 - March '89	Scientific collaborator at the Institute of Atmospheric Physics, ETHZ
Summer 1989	Participation at field measurements of the Institute of Glaciology (ETHZ) at the Colle Gnifetti (Monte Rosa) and in Oberengadin
Summer semester '90	Collaboration in the project "ETH - Umwelttag"
April 1991	**Bachelor's degree from ETH Zürich (Abteilung X B4)**. Diploma thesis in Atmospheric Physics under the guidance of Prof. H. C. Davies
May '91 - February '92	Employee at Infras (environmental consulting)
1992 - 1995	Scientific collaborator and Ph.D. student at the Institute of Atmospheric Physics, ETH Zürich, in the group of Prof. A. Waldvogel